International Telecommunication Union

ITU-R

Radiocommunication Sector of ITU

Report ITU-R RS.2491-0

(09/2021)

Global survey of radio frequency interference observed by the SMAP radar in the 1 215-1 300 MHz band and the SMAP radiometer in the 1 400-1 427 MHz band

RS Series

Remote sensing systems

International Telecommunication Union

Foreword

The role of the Radiocommunication Sector is to ensure the rational, equitable, efficient and economical use of the radio-frequency spectrum by all radiocommunication services, including satellite services, and carry out studies without limit of frequency range on the basis of which Recommendations are adopted.

The regulatory and policy functions of the Radiocommunication Sector are performed by World and Regional Radiocommunication Conferences and Radiocommunication Assemblies supported by Study Groups.

Policy on Intellectual Property Right (IPR)

ITU-R policy on IPR is described in the Common Patent Policy for ITU-T/ITU-R/ISO/IEC referenced in Resolution ITU-R 1. Forms to be used for the submission of patent statements and licensing declarations by patent holders are available from http://www.itu.int/ITU-R/go/patents/en where the Guidelines for Implementation of the Common Patent Policy for ITU-T/ITU-R/ISO/IEC and the ITU-R patent information database can also be found.

Series of ITU-R Reports

(Also available online at http://www.itu.int/publ/R-REP/en)

Series	Title
BO	Satellite delivery
BR	Recording for production, archival and play-out; film for television
BS	Broadcasting service (sound)
BT	Broadcasting service (television)
F	Fixed service
M	Mobile, radiodetermination, amateur and related satellite services
P	Radiowave propagation
RA	Radio astronomy
RS	**Remote sensing systems**
S	Fixed-satellite service
SA	Space applications and meteorology
SF	Frequency sharing and coordination between fixed-satellite and fixed service systems
SM	Spectrum management

Note*: This ITU-R Report was approved in English by the Study Group under the procedure detailed in Resolution ITU-R 1.*

Electronic Publication
Geneva, 2021

REPORT ITU-R RS.2491-0

Global survey of radio frequency interference observed by the SMAP radar in the 1 215-1 300 MHz band and the SMAP radiometer in the 1 400-1 427 MHz band

(Question ITU-R 255/7)

(2021)

TABLE OF CONTENTS

Page

Scope

This Report presents global surveys of radio-frequency interference (RFI) levels observed by soil moisture active passive (SMAP) L-band sensors in the Earth exploration-satellite service (EESS) (active) band 1 215-1 300 MHz and the EESS (passive) band 1 400-1 427 MHz with the goal of informing EESS mission planners in the setting of their mission goals and objectives. This Report and its contents are not intended to prompt any future conference actions or changes to the Radio Regulations (RR).

1 Introduction

This Report is intended to assist EESS operators in their mission planning and to facilitate administration level interference discussions.

This Report presents global surveys of RFI levels observed by SMAP radar in the Earth exploration-satellite service (EESS) (active) frequency band 1 215-1 300 MHz and SMAP radiometer in the EESS (passive) frequency band 1 400-1 427 MHz.

The frequency band 1 215-1 300 MHz is allocated on a primary basis to the radionavigation-satellite service (RNSS) and radiolocation service (RLS), and the frequency band 1 240-1 300 MHz is also allocated on a primary basis to the aeronautical radionavigation service (ARNS). Systems operating under the EESS (active) allocation cannot claim protection from systems operating in the RLS or ARNS in these bands and cannot cause harmful interference to or claim protection from systems operating in the RNSS in the band 1 215-1 260 MHz. However, from the perspective of the active sensors operating in the EESS (active), emissions from the terrestrial radars operating in the RLS and ARNS are RFI to the EESS (active) sensors in the sense that their emissions can degrade the performance of the EESS (active) sensors. However, it is recognized that the EESS (active) sensors operating in this frequency band have to accept the RLS and ARNS emissions in accordance with the provisions of RR No. **5.332**.

The EESS (passive) frequency band 1 400-1 427 MHz is allocated solely for passive operations. The adjacent bands are allocated to the fixed, mobile and radiolocation services. Excessive unwanted emissions in the passive frequency band originating from the active services in adjacent bands, and unauthorised emissions occurring within the passive frequency band can impact the passive sensors operating in this passive frequency band and identified as RFI to these passive sensors. However, it is recognized that unwanted emissions from services in the adjacent bands may be in accordance with the provisions of Resolution **750 (Rev.WRC-19)**.

This document provides the three-day global map of RFI power observed by the SMAP radar around 1 225 MHz during the 2015 period. Presented for comparison is the RF environment observed by the SMAP radiometer in the 1 400-1 427 MHz frequency band in a three-day global map of brightness temperature obtained during the same three-day period as for the radar. The RFI as measured by these two spaceborne active/passive sensors is also described to the extent possible. This information is provided to assist in the design of future spaceborne active/passive sensors in these bands.

2 Related ITU-R Recommendations and Reports

There are the following ITU-R Recommendations and Reports related to this Report on the radio-frequency interference (RFI) observed by the SMAP radar and radiometer:

– Recommendation ITU-R RS.1166-4 – Performance and interference criteria for active spaceborne sensors

– Recommendation ITU-R RS.1859-1 – Use of remote sensing systems for data collections to be used in the event of natural disasters and similar emergencies

– Recommendation ITU-R RS.1883-1 – Use of remote sensing systems in the study of climate change and the effects thereof

– Recommendation ITU-R RS.2017-0 – Performance and interference criteria for satellite passive remote sensing
– Recommendation ITU-R RS.2106-0 – Detection and resolution of radio frequency interference to Earth exploration-satellite service (passive) sensors;
– Report ITU-R RS.2490-0 – Global survey of radio frequency interference observed by the Aquarius scatterometer in 1 215-1 300 MHz band and Aquarius radiometer in the 1 400-1 427 MHz band
– Report ITU-R RS.2492-0 – Global survey of radio frequency interference observed by SMOS radiometer in the EESS (passive) band 1 400-1 427 MHz
– Report ITU-R RS.2178-0 – The essential role and global importance of radio spectrum use for Earth observations and for related applications
– Report ITU-R RS.2311-0 – Pulsed radio frequency signal impact measurements and possible mitigation techniques between Earth exploration-satellite (active) systems and RNSS systems and networks in the band 1 215-1 300 MHz.

3 List of acronyms and abbreviations

ADC	Analogue digital converter
ARNS	Aeronautical radionavigation service
BFPQ	Block floating point quantization
BS	Broadcasting satellite
BSS	Broadcasting satellite system
BT	Brightness temperature
CCDF	Complementary cumulative distribution function
CDF	Cumulative distribution function
CNES	*Centre national d’études spatiales*
EESS	Earth exploration-satellite service
ESA	European Space Agency
IF	Intermediate frequency
MIC	Ministry of Internal Affairs and Communications of Japan
OOBE	Out-of-band emissions
PRF	Pulse repetition frequency
RFI	Radio-frequency interference
RLS	Radiolocation service
RR	Radio Regulations
SMAP	Soil moisture active passive
SMOS	Soil moisture ocean salinity
SNR	Signal-to-noise ratio
TA	Antenna temperature
WRC	World Radiocommunication Conference

4 Regulatory situation in the 1 215-1 300 MHz and 1 400-1 427 MHz frequency bands

4.1 Regulatory situation in the 1 215-1 300 MHz frequency band

The 1 215-1 300 MHz band is allocated on a primary basis to the EESS (active) with constraints given in ITU-R RR No. **5.332** in the 1 215-1 260 MHz sub-band, RR Nos. **5.332** and **5.335** in the 1 240-1 300 MHz sub-band and RR No. **5.335A** in the 1 260-1 300 MHz sub-band. RR No. **5.332** states that "In the band 1 215-1 260 MHz, active spaceborne sensors in the Earth exploration-satellite and space research services shall not cause harmful interference to, claim protection from, or otherwise impose constraints on operation or development of the radiolocation service, the radionavigation-satellite service and other services allocated on a primary basis." Radio Regulation No. **5.335** states that "In Canada and the United States in the band 1 240-1 300 MHz, active spaceborne sensors in the Earth exploration-satellite and space research services shall not cause interference to, claim protection from, or otherwise impose constraints on operation or development of the aeronautical radionavigation service."

Radio Regulation No. **5.335A** states that "In the band 1 260-1 300 MHz, active spaceborne sensors in the Earth exploration-satellite and space research services shall not cause harmful interference to, claim protection from, or otherwise impose constraints on operation or development of the radiolocation service and other services allocated by footnotes on a primary basis."

Since EESS (active) cannot claim protection from the radiolocation service, the aeronautical radionavigation service nor the radionavigation-satellite service in these respective sub-bands, EESS (active) systems have to mitigate the RFI received from these other primary services.

Figure 1 shows the ITU-R frequency allocations in and around the 1 215-1 300 MHz frequency range.

FIGURE 1

ITU-R frequency allocations in the 1 215-1 300 MHz range and adjacent frequency bands

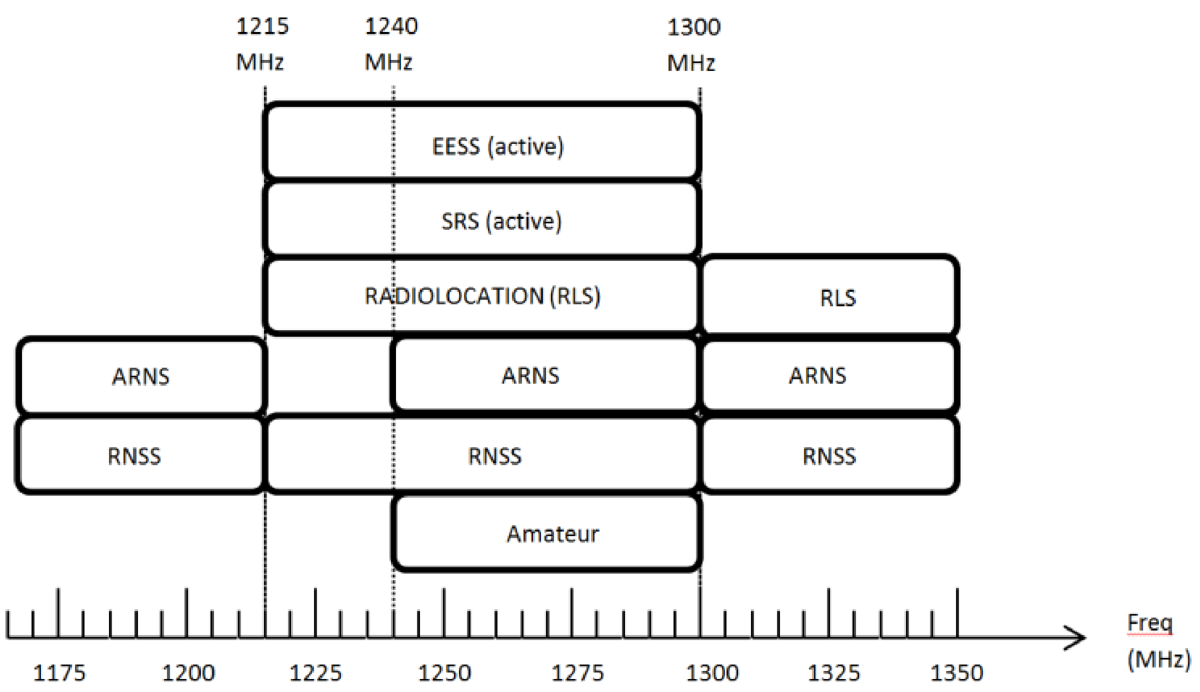

Below the 1 215-1 300 MHz band allocated to EESS (active) is the 1 164-1 215 MHz band, which is allocated on a primary basis to the ARNS and the RNSS (space-to-Earth) (space-to-space). Above the 1 215-1 300 MHz band is the 1 300-1 350 MHz band, which is allocated on a primary basis to the RLS, the ARNS and the RNSS (Earth-to-space).

4.2 Regulatory situation in the 1 400-1 427 MHz frequency band

The band 1 400-1 427 MHz is allocated on a primary basis to the EESS (passive), SRS (passive) and to the radio astronomy service as shown in Fig. 2. All emissions are prohibited in this band according to ITU-R RR No. **5.340**. In addition, WRC-07 adopted Resolution **750** on the compatibility between the EESS (passive) and relevant active services. Concerning the 1 400-1 427 MHz band, Resolution **750 (Rev.WRC-19)** contains the mandatory and recommended maximum levels of unwanted emissions from active service stations within the EESS (passive) band applicable to the ITU-R services allocated in the adjacent bands. This Resolution also resolves to urge administrations to take all reasonable steps to ensure that unwanted emissions of active services do not exceed the specific recommended maximum levels, noting that EESS passive sensors provide worldwide measurements that benefit all countries.

FIGURE 2

ITU-R frequency allocations in the 1 400-1 427 MHz range and adjacent frequency bands

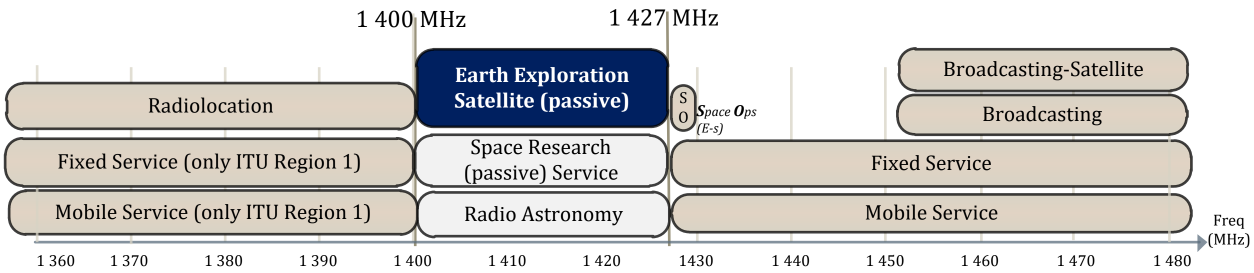

The SMAP mission obtains accurate global observations of emissions originating from land and ocean surfaces since the atmosphere is almost transparent in the 1 400-1 427 MHz frequency band. In addition, the sensitivity to varying emissivity resulting from changes of the water content in the soil and the salinity in the oceans is high for lower microwave frequencies in comparison to the measurements obtained at higher frequencies by operational sensors. The all-weather-all-surfaces capabilities of the 1 400-1 427 MHz frequency band addresses the needs of a large range of user communities and applications.

The following sections describe the RFI as measured during the 2015 period by the SMAP mission spaceborne active sensor and during the 2015 to present period by the SMAP mission spaceborne passive sensor which were operating entirely within their allocated EESS frequency bands of 1 215-1 300 MHz and 1 400-1 427 MHz in L-Band. Section 2 presents the RFI scenario detected by the radar of the SMAP mission. Section 3 presents the RFI scenario detected by the radiometer of the SMAP mission.

The information provided in this Report may be taken into account during the design of future spaceborne sensors which are intended to operate in the 1 215-1 300 MHz and 1 400-1 427 MHz frequency bands.

5 SMAP radar observed RFI

5.1 Description of SMAP radar

The SMAP radar operates in the 1 215-1 300 MHz frequency band and is a synthetic aperture radar designed to acquire radar backscatter signals that are used to estimate surface soil moisture. The spaceborne radar is designed to operate at an altitude of 685 km and inclination of 98° to provide an average revisit time of three days for soil moisture globally. The orbit is dawn/dusk sun-synchronous. The SMAP radar co-points with the radiometer subsystem to actively estimate soil moisture and freeze/thaw state. The radar will collect dual polarimetric returns (VV, HH, and HV transmit-receive polarizations) at 3 km resolution. In order to minimize range/Doppler ambiguities with the baseline antenna and viewing geometry, separate centre frequencies are used for each polarization (e.g. 1 260 MHz for V-pol and 1 263 MHz for H-pol). The centre frequencies are set 3 MHz apart, and the two frequencies can be selectively set within the 80.5 MHz range of 1 217.25-1 297.75 MHz to minimize radio frequency interference (RFI). The frequencies were actually set to around 1 225 MHz on orbit after a period of RFI survey to determine where the least amount of RFI occurred in the range of 1 217.25-1 297.75 MHz. The range bandwidth of each signal is 1 MHz with a corresponding 150 m line of sight range resolution and a ground range resolution of 250 m, resulting in a minimum of 12 looks in range for 3 km cells. The linear FM pulses have pulse durations of 15 ms and bandwidths of 1 MHz. A 6 m diameter reflector is rotated at 13 rpm to maintain contiguity of the measurements in the along-track direction. The incidence angle on the surface is near constant at 40 degrees, giving a 1 017 km swath. The beam from the offset parabolic reflector provides a 38 km wide footprint. The 6 m offset parabolic reflector produces a 3 dB beam width of 2.8 degrees. The beam may be pointed in any direction during spacecraft manoeuvres. Figure 3 illustrates the measurement geometry showing high- and low-resolution radar swaths and the radiometer swath.

The SMAP radar returns measurements of backscatter power obtained continuously over most of the Earth’s surface, including land and ice. The radar operates in two modes: a high-resolution mode for generating 3 km and 10 km geophysical products, and a low-resolution mode or real-aperture mode. In the high-resolution mode, each fully sampled radar return is digitized, compressed using block floating point quantization (BFPQ), recorded by the onboard recorders, and downlinked for range and azimuth compression processing on the ground. The peak data rate transmitting from the radar to a ground station is approximately 30 Mbit/s. In low-resolution mode, each radar return is incoherently averaged in range and azimuth, with no range or azimuth compression performed. This averaging is done on the spacecraft, resulting in 3-km × 30-km cells and a 350 kbit/s peak data rate. To reduce the data volume, the high-resolution mode usually operates only over land and usually only during the descending (AM) portion of the spacecraft orbit.

As far as timing for the hardware, the pulse repetition frequency (PRF) for the radar is approximately 3 000 Hz. This PRF applies to both frequencies (or polarizations) which are transmitted sequentially with the V-pol signal and H-pol signal separated by about 9 microseconds. The PRF is varied slightly over each orbit to correct for the oblateness of the Earth. The maximum aperture length is 42 milliseconds.

FIGURE 3

SMAP measurement geometry showing high and low resolution radar swaths and radiometer swath

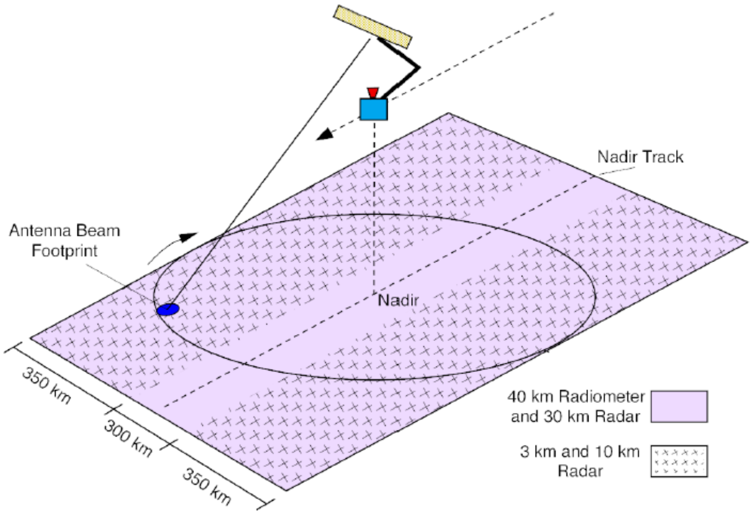

5.2 RFI detection and mitigation

SMAP radar RFI mitigation capabilities include: 1) a tunable operating frequency to allow the instrument to avoid the particularly noisy regions of the spectrum over specific regions of the Earth; 2) sharp RF/digital receiver filtering and a high degree of out-of-band interference rejection (80+ dB); and 3) supplemental radar telemetry for flagging any range lines contaminated by RFI, so that these bad data can be removed in ground data processing.

Several telemetry functions are designed into the receiver electronics to flag data blocks corrupted by RFI. A ‘receive power monitor’ flag is set whenever strong out-of-band interference causes a gain compression error in the RF front-end, upstream of the IF filter. An A/D converter ‘saturation flag’ detects range lines where strong in-band RFI causes one or more voltage samples to be clipped in the receive-window period. ‘Noise-only’ power measurements in the digital processor are accumulated on short time scales (every PRI, or ~350 μs) to facilitate detection of pulsed RFI. These telemetry fields serve as an important tool in ground data processing to identify and throw away contaminated echoes and noise only measurements, before blocks of raw SAR data are processed further.

5.3 Types of maps

The SMAP radar collects dual polarimetric returns (VV, HH, and HV transmit-receive polarizations). The type of map used in this Report is the following:

– Regional RFI maps: regional RFI maps (Regions 1, 2 and 3) with a quarter of a year mapping period show the ADC input power for select CDF values; Figure 5 shows the observed noise power (99.9% CDF value) at SMAP radar ADC input for North America (Region 2) (May 2015).

5.4 Types of RFI sources

The spatial and temporal resolution of the SMAP radar data permit the determination of individual RFI sources and comparisons of the predicted RFI effects with those actually observed. RFI maps show examples of identifying the locations of SMAP radar RFI hot-spots with nearby ATC radars over North America. It is also possible to compare the expected RFI signals generated from RFI and source/receiver modeling to the RFI levels SMAP actually observes.

Figure 5 is an RFI map of observed noise power with CDF of 99.9% at the SMAP radar ADC input for North America in May 2015. The ARNS radars which typically operate above 1240 MHz are not present since the SMAP radar centre frequency is below 1240 MHz. Some RLS radars which typically operate above 1215 MHz can be seen at higher latitudes in Fig. 5.

5.5 Global survey of RFI observed by SMAP radar in the first quarter of 2015

The SMAP radar co-points with the radiometer subsystem to actively estimate soil moisture and freeze/thaw state. The radar collects dual polarimetric returns (VV, HH, and HV transmit-receive polarizations) at 3 km resolution.

The observed noise power for each 3 km resolution cell is sampled once every three days. Over the first quarter of year 2015, there were about 30 samples of noise power at the ADC input per resolution cell over the approximately 90 days from which a histogram and complementary cumulative distribution function (CCDF) of the noise power values were produced. For the following RFI maps of the observed noise for CCDF, the noise power values are pseudocolor-coded. The pseudocolor legend in the ‘ge-colorbar’ shows fifteen noise power bins of powers equally distributed over the range of −20 dBm to +6 dBm. The pseudocolor for each 3 km resolution cell represents the CCDF value with a probability of 99.9% that the noise power is greater than the power value shown in the ‘ge-colorbar’ legend.

Figure 4 shows the RFI map of the observed noise for CCDF value 99.9% in Region 1 for observations in the first quarter of year 2015.

Figure 5 shows the RFI maps of the observed noise for CCDF value 99.9% in Region 2 for observations in the first quarter of year 2015.

Figure 6 shows the RFI maps of the observed noise for CCDF value 99.9% in Region 3 for observations in the first quarter of year 2015.

FIGURE 4

Map of observed noise power (99.9%) at SMAP radar ADC input for Europe and Northern Africa (Region 1) (May 2015)

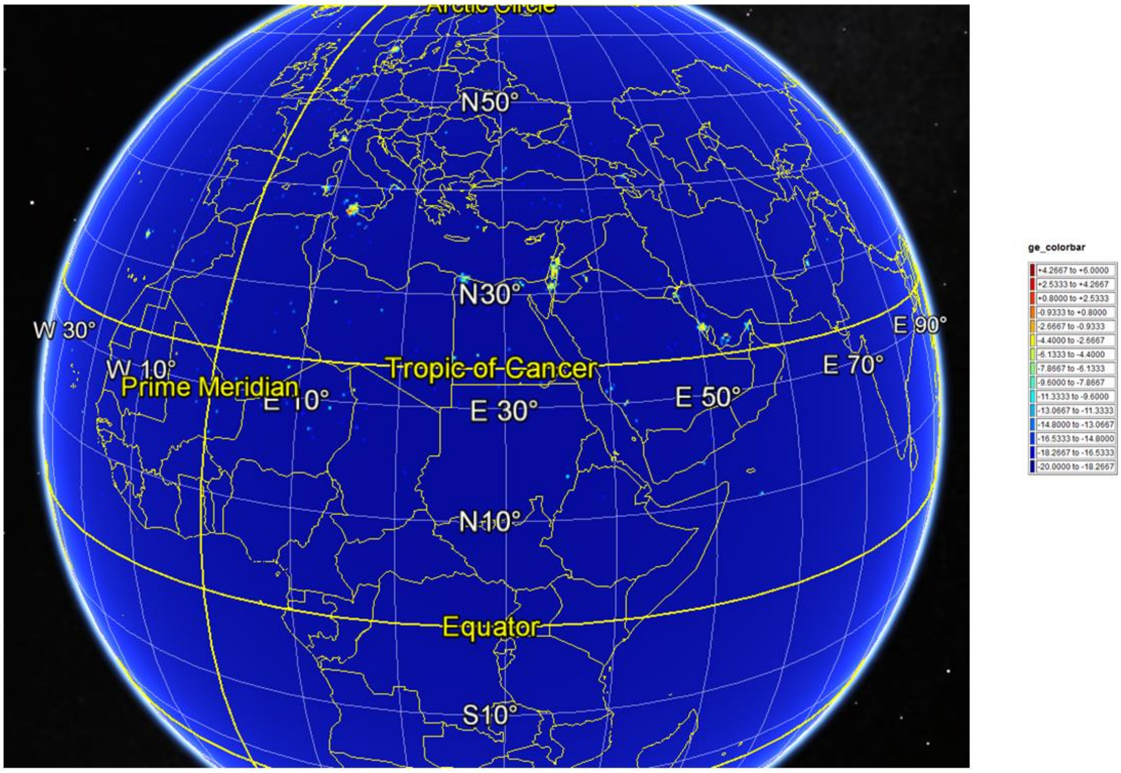

FIGURE 5

Map of observed noise power (99.9%) at SMAP radar ADC input for North America (Region 2) (May 2015)

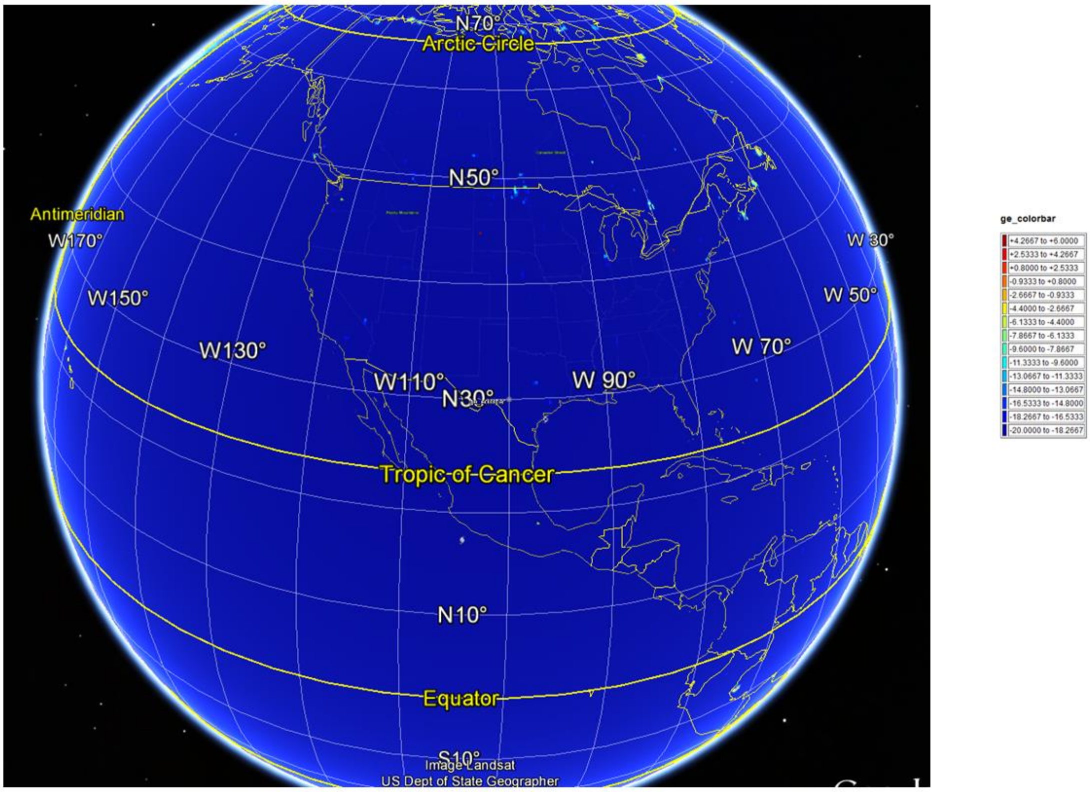

FIGURE 6

Map of observed noise power (99.9%) at SMAP radar ADC input for Asia (Region 3) (May 2015)

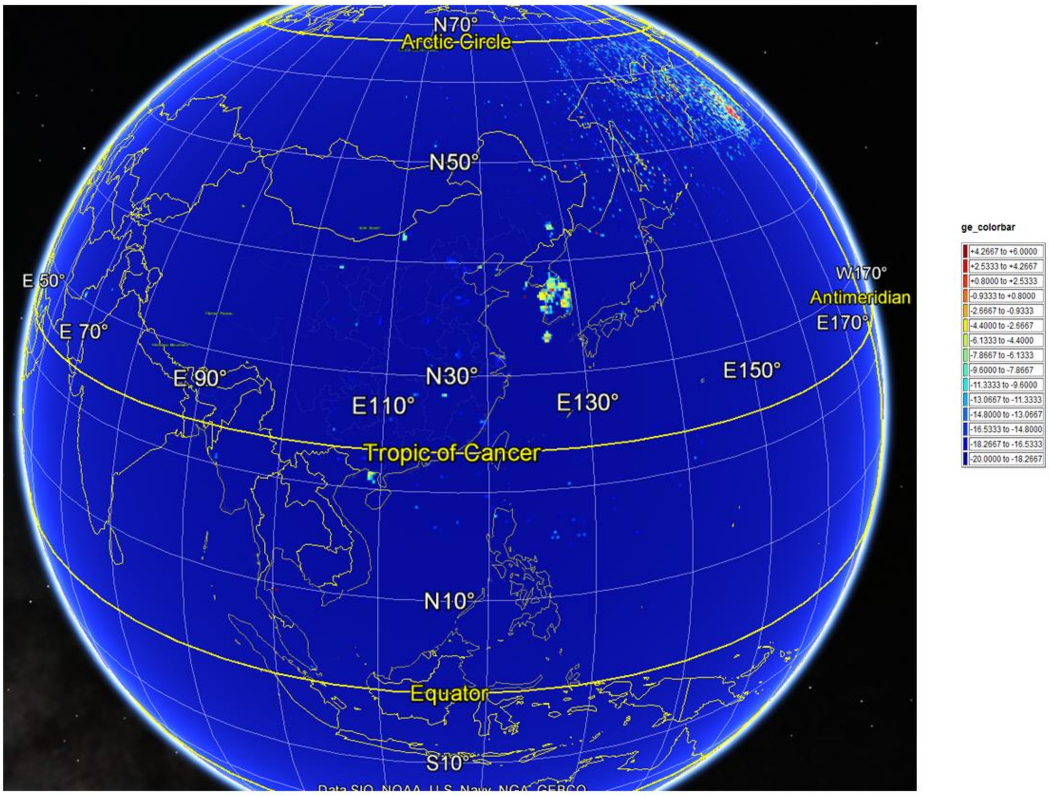

6 SMAP radiometer observed RFI

6.1 Description of SMAP radiometer

The SMAP radiometer maps the world every three days. The SMAP radiometer is a 1.413 GHz Dicke radiometer similar to that used for the Aquarius radiometer, that uses noise injection for calibration. The radiometer operates with V, H, and third and fourth Stokes parameter polarizations at 1.413 GHz. Although the third Stokes parameter measurement is primarily to assist in the correction of Faraday rotation effects, it may provide additional science research benefits.

The SMAP radiometer returns brightness measurements over most of the Earth's surface, including land and ice. The radiometer operates continuously, generating data at a high-resolution rate of 3.2 Mbit/s and at a low-resolution rate of 750 kbit/s. The radiometer and radar operations are simultaneous so that the two sensors look at the same piece of the planet.

6.2 RFI detection

The SMAP radiometer uses multiple RFI detection methods which occur in the ground processing software. The detection methods include pulse detection or time domain detection, cross frequency detection, kurtosis detection, and polarimetric detection using the third and fourth Stokes parameters. All detection algorithms are "double sided", and each algorithm has threshold parameters to control the false alarm rate. The pulse, kurtosis and polarimetric detectors are applied to fullband data samples which are obtained every 350 μs and the cross frequency, kurtosis and polarimetric detectors are applied to the sub-band data samples reported every 1.2 ms. These algorithms are implemented for each footprint formed using 32 fullband measurements and 8 × 16 sub-band measurements. The final brightness temperatures are computed from only the sub-band measurements, but RFI mitigation includes flags from the sub-band and fullband measurements (both fullband and sub-band data are included in the science telemetry).

6.3 RFI characterization

Section 6.7 contains reports of observed RFI by the SMAP radiometer over areas of various administrations. Each report has an interference source detail log with the following parameters which are provided to the national spectrum management authorities so that investigations can be initiated:

– Unique ID for each RFI source
– Location coordinates (longitude, latitude)
– Centre frequency (MHz)
– Source detection characteristics (point or extended, directivity, pulsed or continuous)
– Brightness temperature (degrees kelvin (K))
– e.i.r.p. of transmitting sources (dBW using Friis formula)
– City/State/Region of source
– Number of observations of source over analysis period
– Date/time log (first detected, first reported, or last observation)
– Present status (on, off).

6.4 Types of maps

Section 6.7 contains reports of observed RFI by the SMAP radiometer over areas of various administrations. Each report has several types of maps of observed RFI:

– Peak hold plot on a 0.25 × 0.25 grid of horizontally polarized antenna temperatures (TA) in kelvin before RFI filtering over the time period of reporting

– Map on a 0.25 × 0.25 grid of the percentage of observations over the reporting period with a detected RFI level of 5 K or more in the horizontal polarization
– Location and intensity of RFI sources over the administration.

6.5 Types of RFI sources

The types of RFI sources can be categorized by whether they are in-band or out-of-band and whether they point or extended sources:

– In-band emissions in the protected band 1 400-1 427 MHz: These RFI sources in-band are caused by unauthorized sources.
– Out-of-band emissions from adjacent bands: These RFI sources with high emission levels may belong to the radar systems in the adjacent bands.
– Point sources: These RFI sources are for only one interfering emitter within the sensor spatial resolution on the ground.
– Extended sources: These RFI sources are for multiple emitters within the sensor footprint.

6.6 Observation of RFI into SMAP radiometer in May 2015

On 31 January 2015, NASA launched the SMAP satellite to improve climate and weather forecasts, monitor droughts, and better predict flooding caused by severe rainfall or snowmelt – information that may help save lives and property. SMAP soil moisture measurements can also allow nations to better forecast crop yields and improve global famine early-warning systems.

Based on previous missions that have encountered interference in the 1 400-1 427 MHz band, such as the European Space Agency’s (ESA) Soil Moisture and Ocean Salinity (SMOS) mission, the SMAP mission developed techniques to reduce the impact of RFI from systems operating in adjacent bands. The SMAP microwave radiometer is able to detect RFI that is localized in time and/or frequency with respect to SMAP measurements in the 1 400-1 427 MHz Earth science (passive) primary exclusive allocation.

In 2015, SMAP had detected RFI from both radar and TV receiver systems of BSAT Broadcasting Satellite (BS) over the Americas, Europe and Asia, although both the strength of the detected signals and the probability of occurrence over the Americas were found to be relatively low compared to Europe and Asia.

The detected out-of-band emissions (OOBE) and unauthorized in-band signals degraded the SMAP measurements. Some of the measured data corrupted by them were removed at the cost of instrument SNR (signal-to-noise ratio) and degradation in soil moisture sensing performance. Other measured data corrupted by RFI could not be removed, to such a degree that soil moisture sensing was not possible, and SMAP suffered data loss. In particular, there were specific locations over which SMAP where OOBE and unauthorized in-band signals obliviated natural thermal emissions, rendering this data unusable. One such location where this occurred is Japan (Figure 7) where the measured brightness temperature was found to be higher than physically possible. The SMAP RFI detectors could not extract natural signals from the RFI, particularly when the RFI were generated by the aggregate effects of multiple sources distributed over SMAP’s field of view. This situation became a law-of-large numbers problem whereby the RFI started to look like Gaussian noise that is indistinguishable from thermal noise except for its high amplitude, rendering all of the SMAP’s interference mitigation techniques ineffective. In this situation, SMAP was blind.

FIGURE 7

Global map of percent of SMAP data lost due to RFI in the 1 400-1 427 MHz passive band (horizontal polarization)

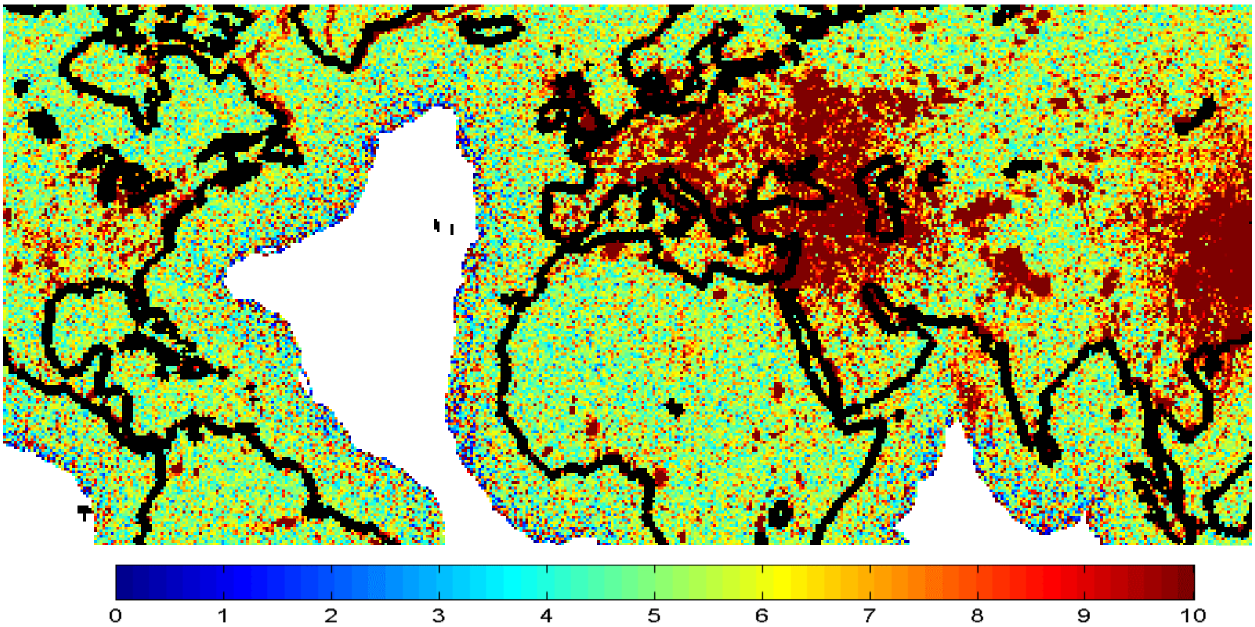

RFI arises from adjacent band radar and communication systems, as well as the use of unauthorized devices within the band.

The RFI detection algorithm works on two types of SMAP data streams. One type is the 'full-band' data stream and corresponds to the entire 24 MHz bandwidth of the SMAP filter and to an integration time of about 300 μs. The other type is the 'sub-band' data stream and consists of 16 frequency channels each corresponding to 1.5 MHz and an integration time of about 1.2 ms. For each data stream, SMAP takes measurements of all four modified Stokes parameters (V-pol, H-pol, 3rd and 4th Stokes parameters).

The RFI detection algorithm uses both data streams and all four modified Stokes parameters. The criteria used to detect RFI are the following:

– Time-domain outlier detection (V- and H-pol; both full-band and sub-band data);

– Kurtosis detection (V- and H-pol; both full-band and sub-band data);

– Cross-frequency outlier detection (V- and H-pol; sub-band data only);

– Polarization detection (3rd and 4th Stokes parameters; both full-band and sub-band data).

The outputs of this RFI detection algorithm are all the RFI flags raised by the detection criteria above and the filtered antenna temperature, i.e. the antenna temperature averaged at every footprint after all the flagged subsamples have been removed.

The SMAP false alarm rate is 5%; detection rates >10% are definitely due to non-thermal sources (indicated by dark red areas).

FIGURE 8

Regional maps of eastern Asia show maximum detected brightness temperature (in kelvins) by SMAP in the 1 400-1 427 MHz passive band (horizontal polarization) in May 2015

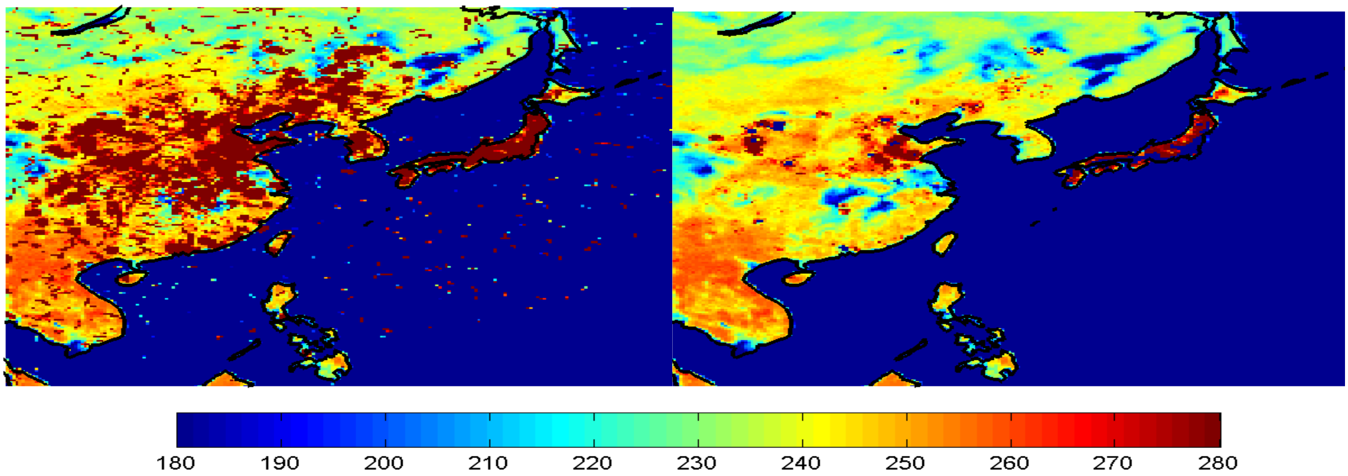

The colour scale has been saturated at 280 K to emphasis values exceeding expected geophysical range. The left panel shows the max-hold brightness temperature without RFI filtering and the right panel shows with RFI filtering performed in ground processing algorithms. Note the persistent dark red areas (and anomalous blue areas) over Japan where SMAP's state-of-the-art RFI filtering techniques were unable to perform.

FIGURE 9

Detection rate of observed RFI in Asia and Japan (with colour scale spanning 0-100% detection rate) in May 2015

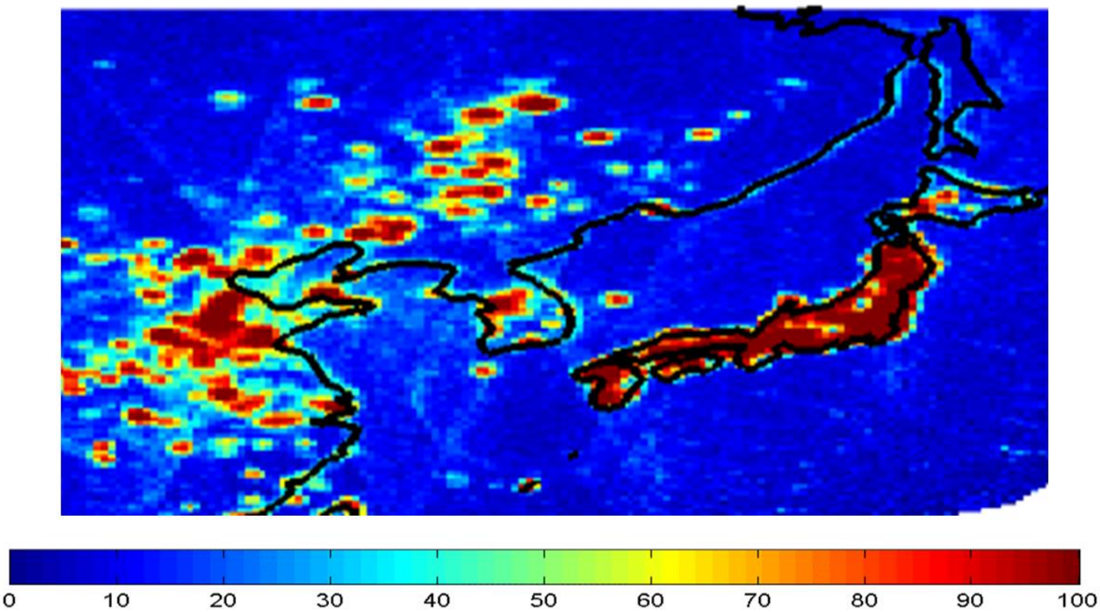

SMAP was unable to observe in the protected 1 400-1 427 MHz band in Japan, parts of China and several other countries. Subsection 4.1 contains detailed information on observed RFI in Japan. Tests facilitated by the Japanese authorities (MIC) confirmed that the RFI observed over Japan was mainly due to the intermediate frequency emissions of malfunctioning TV receiver systems of BSAT Broadcasting Satellite.

Subsection 6.7.2 contains information on observed RFI in China and other subsections in § 6.7 show information on observed RFI in areas of various other administrations.

6.7 Reports of observed RFI by radiometer over areas of various administrations

The following sections contain reports of RFI over areas of various administrations as observed from 2015 to 2019. Each section has a table of the summary of RFI sources, a table of the interference source detail log, a plot of the peak hold data over the area of the administration, a map of the percentage of observations of RFI over the period of the reported observation and a plot of the location and intensity of RFI sources over the area of the administration.

6.7.1 Report of observed RFI over Japan in October 2016

6.7.1.1 Data loss experienced over Japan in October 2016

SMAP has experienced persistent data loss over most of Japan in October 2016. Figure 10 indicates areas of Japan where there was no useable data for soil moisture retrievals in October 2016 because of corruption due to RFI during that time. Figure 11 is a probability map showing the percentage of time that SMAP detected an RFI level of 5 K or more in the horizontal polarization for data from 1 to 31 October 2016 over Japan.

FIGURE 10

Areas (yellow) of Japan where there was no useable data in October 2016 and no soil moisture retrievals were possible

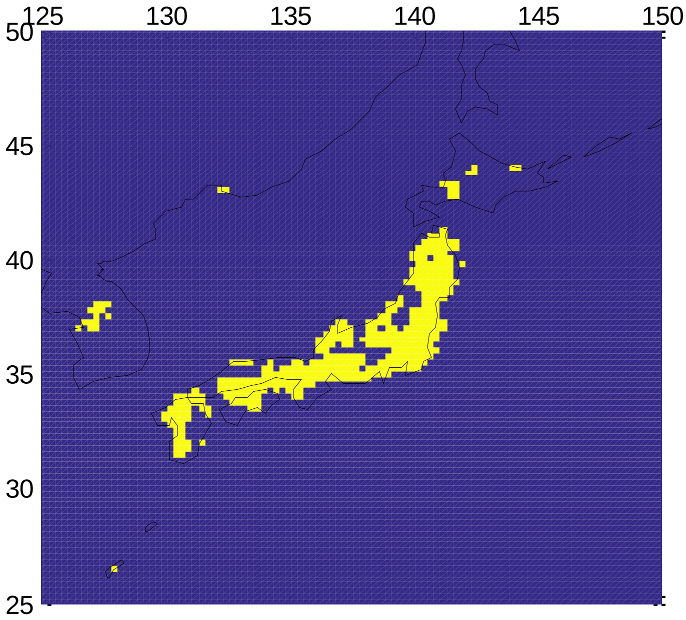

Note to Fig. 10: Data taken over the period 1 October 2016 to 7 October 2016 and displayed on a 0.25°×0.25° grid. Vertical polarization exhibited similar results.

FIGURE 11

Percentage of the time that SMAP detected an RFI level of 5 K or more in the horizontal polarization for data from 1 to 31 October 2016 over Japan

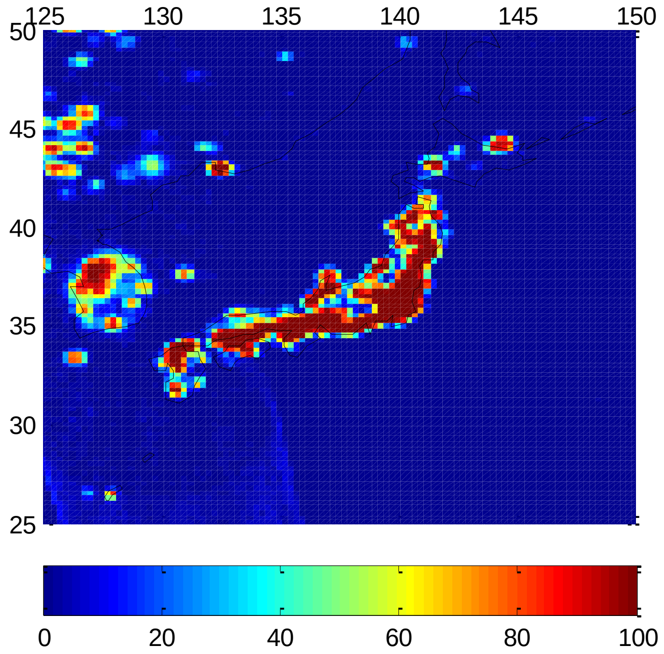

Note to Fig. 11: Vertical polarization exhibited similar results. Data shown on a 0.25° × 0.25° grid.

6.7.1.2 RFI of BSAT-3C BS TV emissions over Japan

The ESA has done analyses of images from their SMOS mission and determined that the intermediate frequency (IF) emissions of malfunctioning TV receiver systems of BSAT Broadcasting Satellite are the main contributor to the extended RFI observed by SMOS over Japan. SMOS like SMAP operates in the protected EESS (passive) allocation in the 1 400-1 427 MHz band. It was determined that the BSAT channels, numbers 19 and 21, correspond to those with intermediate frequencies within the 1 400-1 427 MHz passive sensing band. The BSAT channels 19 and 21 intermediate frequencies occupy the bandwidths 1 377.47 MHz – 1 411.97 MHz and 1 415.83 MHz – 1 450.33 MHz, respectively. Thus, they overlap with the EESS allocation from 1 400 MHz – 1 411.97 MHz and 1 415.83 MHz – 1 427 MHz. Since SMAP science telemetry includes frequency information, spectral data over Japan was analyzed. The images produced from SMAP data provide evidence of corruption of data due to RFI in the frequencies corresponding to the BSAT Broadcasting Satellite intermediate frequencies.

6.7.1.3 Spectra measured by SMAP over the main Japanese cities

SMAP spectral data is provided in Figs 12 to 15 over major Japanese cities using data from 1 to 31 October 2016. The middle frequencies from ~1 412 MHz – 1 415 MHz had much reduced TAs compared to the edges. TAs of 350 K and above are beyond the geophysical limits and thus can definitively be classified as RFI. Each data point is the average of the sub-band TA measured within a 50 km radius, centred approximately at the centre of the city. Figure 16 is a peak hold image of antenna temperatures for each of the 16 sub-bands. Although the middle sub-bands indicate much less corruption due to RFI, there still appeared to be point sources of RFI in the images at these frequencies. The data from these channels were further processed to geolocate these sources.

FIGURE 12

Osaka

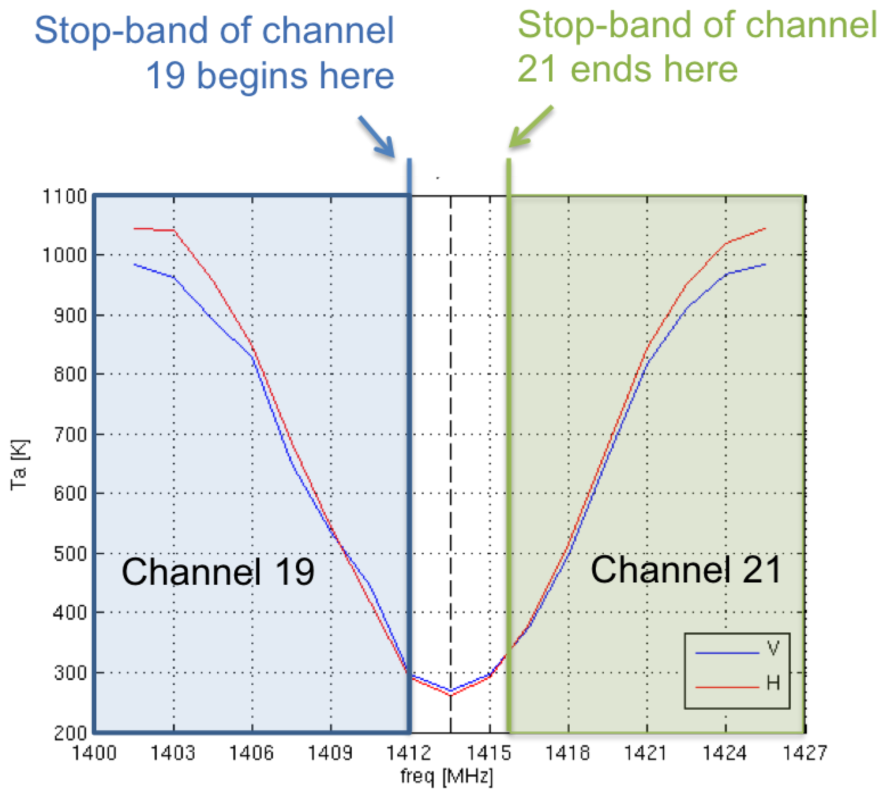

Note to Fig. 12: The Figure shows the SMAP frequency response to BSAT interference. Superimposed are the frequencies used by channels 19 and 21 of the BSAT system.

FIGURE 13

Tokyo

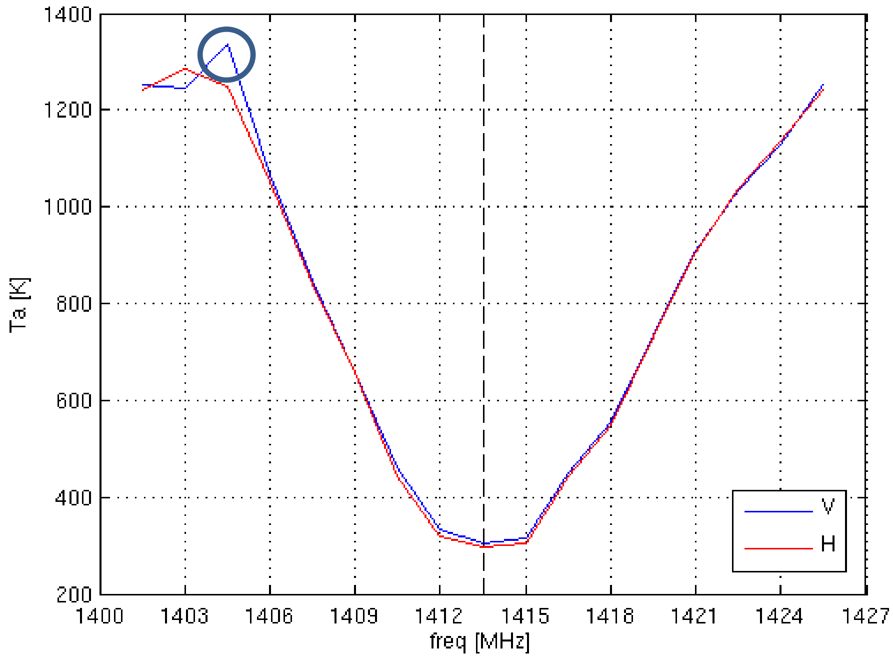

Note to Fig. 13: The Figure shows the SMAP frequency response to BSAT interference. Note that V-pol has a peak around 1 404.5 MHz. In addition to the BSAT interference there is an additional interferer at this frequency. This hypothesis was supported by the fact that an RFI source was visible in Tokyo when the BSAT system was under maintenance.

FIGURE 14

Nagoya

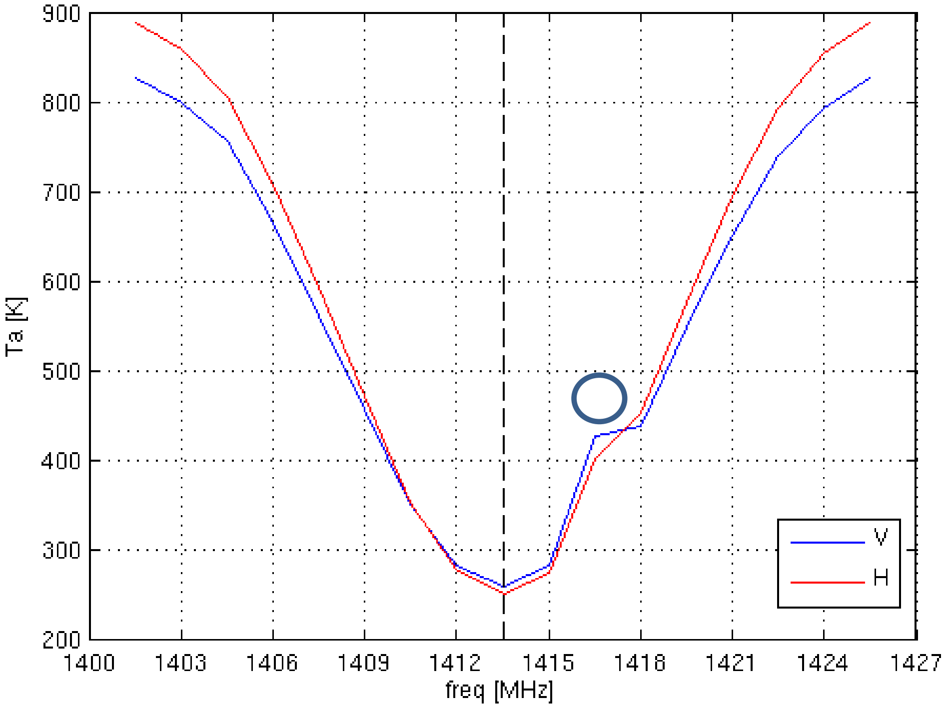

Note to Fig. 14: The Figure shows the SMAP frequency response to BSAT interference. Additional interferer around 1 416.5 MHz likely not belonging to the BSAT system.

FIGURE 15

Hiroshima

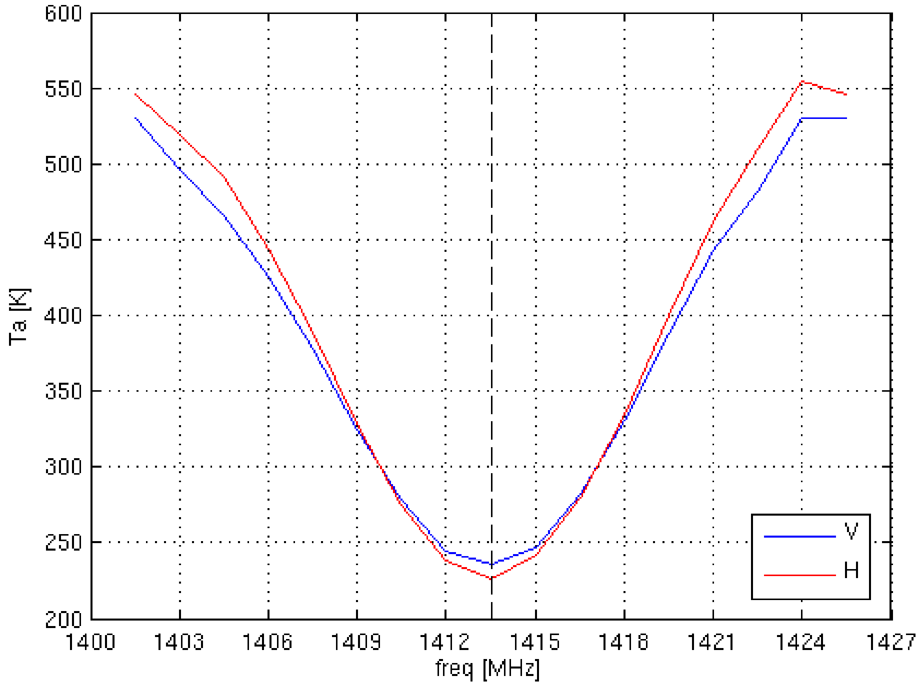

Note to Fig. 15: The Figure shows the SMAP frequency response to the BSAT interference.

FIGURE 16

Peak hold data over Japan on a 0.25° × 0.25° grid of horizontally polarized TAs in kelvin before RFI filtering for the period 1 October 2016 to 7 October 2016

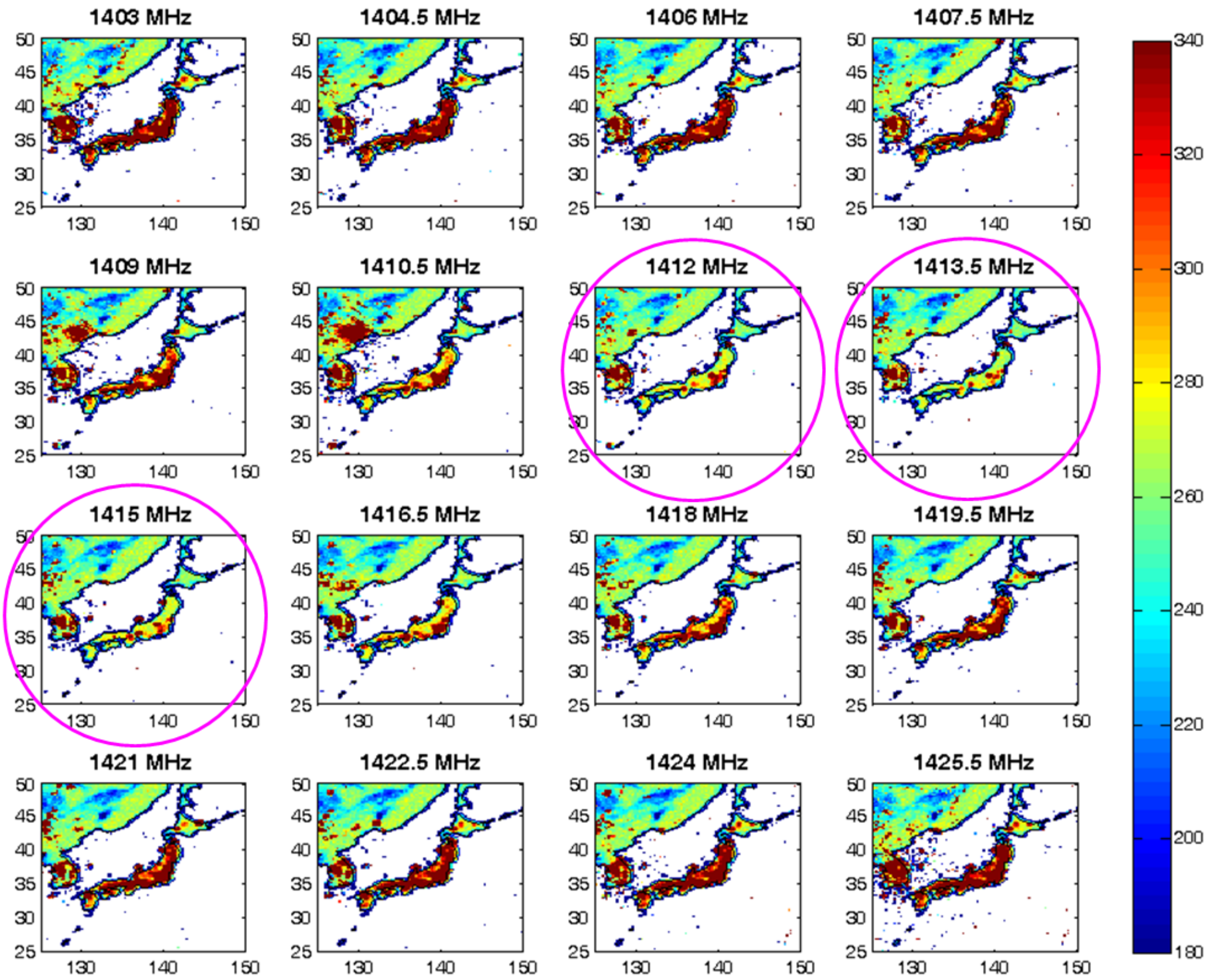

Note to Fig. 16: The colour scale was limited to 180 to 340 K to better show the RFI events. The middle channels from 1 412 MHz to 1 415 MHz show significantly less corruption compared to the outer channels.

6.7.1.4 Geolocation of RFI sources (within the guard band) not due to BSAT as determined from observations in October 2016

The middle three channels are located in the BSAT guard bands from 1 412 MHz to 1 425 MHz. Table 1 includes the following detailed information for each RFI source identified using the middle three channels (see Fig. 17) of SMAP spectral data: latitude and longitude, average RFI level in kelvin, as well as number of observations used to geolocate the source to determine RFI level. The centre frequencies of the sources were not provided since it was difficult to determine using only 3 channels. There are 15 sources listed in Table 1. Data from 1 to 31 October 2016 was used to create Table 1. The sources are ordered in the table from largest to smallest levels.

The localization of RFI sources is based on the difference between SMAP measurements before and after RFI filtering. This difference corresponds to the effect that RFI have on the data. A machine learning algorithm is then applied to automatically find the points where the effect of RFI is highest (local maxima). These points define the location of RFI sources. Since every RFI source is observed multiple times during the course of one month, the coordinates and RFI level provided in this report are the result of an average of the individual observations from 1 to 31 October 2016.

FIGURE 17

Location and intensity of RFI sources over Japan not due to BSAT

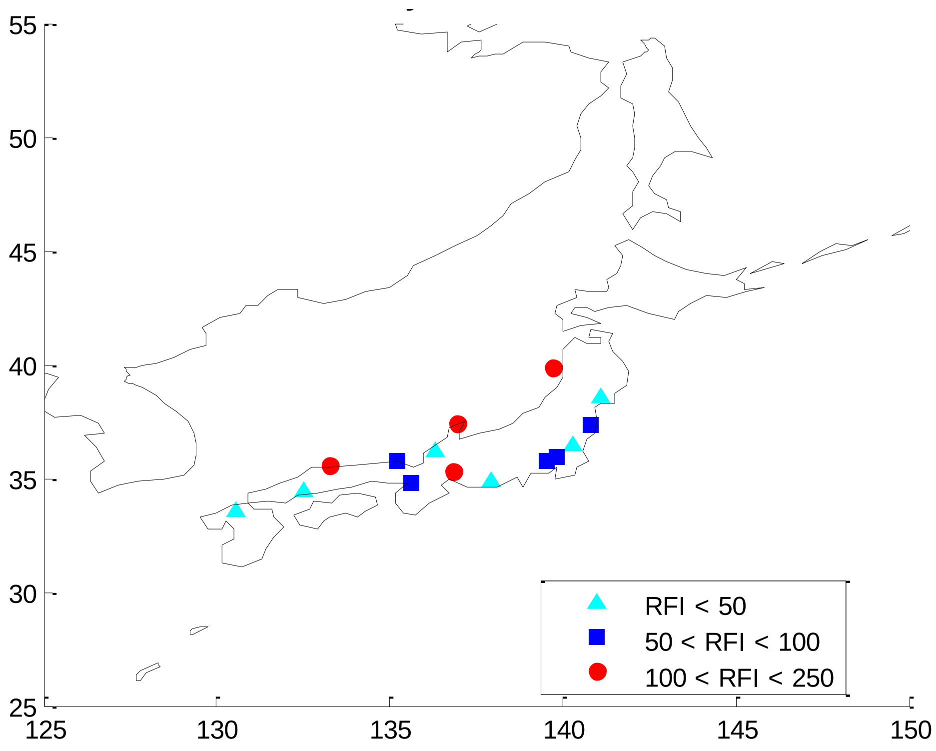

Note to Fig. 17: Sources were located using the middle three channels of the spectral data. Colours indicate range of RFI levels in kelvin (1-31 October 2016).

TABLE 1

Interference source detail log
Number of active sources listed not due to BSAT
Time period: 1-31 October 2016

ID	Number	Latitude (degrees)	Longitude (degrees)	Average RFI level (kelvin)	Number of observations
J	1	37.42	136.96	244	49
J	2	35.58	133.25	204	18
J	3	39.87	139.74	192	14
J	4	35.3	136.86	109	28
J	5	35.94	139.86	84	40
J	6	37.35	140.83	76	17
J	7	35.76	135.23	67	26
J	8	35.75	139.57	62	35
J	9	34.82	135.65	53	28
J	10	33.56	130.58	48	39
J	11	36.45	140.29	35	8
J	12	34.86	137.96	32	42
J	13	38.57	141.1	19	32

TABLE 1 (*end*)

ID	Number	Latitude (degrees)	Longitude (degrees)	Average RFI level (kelvin)	Number of observations
J	14	36.15	136.32	13	8
J	15	34.44	132.49	12	15

6.7.2 Report of observed RFI over China in October 2016

6.7.2.1 Detailed information on RFI over China as observed in October 2016

Table 2 includes the following detailed information for each RFI source: latitude and longitude, centre frequency, average RFI level in kelvin, number of observations used to geolocate the source and determine RFI level and the region where the source is located. There are 240 sources listed in Table 2. Data from 1 to 31 October 2016 was used to create Table 2 as well as supporting Figures in § 6.7.2.1.

The localization of RFI sources was based on the difference between SMAP measurements before and after RFI filtering. This difference corresponds to the effect that RFI have on the data. A machine learning algorithm was then applied to automatically find the points where the effect of RFI is highest (local maxima). These points defined the location of RFI sources. Since every RFI source is observed multiple times during the course of one month, the coordinates and RFI level provided in this report were the result of an average of the individual observations from 1 to 31 October 2016. SMAP science telemetry includes frequency information thus the RFI centre frequency was also identified for the RFI sources. A range is given if there appeared to be an observable bandwidth in the spectrum for the RFI source. Multiple centre frequencies were given if there were multiple peaks across the 16 sub-bands that were obviously RFI (TA > 350 K). The sources are ordered in the Table from the largest to the smallest interference levels.

TABLE 2

Interference source detail log
Number of active sources listed: [240]
Time period: 1-31 October 2016

ID	Number	Latitude (degree)	Longitude (degree)	Centre frequency (MHz)	Average RFI, TA (K)	Number of observations 1-31 October 2016	Region
CHN	1	36.27	114.64	1 401-1 424	967	4	Hebei Shěng
CHN	2	34.27	108.95	1 401-1 424	786	44	Shaanxi Shěng
CHN	3	29.53	114.05	1 401-1 424	564	41	Hubei Shěng
CHN	4	30.26	119.14	1 401, 1 403, 1 421	516	22	Zhejiang Shěng
CHN	5	27.65	106.72	1 412-1 422	455	12	Guizhou Shěng
CHN	6	50.58	123.15	1 402-1 409	440	10	Nei Mongol Zìzhìqu
CHN	7	29.96	105.28	1 408-1 418, 1 419.5	412	8	Sichuan Shěng
CHN	8	22.79	113.05	1 424	404	7	Guangdong Shěng
CHN	9	38.49	106.18	1 404-1 418	401	49	Ningxia Hui Zìzhìqu
CHN	10	39.95	116.36	1 410.5	393	47	Beijing Zhíxiáshì
CHN	11	24.49	117.97	1 401-1 415	387	17	Fujian Shěng
CHN	12	30.95	121.24	1 402-1 408, 1 421	359	40	Shanghai Zhíxiáshì
CHN	13	38.62	108.39	1 401-1 406, 1 421-1 424	345	52	Nei Mongol Zìzhìqu
CHN	14	39.94	98.3	1 409, 1 420	329	3	Gansu Shěng
CHN	15	39.72	98.45	1 421	326	45	Gansu Shěng
CHN	16	41.18	114.72	1 401-1 424	324	3	Hebei Shěng
CHN	17	31.47	92.06	1 412-1 416, 1 418-1 422	315	41	Xizang Zìzhìqu
CHN	18	22.95	113.1	1 401-1 424	291	3	Guangdong Shěng
CHN	19	34.47	113.44	1 402-1 403, 1 424	288	28	Henan Shěng
CHN	20	25.82	105.22	1 410.5, 1 416.5	286	45	Guizhou Shěng
CHN	21	43	129.38	1 406-1 410	282	20	Jilin Shěng
CHN	22	36.15	103.77	1 407.5, 1 413.5, 1 419.5	275	44	Gansu Shěng

TABLE 2 (*continued*)

ID	Number	Latitude (degree)	Longitude (degree)	Centre frequency (MHz)	Average RFI, TA (K)	Number of observations 1-31 October 2016	Region
CHN	23	41.65	86.24	1 401, 1 403, 1 421	274	6	Xinjiang Uygur Zìzhìqu
CHN	24	33.26	111.53	1 404.5, 1 407-1 409	270	6	Henan Shěng
CHN	25	29.58	105.3	1 418-1 422	270	22	Sichuan Shěng
CHN	26	38.82	115.27	1 401.5, 1 424	248	45	Hebei Shěng
CHN	27	30.44	114.34	1 410-1 413, 1 416.5	243	39	Hubei Shěng
CHN	28	29.31	108.15	1 410.5, 1 416.5	237	17	Chongqing Zhíxiáshì
CHN	29	23.09	113.08	1 418, 1 424	235	24	Guangdong Shěng
CHN	30	26.38	119.6	1 409	230	5	Fujian Shěng
CHN	31	22.39	113.03	1 401.5, 1 424	216	8	Guangdong Shěng
CHN	32	22.21	112.8	1 401.5, 1 424	213	6	Guangdong Shěng
CHN	33	38.98	103.56	1 404, 1 418	208	11	Gansu Shěng
CHN	34	23.16	112.9	1 401-1 424	207	3	Guangdong Shěng
CHN	35	39.08	117.18	1 412	204	46	Tianjin Zhíxiáshì
CHN	36	22.54	114.06	1 402-1 414	199	31	Guangdong Shěng
CHN	37	30.95	103.98	1 401, 1 419.5, 1 424	199	19	Sichuan Shěng
CHN	38	45.17	127.98	1 416-1 420	198	9	Heilongjiang Shěng
CHN	39	31.84	117.29	1 410.5, 1 416.5	192	31	Anhui Shěng
CHN	40	30.79	106.07	1 408.5, 1 416, 1 421	189	16	Sichuan Shěng
CHN	41	30.24	103.53	1 414, 1 421	183	39	Sichuan Shěng
CHN	42	32.58	118.16	1 409	180	3	Anhui Shěng
CHN	43	42.8	125.44	1 411-1 415, 1 418-1 421	180	28	Jilin Shěng
CHN	44	35.23	109.58	1 404, 1 411-1 415, 1 419.5	177	28	Shaanxi Shěng
CHN	45	45.15	122.71	1 407-1 409, 1 413-1 415	176	9	Jilin Shěng
CHN	46	41.8	123.41	1 403-1 424	176	35	Liaoning Shěng

TABLE 2 (*continued*)

ID	Number	Latitude (degree)	Longitude (degree)	Centre frequency (MHz)	Average RFI, TA (K)	Number of observations 1-31 October 2016	Region
CHN	47	30.93	106.11	1 409, 1 416, 1 421	168	3	Sichuan Shěng
CHN	48	29.48	121.68	1 406-1 413	168	30	Zhejiang Shěng
CHN	49	28.15	112.93	1 402, 1 403, 1 416, 1 424	164	22	Hunan Shěng
CHN	50	25.53	118.24	1 421	158	24	Fujian Shěng
CHN	51	29.5	90.91	1 415, 1 422	158	36	Xizang Zìzhìqu
CHN	52	44.32	85	1 418	157	42	Xinjiang Uygur Zìzhìqu
CHN	53	26.58	119.53	1 409	155	19	Fujian Shěng
CHN	54	27.03	118.32	1 403	154	13	Fujian Shěng
CHN	55	38.08	117.58	1 406-1 410	154	8	Hebei Shěng
CHN	56	32.65	117.04	1 419.5	150	26	Anhui Shěng
CHN	57	25.57	119.78	1 421	150	18	Fujian Shěng
CHN	58	40.67	109.83	1 412	149	59	Nei Mongol Zìzhìqu
CHN	59	45.62	122.8	1 415	148	8	Jilin Shěng
CHN	60	26.88	114.84	1 404-1 406	138	10	Jiangxi Shěng
CHN	61	43.91	125.36	1 409, 1 412, 1 418-1 420	138	25	Jilin Shěng
CHN	62	22.93	113.97	1 402-1 409	137	3	Guangdong Shěng
CHN	63	36.19	117.07	1 403, 1 424	136	19	Shandong Shěng
CHN	64	31.26	118.34	1 410.5	132	17	Anhui Shěng
CHN	65	50.16	125.97	1 410-1 415	130	65	Heilongjiang Shěng
CHN	66	33.97	116.37	1 410.5-1 415	130	32	Henan Shěng
CHN	67	34.37	107.12	1 421	130	41	Shaanxi Shěng
CHN	68	37.94	114.65	1 417.5	127	26	Hebei Shěng
CHN	69	39.11	101.82	1 411-1 415	127	43	Nei Mongol Zìzhìqu
CHN	70	36.93	117.16	1 401-1 424	127	18	Shandong Shěng

TABLE 2 (*continued*)

ID	Number	Latitude (degree)	Longitude (degree)	Centre frequency (MHz)	Average RFI, TA (K)	Number of observations 1-31 October 2016	Region
CHN	71	36.73	117.21	1 405-1 408, 1 424	127	3	Shandong Shěng
CHN	72	45.04	125.98	1 411.5, 1 416-1 421	126	27	Jilin Shěng
CHN	73	34.46	115.6	1 410.5	124	25	Henan Shěng
CHN	74	33.61	119.58	1 421	122	8	Jiangsu Shěng
CHN	75	43.87	126.54	1 406, 1 416, 1 422	122	36	Jilin Shěng
CHN	76	45.5	122.92	1 415	119	3	Jilin Shěng
CHN	77	45.34	121.59	1 409	119	3	Nei Mongol Zìzhìqu
CHN	78	33.27	108.34	1 418	118	18	Shaanxi Shěng
CHN	79	35.99	116.9	1 403, 1 418, 1 424	118	12	Shandong Shěng
CHN	80	24.36	117.34	1 403	117	7	Fujian Shěng
CHN	81	36.46	114.65	1 401-1 424	117	22	Hebei Shěng
CHN	82	42.21	116.45	1 409	117	34	Nei Mongol Zìzhìqu
CHN	83	28.66	121.26	1 401, 1 424	117	33	Zhejiang Shěng
CHN	84	25.08	116.1	1 402, 1 424	116	26	Fujian Shěng
CHN	85	28.25	119.76	1 406-1 410, 1 417-1 420	116	15	Zhejiang Shěng
CHN	86	34.9	119.05	1 401, 1 424	115	7	Jiangsu Shěng
CHN	87	44.86	126.04	1 410-1 413, 1 416-1 421	115	4	Jilin Shěng
CHN	88	36.71	117.99	1 402, 1 424	114	9	Shandong Shěng
CHN	89	26.95	119	1 406	111	13	Fujian Shěng
CHN	90	34.45	114.69	1 401, 1 407.5, 1 413.5, 1 421	109	22	Henan Shěng
CHN	91	49.27	120.62	1 401-1 403, 1 422-1 424	105	61	Nei Mongol Zìzhìqu
CHN	92	39.47	106.76	1 416	104	3	Nei Mongol Zìzhìqu
CHN	93	42.93	90.28	1 407-1 412	103	7	Xinjiang Uygur Zìzhìqu
CHN	94	40.11	114.13	1 401-1 424	101	12	Hebei Shěng

TABLE 2 (*continued*)

ID	Number	Latitude (degree)	Longitude (degree)	Centre frequency (MHz)	Average RFI, TA (K)	Number of observations 1-31 October 2016	Region
CHN	95	43.52	124.99	1 409	100	4	Jilin Shěng
CHN	96	42.7	126.04	1 411-1 418	98	13	Jilin Shěng
CHN	97	37.71	117.62	1 402-1 410	98	20	Shandong Shěng
CHN	98	31.33	120.34	1 411-1 414	96	7	Jiangsu Shěng
CHN	99	34.62	114.65	1 407.5, 1 413	95	3	Henan Shěng
CHN	100	32.75	116.79	1 407.5, 1 419, 1 422.5	94	3	Anhui Shěng
CHN	101	35.46	115.13	1 403-1 406	91	14	Henan Shěng
CHN	102	41.11	108.33	1 418	89	9	Nei Mongol Zìzhìqu
CHN	103	35.1	118.5	1 404, 1 410	89	4	Shandong Shěng
CHN	104	30.99	119.52	1 403	88	7	Anhui Shěng
CHN	105	29.04	100.29	1 416.5	88	31	Sichuan Shěng
CHN	106	31.02	117.86	1 404.5, 1 415, 1 421	87	4	Anhui Shěng
CHN	107	33.99	116.76	1 411-1 414, 1 416-1 418	85	4	Anhui Shěng
CHN	108	29.22	119.62	1 413	85	6	Zhejiang Shěng
CHN	109	26.57	106.69	1 407.5, 1 416.5	84	23	Guizhou Shěng
CHN	110	38.59	116.46	1 401	84	3	Hebei Shěng
CHN	111	45.56	126.56	1 416.5	83	8	Heilongjiang Shěng
CHN	112	36.62	101.77	1 412	83	6	Qinghai Shěng
CHN	113	30.53	108.2	1 413-1 415, 1 419.5	82	10	Chongqing Zhíxiáshì
CHN	114	25.86	114.92	1 404.5	82	9	Jiangxi Shěng
CHN	115	37.43	121.32	1 421	82	37	Shandong Shěng
CHN	116	39.34	106.63	1 414-1 419	81	8	Ningxia Hui Zìzhìqu
CHN	117	36.16	114.4	1 401, 1 424	80	12	Henan Shěng
CHN	118	42.3	118.85	1 422	80	20	Nei Mongol Zìzhìqu

TABLE 2 (*continued*)

ID	Number	Latitude (degree)	Longitude (degree)	Centre frequency (MHz)	Average RFI, TA (K)	Number of observations 1-31 October 2016	Region
CHN	119	41.55	110.03	1 412-1 414	79	7	Nei Mongol Zìzhìqu
CHN	120	44.42	121.9	1 405-1 409	79	4	Nei Mongol Zìzhìqu
CHN	121	22.79	115.36	1 401.5, 1 424	78	27	Guangdong Shěng
CHN	122	34.8	115.95	1 406	78	3	Shandong Shěng
CHN	123	42.53	128.34	1 415, 1 422	77	5	Jilin Shěng
CHN	124	48.29	126.55	1 422.5	76	22	Heilongjiang Shěng
CHN	125	34.72	112.16	1 401-1 403	76	38	Henan Shěng
CHN	126	27.98	108.03	1 410.5, 1 419.5	75	14	Guizhou Shěng
CHN	127	27.08	110.58	1 403	74	9	Hunan Shěng
CHN	128	45.18	124.83	1 404, 1 407	74	21	Jilin Shěng
CHN	129	35.47	106.88	1 406, 1 410.5, 1 422.5	72	12	Gansu Shěng
CHN	130	37.92	116.51	1 422	70	24	Hebei Shěng
CHN	131	35	118.3	1 404	70	3	Shandong Shěng
CHN	132	47.49	131.36	1 401-1 424	69	3	Heilongjiang Shěng
CHN	133	32.43	104.51	1 413, 1 418, 1 421	66	12	Sichuan Shěng
CHN	134	45.72	126.59	1 416.5	64	12	Heilongjiang Shěng
CHN	135	40.75	107.44	1 406-1 408	64	11	Nei Mongol Zìzhìqu
CHN	136	42.03	116.5	1 409, 1 421	64	4	Nei Mongol Zìzhìqu
CHN	137	32.79	106.3	1 406	64	5	Shaanxi Shěng
CHN	138	23.36	116.68	1 406, 1 412	62	23	Guangdong Shěng
CHN	139	44.66	123.78	1 413	62	3	Jilin Shěng
CHN	140	40.91	122.91	1 405	62	3	Liaoning Shěng
CHN	141	39.52	94.91	1 419.5	61	4	Gansu Shěng
CHN	142	43.63	121.09	1 403	61	25	Nei Mongol Zìzhìqu

TABLE 2 (*continued*)

ID	Number	Latitude (degree)	Longitude (degree)	Centre frequency (MHz)	Average RFI, TA (K)	Number of observations 1-31 October 2016	Region
CHN	143	22.96	104.23	1 421	61	41	Yunnan Shěng
CHN	144	44.39	121.08	1 407.5	60	30	Nei Mongol Zìzhìqu
CHN	145	43.98	120.83	1 422.5	60	3	Nei Mongol Zìzhìqu
CHN	146	23.71	116.1	1 401.5, 1 410.5	59	4	Guangdong Shěng
CHN	147	49.35	127.03	1 404.5, 1 410.5, 1 419.5	59	11	Heilongjiang Shěng
CHN	148	33.62	114.68	1 411-1 414	59	22	Henan Shěng
CHN	149	25.28	110.38	1 407.5, 1 416-1 420	58	20	Guangxi Zìzhìqu
CHN	150	46.57	125.17	1 401-1 424	58	7	Heilongjiang Shěng
CHN	151	45.74	122.66	1 415	58	3	Nei Mongol Zìzhìqu
CHN	152	49.21	128.45	1 413.5, 1 422.5	57	5	Heilongjiang Shěng
CHN	153	34.69	113.67	1 401, 1 410.5, 1 424	57	12	Henan Shěng
CHN	154	30.51	108.31	1 413-1 415, 1 419.5	56	6	Chongqing Zhíxiáshì
CHN	155	24.51	117.41	1 403	56	3	Fujian Shěng
CHN	156	23.76	115.92	1 409-1 415	56	12	Guangdong Shěng
CHN	157	45.4	126.76	1 404.5, 1 415	56	3	Heilongjiang Shěng
CHN	158	35.25	118.36	1 411	56	11	Shandong Shěng
CHN	159	35.45	118.48	1 403	56	3	Shandong Shěng
CHN	160	44.41	129.29	1 406, 1 419.5	55	3	Heilongjiang Shěng
CHN	161	47.57	131.23	1 401-1 424	55	4	Heilongjiang Shěng
CHN	162	32.84	114.98	1 413	55	6	Henan Shěng
CHN	163	43.98	116.12	1 410, 1 421	53	26	Nei Mongol Zìzhìqu
CHN	164	25.43	110.2	1 407.5, 1 418	52	4	Guangxi Zìzhìqu
CHN	165	27.77	113.01	1 424	51	3	Hunan Shěng
CHN	166	40.59	119.44	1 409, 1 413.5	51	13	Liaoning Shěng

TABLE 2 (*continued*)

ID	Number	Latitude (degree)	Longitude (degree)	Centre frequency (MHz)	Average RFI, TA (K)	Number of observations 1-31 October 2016	Region
CHN	167	42.79	90.34	1 407-1 412	51	3	Xinjiang Uygur Zìzhìqu
CHN	168	41.56	125.86	1 409	50	10	Jilin Shěng
CHN	169	31.06	116.94	1 416.5	49	10	Anhui Shěng
CHN	170	32.63	106.37	1 407, 1 412, 1 415	49	3	Sichuan Shěng
CHN	171	23.71	106.89	1 421	48	13	Guangxi Zìzhìqu
CHN	172	23.49	108.49	1 419.5	48	4	Guangxi Zìzhìqu
CHN	173	36.07	113.79	1 422.5	47	5	Henan Shěng
CHN	174	32.36	119.43	1 418	47	15	Jiangsu Shěng
CHN	175	39.75	118.33	1 413.5	46	8	Hebei Shěng
CHN	176	44.55	129.34	1 419.5	46	3	Heilongjiang Shěng
CHN	177	28.68	118.19	1 418	46	9	Jiangxi Shěng
CHN	178	50.25	120.03	1 409	46	3	Nei Mongol Zìzhìqu
CHN	179	22.68	110.29	1 410.5, 1 419.5	44	24	Guangxi Zìzhìqu
CHN	180	29	117.17	1 413.5	44	8	Jiangxi Shěng
CHN	181	40.81	111.73	1 422	44	40	Nei Mongol Zìzhìqu
CHN	182	22.33	106.79	1 421	42	22	Guangxi Zìzhìqu
CHN	183	46.8	130.34	1 401	42	4	Heilongjiang Shěng
CHN	184	33.85	113.26	1 403, 1 413	42	6	Henan Shěng
CHN	185	23.5	100.71	1 406	42	20	Yunnan Shěng
CHN	186	21.97	100.75	1 406	42	4	Yunnan Shěng
CHN	187	29.75	112.33	1 402	41	4	Hubei Shěng
CHN	188	35.73	118.75	1 406	41	4	Shandong Shěng
CHN	189	21.6	109.63	1 407.5	40	3	Guangxi Zìzhìqu
CHN	190	32.85	112.52	1 403, 1 410, 1 424	40	3	Henan Shěng

TABLE 2 (*continued*)

ID	Number	Latitude (degree)	Longitude (degree)	Centre frequency (MHz)	Average RFI, TA (K)	Number of observations 1-31 October 2016	Region
CHN	191	27.67	113.82	1 416.5	40	8	Jiangxi Shěng
CHN	192	37.94	102.61	1 403	37	3	Gansu Shěng
CHN	193	23.57	106.75	1 421	37	3	Guangxi Zìzhìqu
CHN	194	35.09	117.73	1 404.5	37	3	Shandong Shěng
CHN	195	32.14	112.14	1 422.5	36	31	Hubei Shěng
CHN	196	42.29	118.56	1 422.5	36	3	Nei Mongol Zìzhìqu
CHN	197	43.81	87.55	1 409	36	12	Xinjiang Uygur Zìzhìqu
CHN	198	28.85	92.13	1 424	36	4	Xizang Zìzhìqu
CHN	199	37.6	114.95	1 418	35	3	Hebei Shěng
CHN	200	35.88	115.31	1 404.5	35	9	Henan Shěng
CHN	201	40.02	113.03	1 404.5, 1 412	35	3	Shanxi Shěng
CHN	202	25.18	110.6	1 419	34	3	Guangxi Zìzhìqu
CHN	203	33.32	120.13	1 406	34	5	Jiangsu Shěng
CHN	204	37.37	122.19	1 422	34	4	Shandong Shěng
CHN	205	22.41	110.2	1 422	33	14	Guangxi Zìzhìqu
CHN	206	33.3	113.86	1 412	32	4	Henan Shěng
CHN	207	31.12	113.31	1 404.5	32	3	Hubei Shěng
CHN	208	27.96	113.15	1 401, 1 416, 1 424	32	3	Hunan Shěng
CHN	209	35.18	117.88	1 404	31	3	Shandong Shěng
CHN	210	25.37	110.05	1 407.5, 1 419	30	4	Guangxi Zìzhìqu
CHN	211	27.48	121.08	1 406	30	11	Zhejiang Shěng
CHN	212	33.94	113.07	1 402.5, 1 413	29	4	Henan Shěng
CHN	213	33.97	118.18	1 407	29	6	Jiangsu Shěng
CHN	214	40.2	122.1	1 404.5	29	14	Liaoning Shěng

TABLE 2 (*continued*)

ID	Number	Latitude (degree)	Longitude (degree)	Centre frequency (MHz)	Average RFI, TA (K)	Number of observations 1-31 October 2016	Region
CHN	215	43.26	117.03	1 421	29	5	Nei Mongol Zìzhìqu
CHN	216	22.97	107.02	1 416.5	28	3	Guangxi Zìzhìqu
CHN	217	34.77	116.35	1 403	28	5	Shandong Shěng
CHN	218	36.62	109.46	1 413.5	27	3	Shaanxi Shěng
CHN	219	26.15	99.99	1 404, 1 412	27	11	Yunnan Shěng
CHN	220	42.05	127.12	1 415	26	7	Jilin Shěng
CHN	221	36.83	119.48	1 410-1 412	26	4	Shandong Shěng
CHN	222	40.09	118.74	1 401-1 424	25	4	Hebei Shěng
CHN	223	30.24	108.96	1 404.5, 1 412	25	8	Hubei Shěng
CHN	224	34.27	119.39	1 411	25	3	Jiangsu Shěng
CHN	225	36.8	120.4	1 406	25	3	Shandong Shěng
CHN	226	34.09	119.56	1 415	24	3	Jiangsu Shěng
CHN	227	42.04	121.62	1 415	24	4	Liaoning Shěng
CHN	228	24.98	111.35	1 421	23	5	Guangxi Zìzhìqu
CHN	229	48.01	86.4	1 406	23	6	Xinjiang Uygur Zìzhìqu
CHN	230	30.66	112.39	1 402	22	5	Hubei Shěng
CHN	231	23.43	102.44	1 404, 1 412	22	9	Yunnan Shěng
CHN	232	23.2	108.26	1 421	21	6	Guangxi Zìzhìqu
CHN	233	23.85	111.49	1 418	21	3	Guangxi Zìzhìqu
CHN	234	24.33	111.66	1 412, 1 420	20	4	Guangxi Zìzhìqu
CHN	235	26.68	112.71	1 401	19	3	Hunan Shěng
CHN	236	40.07	113.25	1 404.5, 1 412	19	5	Shanxi Shěng
CHN	237	25.21	111.61	1 421	18	3	Hunan Shěng
CHN	238	32.85	115.18	1 412	17	3	Henan Shěng

TABLE 2 (*end*)

ID	Number	Latitude (degree)	Longitude (degree)	Centre frequency (MHz)	Average RFI, TA (K)	Number of observations 1-31 October 2016	Region
CHN	239	23.36	108.41	1 415, 1 421	16	3	Guangxi Zìzhìqu
CHN	240	39.85	108.71	1 412, 1 418-1 420	16	3	Nei Mongol Zìzhìqu

6.7.2.2 Supporting information on detailed information of RFI over China as observed in October 2016

Figure 18 provides a map on a 0.25° × 0.25° grid of the percentage of observations over the period 1-31 October 2016 that obtained a detected RFI level of 5K or more in vertical polarization. Points having values greater than approximately 25-30% (i.e. light blue to red) are persistent sources of interference during this period. This ‘frequency’ plot does not distinguish between large amplitude and small amplitude, but rather highlights the temporal persistence of specific sources.

In contrast, Fig. 19 provides a ‘peak hold’ (i.e. the maximum value observed) map on a 0.25° × 0.25° grid for the period 1 to 7 October 2016 of horizontally polarized brightness temperatures. This map emphasizes large RFI contributions since geophysical contributions to the brightness background are also included. Again, a large number of RFI sources were observed.

Finally, Fig. 20 provides a summary plot of the information in Table 2 and is colour coded by the amplitude of the observed RFI during the October 2016 time period. A general correspondence between the source locations and the obvious interference locations in Figs 18 and 19 was observed.

FIGURE 18

Percentage of the time that SMAP detected an RFI level of 5 K or more in the horizontal polarization for data from 1-31 October 2016 over China

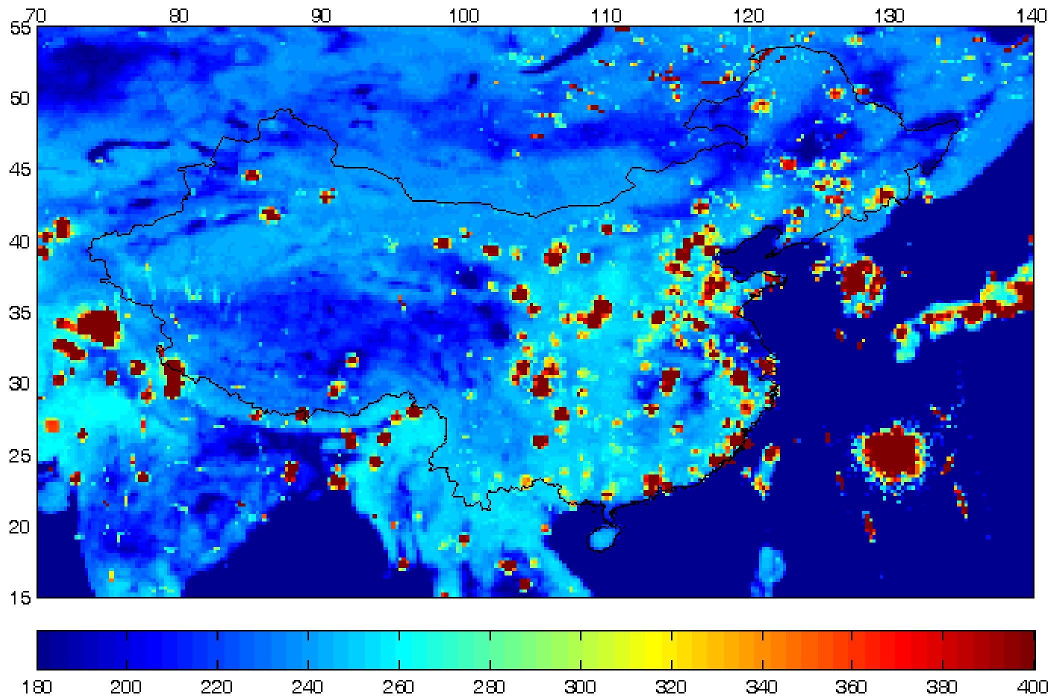

Note to Fig. 18: Vertical polarization exhibited similar results. Data shown on a 0.25° × 0.25° grid.

FIGURE 19

Peak hold data over China on a 0.25° × 0.25° grid of horizontally polarized TAs in kelvin before RFI filtering for the period 1 October 2016 to 7 October 2016

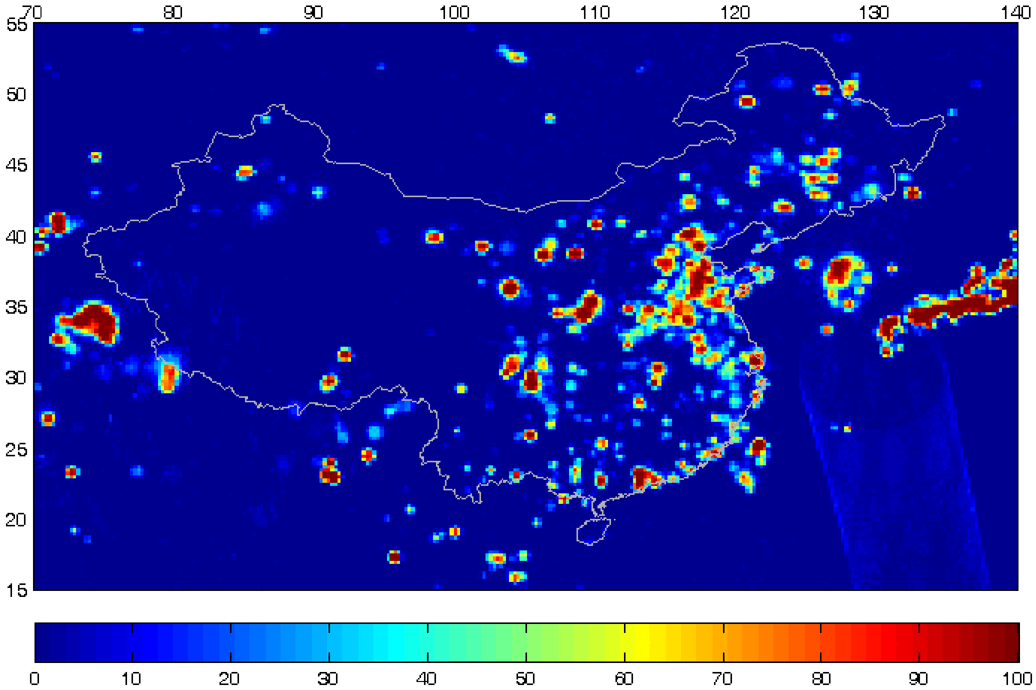

FIGURE 20

Location and intensity of RFI sources over China. Colours indicate range of RFI levels in kelvin (1-31 October 2016)

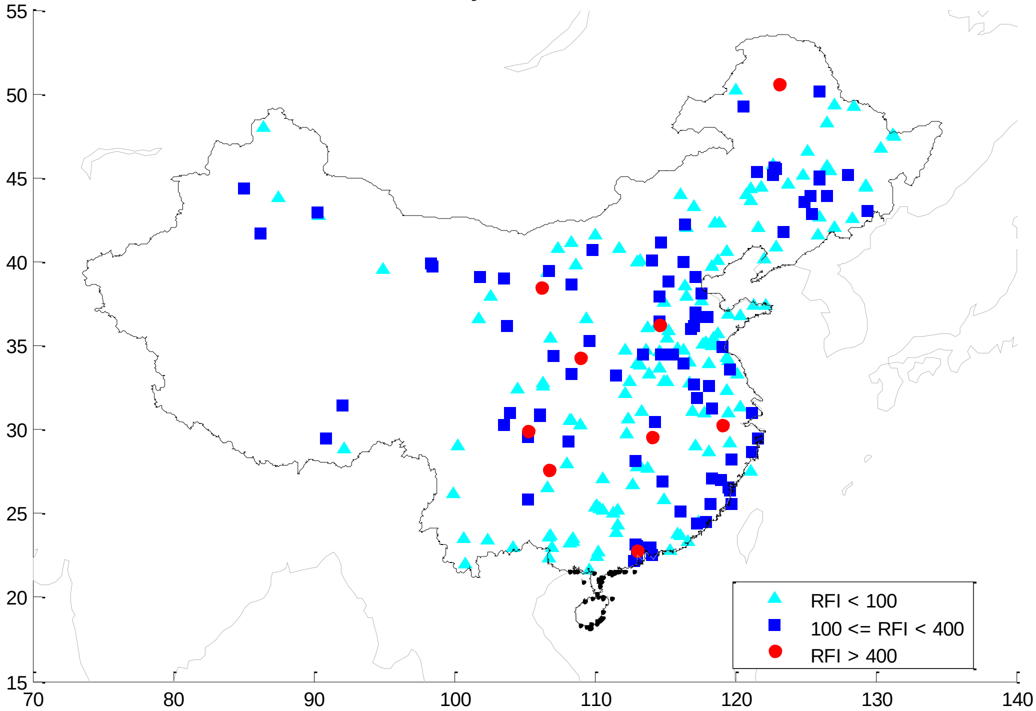

6.7.2.3 Classification of RFI sources in China per intensity (1-31 October 2016)

A general summary of the prevalence of moderate, strong, and very strong sources in China is summarized from Table 2 as follows:

Very strong RFI (RFI level > 400 K)	9 RFI sources (4%)
Strong RFI (100 K ≤ RFI level < 400 K)	86 RFI sources (36%)
Moderate RFI (RFI level < 100 K)	145 RFI sources (60%)

It is noted that the SMAP radiometer is capable of detecting additional RFI sources at amplitudes less than 15 K.

6.7.3 Report of observed RFI over United States of America over a 14-month timeframe from 1 January 2017 to 4 March 2018

6.7.3.1 Summary of the RFI sources

Table 3 defines the fields in the Summary of RFI sources form, that was completed by the United States of America when it reported an RFI event.

TABLE 3

Summary of RFI sources

Date of this RFI status update	1 January 2017 to 4 March 2018
Total number of RFI cases detected	23
Active RFI sources	23 reported
** **Old RFI active sources**	N/A
** **New RFI active sources**	23 reported, see Table 4 for RFI level and geolocation details
RFI sources OFF	N/A

6.7.3.2 Geolocation and other detailed RFI information

Table 4 includes the following detailed information for the RFI source: latitude and longitude, centre frequency, average RFI level in kelvin, number of observations used to geolocate the source and determine RFI level and the region where the source is located as well as the time the source was last seen as of this writing. There were 23 sources identified over the United States including Alaska and Hawaii. Data from 1 January 2018 to 4 March 2018 was used to create Table 4 as well as supporting Figures.

The localization of RFI sources was based on the difference between SMAP measurements before and after RFI filtering. This difference corresponds to the effect that RFI has on the data. A machine learning algorithm was then applied to automatically find the points where the effect of RFI was the highest (local maxima). These points defined the location of RFI sources. Since every RFI source was observed multiple times during the course of the reporting period, the coordinates and RFI level provided in this report are the result of an average of the individual observations from 1 January 2018 to 4 March 2018. SMAP science telemetry includes frequency information thus the RFI centre frequency was also identified for the RFI sources. A range was given if there appeared to be an observable bandwidth in the spectrum for the RFI source. Multiple centre frequencies were given if there were multiple peaks across the 16 sub-bands that were obviously RFI (TA > 330 K).

TABLE 4

Interference source detail log
Number of active sources listed: [23]

Source ID	Observed geolocation		Centre frequency (MHz)	Source detection characteristics	Level of interference detected by sensor (K)	Received power or (dBm or watts)	City/ State/ Region	Number of observations	Last seen (UTC)	Present status (status as per 04/03/2018)
	Longitude (degrees)	Latitude (degrees)								
USA-1	−87.8	41.51	1 406		298		Chicago, IL	119	4/03/2018 23:29	ON
USA-2	−93.52	37.03	1 400, 1 424		133		Springfield, MO	64	4/03/2018 12:27	ON
USA-3	−76.66	39.93	1 402		115		York, PA	28	3/03/2018 22:51	ON
USA-4	−159.65	22.16	1 400-1 410		82		Kokee AFS	49	3/03/2018 4:43	ON
USA-5	−153.68	66.09	1 400-1 424		72		Indian Mountain AFS	104	4/03/2018 17:14	ON
USA-6	−84.3	42.75	1 402		65		Lansing, MI	44	4/03/2018 23:27	ON
USA-7	−162.02	58.7	1 400-1 424		56		Cape Newenham AFS	14	27/02/2018 17:29	ON
USA-8	−156.04	62.92	1 400-1 406		55		Tatalina AFS	85	4/03/2018 17:15	ON
USA-9	−88.04	44.52	1 402		53		Green Bay, WI	38	4/03/2018 23:29	ON
USA-10	−122.58	44.81	1 409		52		Salem, OR	58	3/03/2018 15:02	ON
USA-11	−162.81	55.26	1 400-1 424		43		COB M station	30	4/03/2018 17:15	ON

TABLE 4 (*end*)

Source ID	Observed geolocation		Centre frequency (MHz)	Source detection characteristics	Level of interference detected by sensor (K)	Received power or (dBm or watts)	City/ State/ Region	Number of observations	Last seen (UTC)	Present status (status as per 04/03/2018)
	Longitude (degrees)	Latitude (degrees)								
USA-12	−167.89	65.62	1 400-1 424		43		Tin City AFS	10	27/02/2018 19:04	ON
USA-13	−76.65	37.22	1 409		42		Williamsburg, VA	52	3/03/2018 22:48	ON
USA-14	−156.62	58.68	1 400, 1 424		41		King Salmon AFS	28	1/03/2018 17:02	ON
USA-15	−82.29	41.39	1 423		40		Amherst, OH	38	3/03/2018 22:49	ON
USA-16	−166.14	68.87	1 400-1 424		40		LIZ-1 station	24	4/03/2018 18:49	ON
USA-17	−162.62	66.86	1 420		38		Kotzebue AFS	37	4/03/2018 3:52	ON
USA-18	−82.31	36.57	1 400-1 407		38		Bristol, TN	16	3/03/2018 11:48	ON
USA-19	−79.39	36.6	1 422		37		Danville, VA	26	3/03/2018 22:50	ON
USA-20	−81.93	26.53	1 423		34		Cape Coral, FL	22	4/03/2018 23:24	ON
USA-21	−77.19	40.8	1 418		32		Sunbury, PA	22	3/03/2018 11:49	ON
USA-22	−92.73	45.03	1 411		27		Minneapolis, MN	52	4/03/2018 12:23	ON
USA-23	−89.56	44.1	1 409, 1 414		25		Coloma, WI	41	4/03/2018 12:23	ON

6.7.3.3 Supporting information

Figure 21 shows the peak hold data over the United States on a 0.25° × 0.25° grid of horizontally polarized TAs in kelvin before RFI filtering. Figure 24 shows the map of observed RFI on a 0.25° × 0.25° grid of the percentage of observations. Figure 25 shows the location and intensity of RFI sources over the US.

FIGURE 21

Peak hold data over the United States on a 0.25° × 0.25° grid of horizontally polarized TAs in kelvin before RFI filtering for the week of 21/02/2018 to 27/02/2018

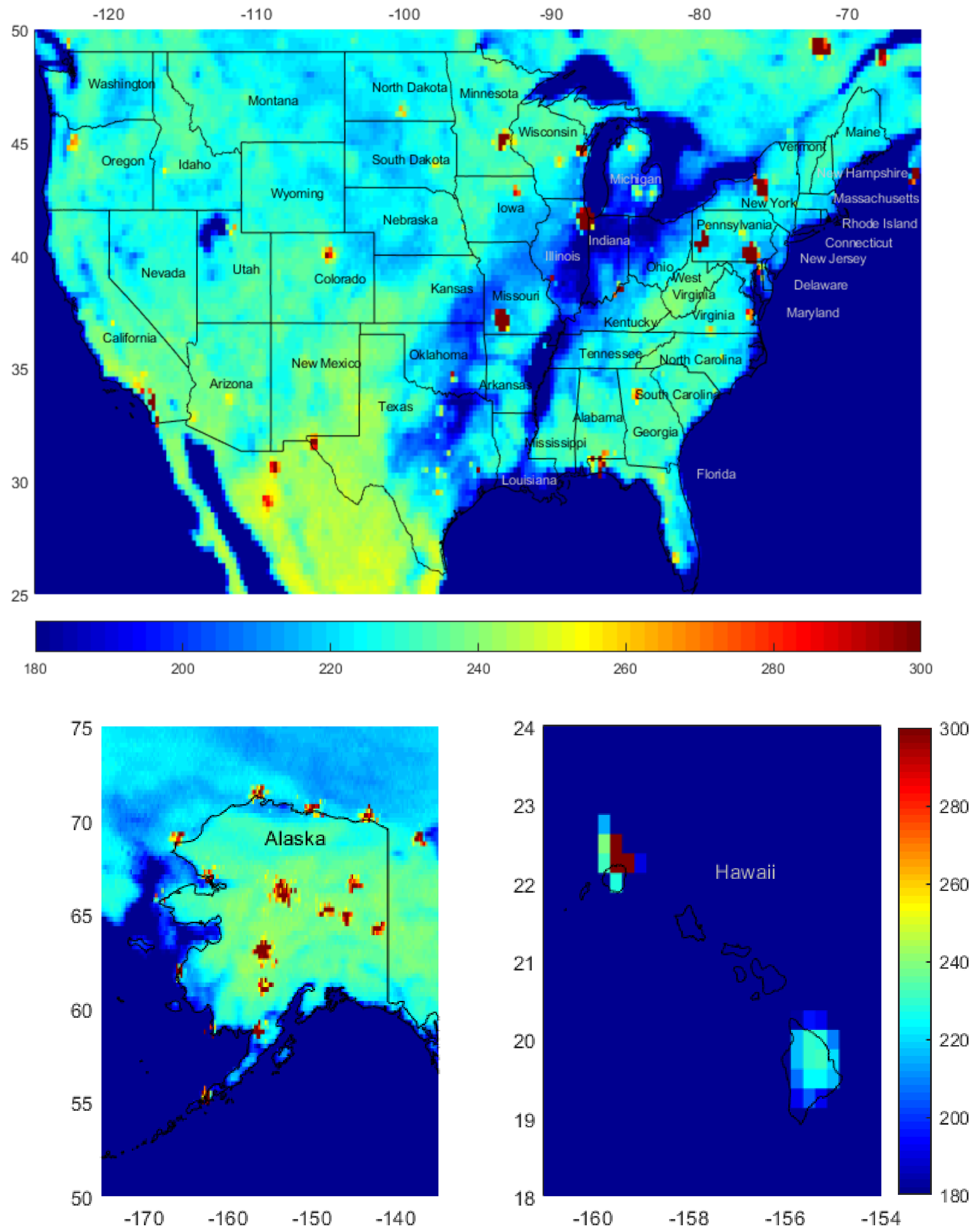

Note to Fig. 21: Similar results are seen in vertical polarization. A ‘peak hold”\’ plot (i.e. the maximum value observed) emphasized large RFI contributions since geophysical contributions to the brightness background are also included. Anything greater than 330 K was considered to be RFI.

FIGURE 22

Map on a 0.25° × 0.25° grid of the percentage of observations over the period January 2018 and February 2018 that obtained a detected RFI level of 5K or more in the horizontal polarization

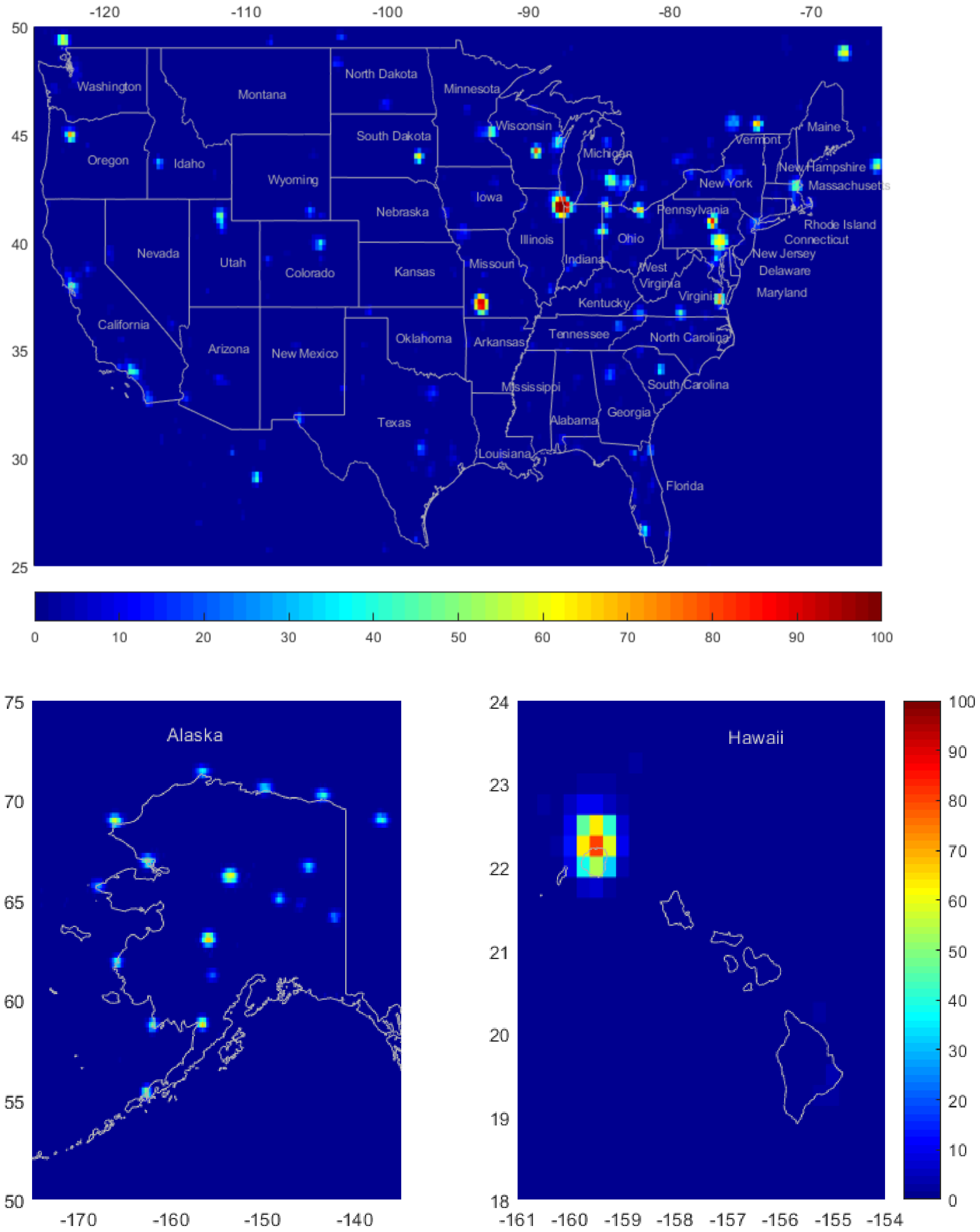

Note to Fig. 22: Vertical polarization shows similar results. Points having values greater than approximately 25-30% (i.e. light blue to red) were persistent sources of interference during this period. This plot did not distinguish between large amplitude and small amplitude, but rather highlighted the temporal persistence of specific sources.

FIGURE 23

Location and intensity of RFI sources over the US

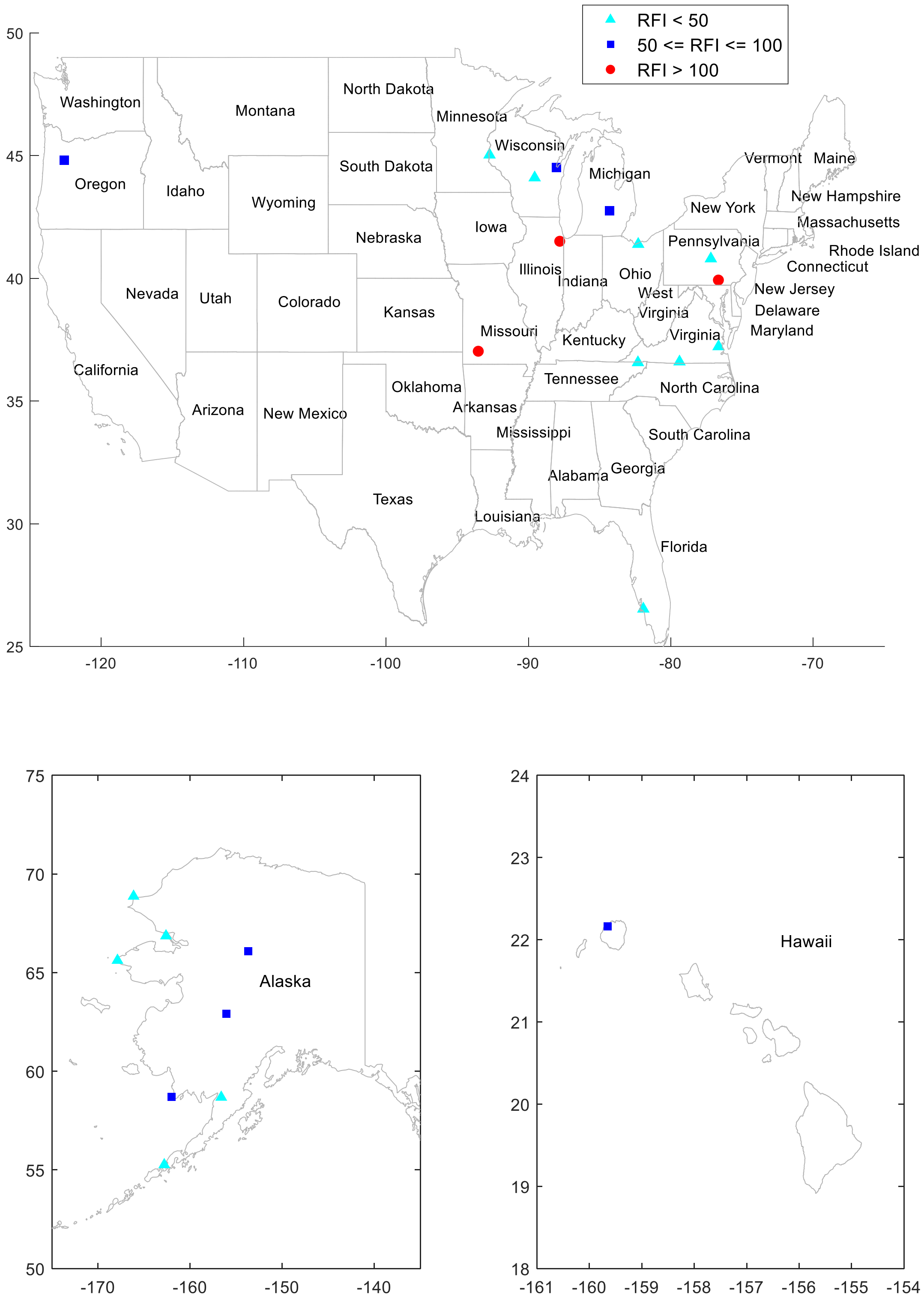

Note to Fig. 23: Colours indicate range of RFI levels in kelvin These locations could be easily seen in the probability map. The strong and very strong sources were also easily seen in the peak hold map. Some of the moderate level RFI sources were more difficult to identify on the peak hold map since the peak hold map also included geophysical contributions.

6.7.3.4 Classification of RFIs over the USA per intensity (status as per 04/03/2018)

A general summary of the prevalence of moderate, strong, and very strong sources over the US is summarized from Table 4 as follows:

Very strong RFI (RFI level > 100 K) 3 RFI sources

Strong RFI (50 K ≤ RFI level < 100 K) 7 RFI sources

Moderate RFI (RFI level < 50 K) 13 RFI sources

6.7.4 Report of observed RFI over The Netherlands over a 13-month timeframe from 1 January 2017 to 14 February 2018

6.7.4.1 Summary of the RFI sources over The Netherlands

Table 5 defines the fields in the Summary of RFI sources form that was completed by the USA when it reported an RFI event over The Netherlands.

TABLE 5

Summary of RFI sources

Date of this RFI status update	1 November 2017 to 14 February 2018
Total number of RFI cases detected	1
Active RFI sources	1 reported
** **Old RFI active sources**	N/A
** **New RFI active sources**	1 reported, see Table 6 for RFI level and geolocation details
RFI sources OFF	N/A

6.7.4.2 Geolocation and other detailed RFI information

Table 6 includes the following detailed information for the RFI source: latitude and longitude, centre frequency, average RFI level in kelvin, number of observations used to geolocate the source and determine RFI level and the region where the source is located. There was only one source identified over The Netherlands. Data from 1 November 2017 to 14 February 2018 was used to create Table 6 as well as supporting Figures.

The localization of RFI sources was based on the difference between SMAP measurements before and after RFI filtering. This difference corresponded to the effect that RFI had on the data. A machine learning algorithm was then applied to automatically find the points where the effect of RFI was highest (local maxima). These points defined the location of RFI sources. Since every RFI source was observed multiple times during the course of the reporting period, the coordinates and RFI level provided in this report are the result of an average of the individual observations from 1 November 2017 to 14 February 2018. SMAP science telemetry includes frequency information thus the RFI centre frequency was also identified for the RFI sources. A range was given if there appeared to be an observable bandwidth in the spectrum for the RFI source. Multiple centre frequencies were given if there were multiple peaks across the 16 sub-bands that were obviously RFI (TA > 330 K).

TABLE 6

Interference source detail log
Number of active sources listed: [1]

Source ID.	Observed geolocation		Centre frequency (MHz)	Source detection characteristics	Level of interference detected by sensor (K)	Received power or (dBm or watts)	City/ State/ Region	Number of observations	Last seen (UTC)	Present status (status as per 14/02/2018)
	Longitude (degrees)	Latitude (degrees)								
NLD-1	5.29	51.75	1 404		140		`s-Hertogenbosch	153		ON

6.7.4.3 Supporting information

Figure 24 provides a map on a 0.25° × 0.25° grid of the percentage of observations over the period 1-31 January 2018 that obtained a detected RFI level of 5K or more in vertical polarization. Points having values greater than approximately 25-30% (i.e. light blue to red) are persistent sources of interference during this period. This plot does not distinguish between large amplitude and small amplitude, but rather highlights the temporal persistence of specific sources.

In contrast, Fig. 25 provides a 'peak hold' (i.e. the maximum value observed) map on a 0.25° × 0.25° grid for the period 7 February 2018 to 13 February 2018 of horizontally polarized brightness temperatures. This map emphasizes large RFI contributions since geophysical contributions to the brightness background are also included.

FIGURE 24

Percentage of the time that SMAP detects an RFI level of 5 K or more in horizontal polarization for data from 1 to 31 January 2018 over The Netherlands. Vertical polarization exhibits similar results. Data shown on a 0.25° × 0.25° grid

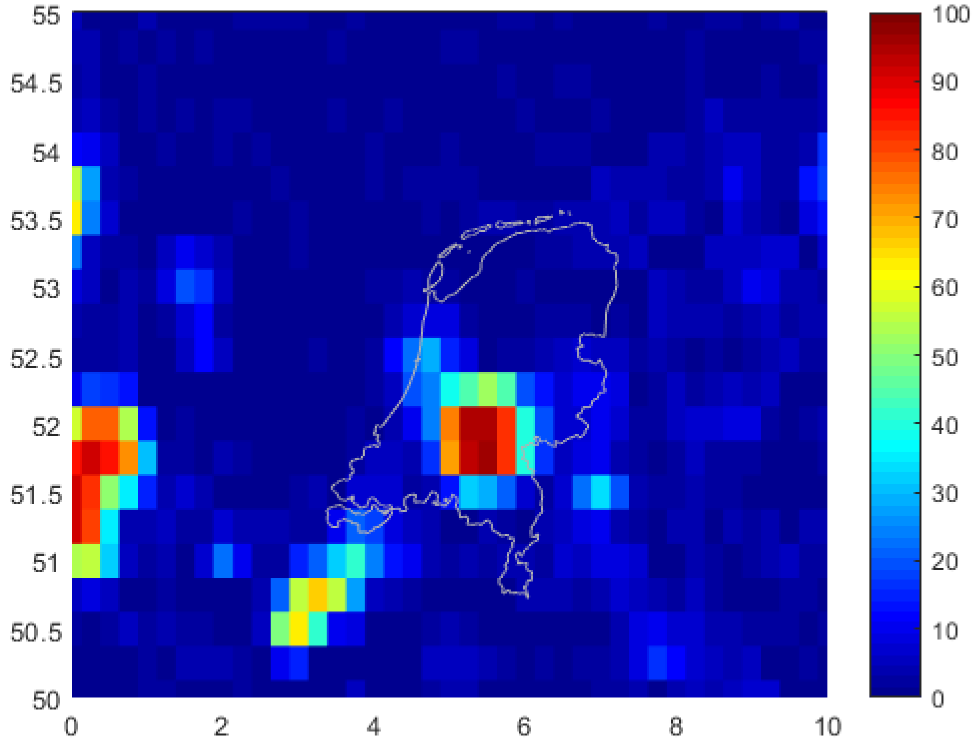

FIGURE 25

Peak hold data over The Netherlands on a 0.25° × 0.25° grid of horizontally polarized TAs in kelvin before RFI filtering for the period 07/02/2018 to 13/02/2018

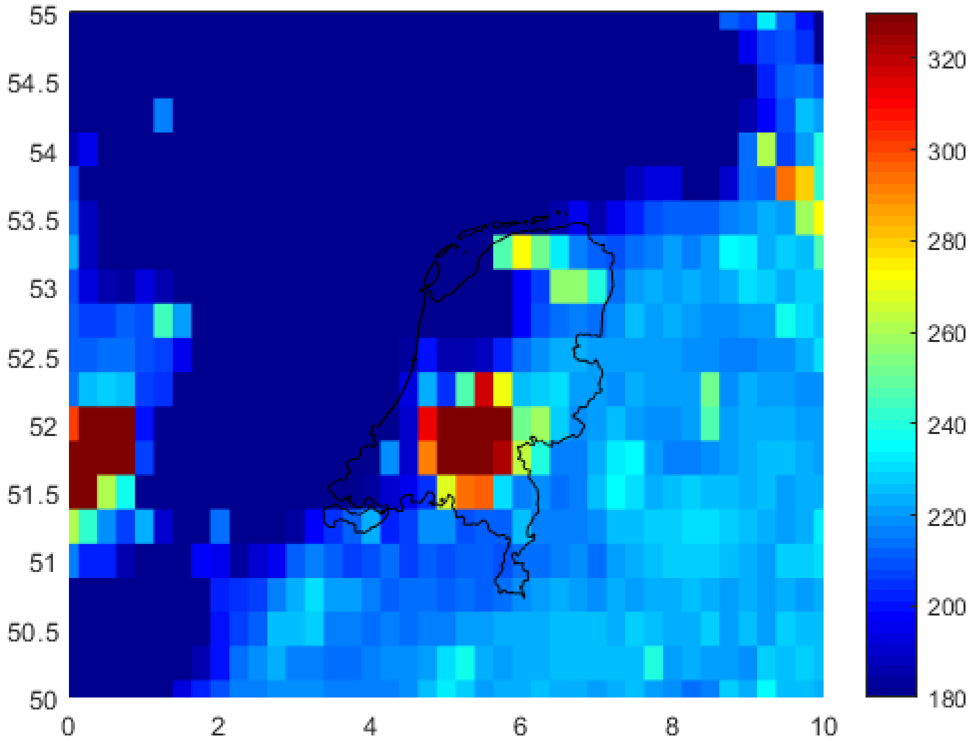

6.7.5 Report of observed RFI over Brazil over a three-month timeframe from 9 April 2018 to 12 July 2018

6.7.5.1 Summary of the RFI sources

Table 7 defined the fields in the Summary of RFI Sources form that was completed by the USA when it reported the RFI events over Brazil.

TABLE 7

Summary of RFI sources

Date of this RFI status update	9 April 2018 to 12 July 2018
Total number of RFI cases detected	21
Active RFI sources	21 reported
** **Old RFI active sources**	N/A
** **New RFI active sources**	21 reported, see Table 8 for RFI level and geolocation details
RFI sources OFF	N/A

6.7.5.2 Geolocation and other detailed RFI information

Table 8 includes the following detailed information for the RFI source: latitude and longitude, centre frequency, average RFI level in kelvin, number of observations used to geolocate the source and determine RFI level and the region where the source was located as well as the time the source was last seen as of this writing. There were 21 sources identified over Brazil. Data from 9 April 2018 to 12 July 2018 was used to create Table 8 as well as supporting Figures.

The localization of RFI sources was based on the difference between SMAP measurements before and after RFI filtering. This difference corresponds to the effect that RFI has on the data. A machine learning algorithm was then applied to automatically find the points where the effect of RFI is highest (local maxima). These points defined the location of RFI sources. Since every RFI source was observed multiple times during the course of the reporting period, the coordinates and RFI level provided in this report are the result of an average of the individual observations from 9 April 2018 to 12 July 2018. SMAP science telemetry includes frequency information thus the RFI centre frequency was also identified for the RFI sources. A range was given if there appeared to be an observable bandwidth in the spectrum for the RFI source. Multiple centre frequencies were given if there were multiple peaks across the 16 sub-bands that were obviously RFI (TA > 330 K).

TABLE 8

Interference source detail log
Number of active sources listed: [21]

Source ID	Observed geolocation		Centre frequency (MHz)	Source detection characteristics	Level of interference detected by sensor (K)	Received power or (dBm or watts)	City/ State/ Region	Number of observations	Last seen (UTC)	Present status (status as per 12/07/2018)
	Longitude (degrees)	Latitude (degrees)								
BRA-1	−53.98	−28.54	1 412		216			99	12/07/2018 9:02	ON
BRA-2	−49.28	−25.44	1 412		153			133	12/07/2018 9:01	ON
BRA-3	−46.57	−23.64	1 400, 1 424		118			83	12/07/2018 9:01	ON
BRA-4	−34.92	−8.1	1 417		178			28	11/07/2018 8:19	ON
BRA-5	−46.99	−18.9	1 404, 1 424		341			94	12/07/2018 8:59	ON
BRA-6	−39.31	−5.21	1 415		134			102	28/06/2018 8:36	ON
BRA-7	−43.34	−21.82	1 400		82			110	29/06/2018 9:11	ON
BRA-8	−48.51	−22.85	1 416		55			10	4/03/2018 17:15	ON
BRA-9	−44.9	−20.16	1 409, 1 414		28			71	12/07/2018 8:59	ON
BRA-10	−47.91	−22.08	1 412, 1 416		21			58	9/07/2018 8:46	ON
BRA-11	−39.9	−6.53	1 417		18			51	11/07/2018 20:34	ON
BRA-12	−39.01	−7.46	1 409, 1 414		22			36	11/07/2018 8:19	ON

TABLE 8 (*end*)

Source ID	**Observed geolocation**		**Centre frequency (MHz)**	**Source detection characteristics**	**Level of interference detected by sensor (K)**	**Received power or (dBm or watts)**	**City/ State/ Region**	**Number of observations**	**Last seen (UTC)**	**Present status (status as per 12/07/2018)**
	Longitude (degrees)	**Latitude (degrees)**								
BRA-13	−35.19	−8.8	1 412, 1 417		32			35	11/07/2018 20:33	ON
BRA-14	−42.49	−18.81	1 412, 1 417, 1 422		41			46	1/07/2018 8:45	ON
BRA-15	−49.35	−23.48	1 408		29			17	10/07/2018 21:31	ON
BRA-16	−49.22	−21.46	1 412, 1 417		24			19	10/07/2018 21:29	ON
BRA-17	−44.49	−23.02	1 423		30			24	12/07/2018 9:00	ON
BRA-18	−53.34	−22.24	1 423		47			17	7/07/2018 9:11	ON
BRA-19	−46.73	−22.24	1 410, 1 417		19			23	12/07/2018 9:00	ON
BRA-20	−46.44	−22.04	1 422		20			17	12/07/2018 9:00	ON
BRA-21	−43.2	−22.88	1 406, 1 423		26			49	11/07/2018 8:23	ON

6.7.5.3 Supporting information

Figure 26 shows the peak hold data over Brazil on a 0.25° × 0.25° grid of horizontally polarized TAs in kelvin before RFI filtering. Figure 27 shows a map on a 0.25° × 0.25° grid of the percentage of observations that obtained a detected RFI level of 5K or more in the horizontal polarization. Figure 28 shows the location and intensity of RFI sources over Brazil.

FIGURE 26

Peak hold data over Brazil on a 0.25° × 0.25° grid of horizontally polarized TAs in kelvin before RFI filtering for the week of 04/07/2018 to 10/07/2018

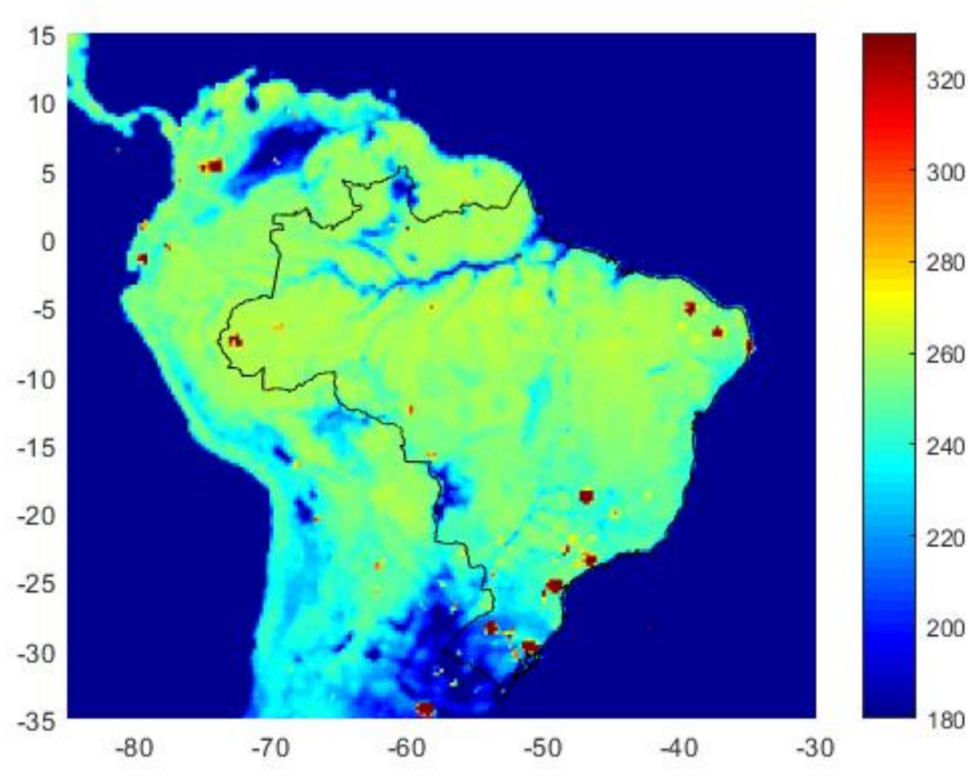

Note to Fig. 26: Similar results were seen in the vertical polarization. A 'peak hold' plot (i.e. the maximum value observed) emphasized large RFI contributions since geophysical contributions to the brightness background were also included. The colour scale is limited to 180 to 330 K. Footprints 180 K and under appear dark blue and those 330 K and above are dark red. Anything greater than 330 K is automatically flagged as RFI since this is the geophysical limit for measurements.

FIGURE 27

Map on a 0.25° × 0.25° grid of the percentage of observations over the period April to June 2018 that obtained a detected RFI level of 5K or more in the horizontal polarization

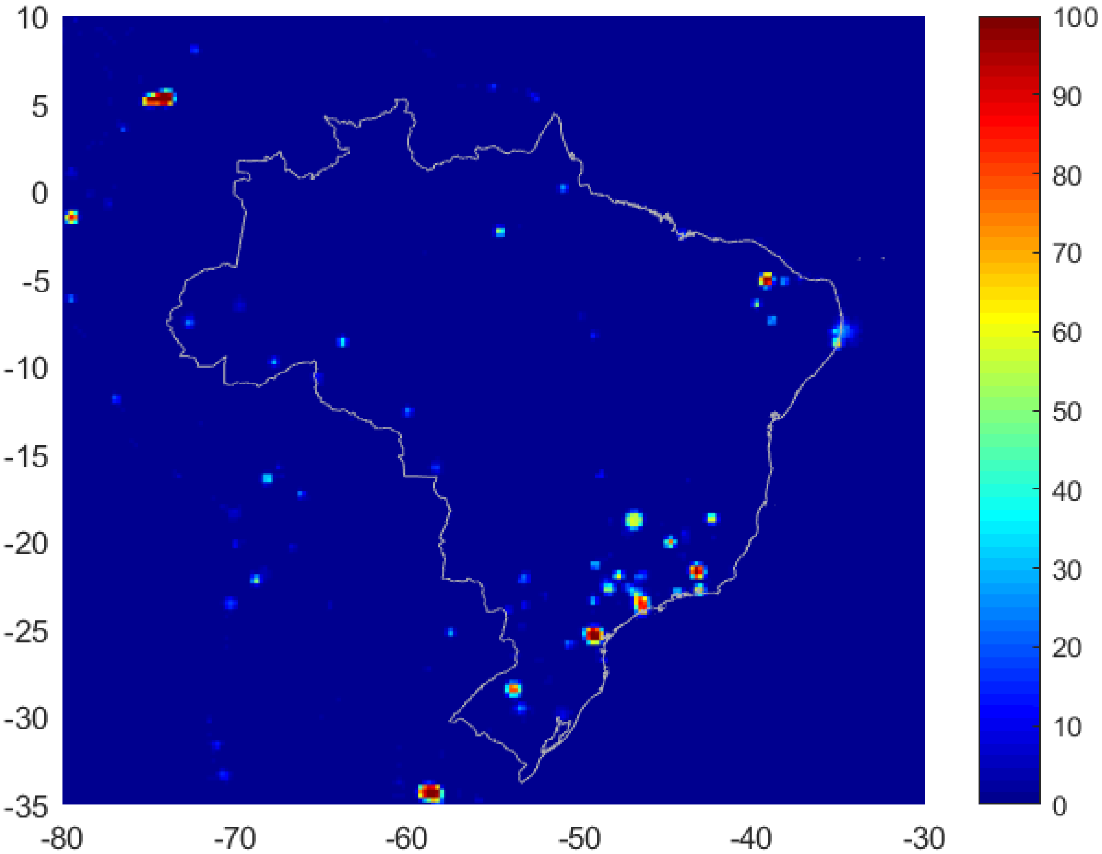

Note to Fig. 27: Vertical polarization showed similar results. Points having values greater than approximately 25-30% (i.e. light blue to red) were persistent sources of interference during this period. This plot does not distinguish between large amplitude and small amplitude, but rather highlights the temporal persistence of specific sources.

FIGURE 28

Location and intensity of RFI sources over Brazil

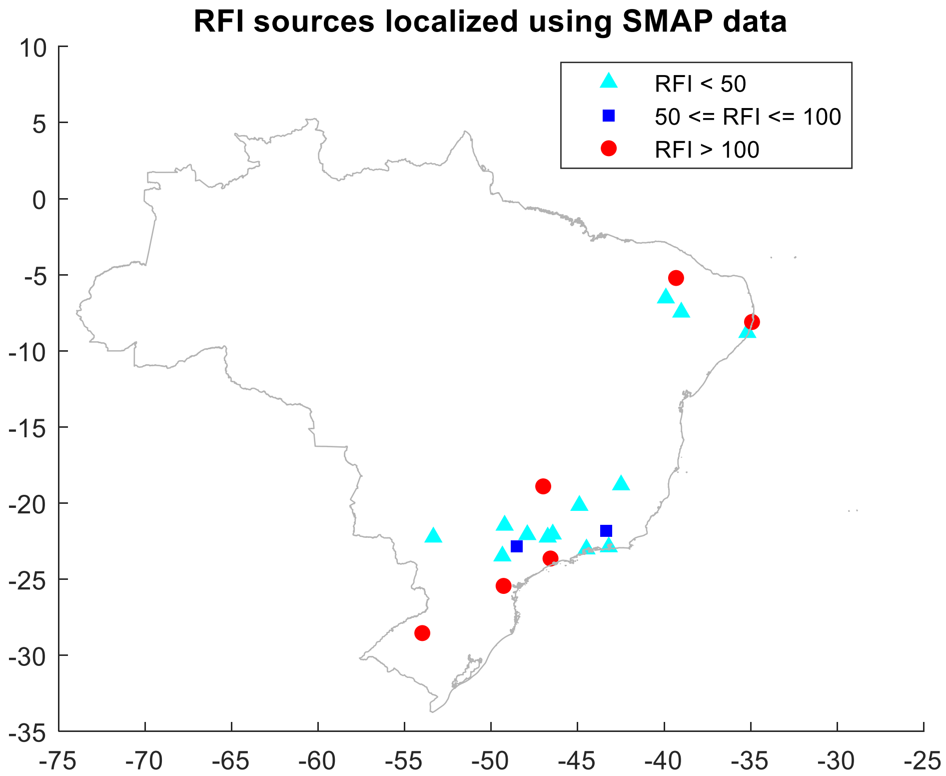

Note to Fig. 28: Colours indicate range of RFI levels in kelvin. These locations can be easily seen in the probability map. The strong and very strong sources are also easily seen in the peak hold map. Some of the moderate level RFI sources are a more difficult to identify on the peak hold map since the peak hold map also includes geophysical contributions.

6.7.5.4 Classification of RFIs over Brazil per intensity (status as of 12/07/2018)

A general summary of the prevalence of moderate, strong, and very strong sources over the US is summarized from Table 8 as follows:

Very strong RFI (RFI level > 100 K)	6 RFI sources
Strong RFI (50 K ≤ RFI level < 100 K)	2 RFI sources
Moderate RFI (RFI level < 50 K)	13 RFI sources

6.7.6 Report of observed RFI over Russia over a three-month timeframe from 18 June 2018 to 17 September 2018

6.7.6.1 Summary of the RFI sources over Russia

Table 9 defines the fields in the Summary of RFI sources form that should be completed by the administration reporting an RFI event.

TABLE 9

Summary of RFI sources

Date of this RFI status update	18 June 2018 to 17 September 2018
Total number of RFI cases detected	44
Active RFI sources	44 reported
**** Old RFI active sources**	N/A
**** New RFI active sources**	44 reported, see Table 10 for RFI level and geolocation details
RFI sources OFF	N/A

6.7.6.2 Geolocation and other detailed RFI information

Table 10 includes the following detailed information for the RFI source: latitude and longitude, centre frequency, average RFI level in kelvin, number of observations used to geolocate the source and determine RFI level where the source was located as well as the time the source was last seen as of this writing. There were 44 sources identified over the Russian Federation. Data from 18 June 2018 to 17 September 2018 was used to create Table 10 as well as supporting Figures.

The localization of RFI sources was based on the difference between SMAP measurements before and after RFI filtering. This difference corresponds to the effect that RFI has on the data. A machine learning algorithm was then applied to automatically find the points where the effect of RFI is highest (local maxima). These points define the location of RFI sources. Since every RFI source was observed multiple times during the course of the reporting period, the coordinates and RFI level provided in this Report were the result of an average of the individual observations from 18 June 2018 to 17 September 2018. SMAP science telemetry includes frequency information thus the RFI centre frequency was also identified for the RFI sources. A range is given if there appeared to be an observable bandwidth in the spectrum for the RFI source. Multiple centre frequencies were given if there were multiple peaks across the 16 sub-bands that were obviously RFI (TA > 330 K).

TABLE 10

Interference source detail log
Number of active sources listed: [44]

Source ID.	Observed geolocation		Centre frequency (MHz)	Source detection characteristics	Level of interference detected by sensor (K)	e.i.r.p. of transmitting source(s) (dBW)	City/ State/ Region	Number of observations	Last seen (UTC)	Present status (status as per 17/09/2018)
	Longitude (degrees)	Latitude (degrees)								
RUS-1	41.86	44.96	1 405, 1 424		490	−11.307		126	14/09/2018 3:47	ON
RUS-2	42.06	57.49	1 405, 1 424		528	−10.9826		225	17/09/2018 3:56	ON
RUS-3	39.67	47.23	1 405, 1 424		345	−12.8307		170	17/09/2018 15:05	ON
RUS-4	33.16	68.74	1 415		394	−12.254		99	15/07/2018 5:30	ON
RUS-5	60.34	58.07	1 421		493	−11.280 5		73	10/09/2018 2:54	ON
RUS-6	103.07	53.14	1 402, 1 424		575	−10.612 2		64	3/09/2018 0:15	ON
RUS-7	45.02	53.13	1 400-1 408, 1 420-1 424		385	−12.354 3		129	17/09/2018 3:55	ON
RUS-8	53.51	63.41	1 400-1 408, 1 424		414	−12.038 9		98	6/09/2018 3:42	ON
RUS-9	60.71	55.74	1 400-1 408, 1 424		384	−12.365 6		111	17/09/2018 13:29	ON
RUS-10	51.57	56.29	1 400-1 424		148	−16.506 3		225	17/09/2018 13:29	ON
RUS-11	47.95	52.1	1 400-1 410, 1 420-1 424		279	−13.752 9		70	23/07/2018 3:56	ON
RUS-12	79.59	66.79	1 402, 1 424		161	−16.140 7		338	17/09/2018 11:53	ON

TABLE 10

Source ID.	Observed geolocation		Centre frequency (MHz)	Source detection characteristics	Level of interference detected by sensor (K)	e.i.r.p. of transmitting source(s) (dBW)	City/ State/ Region	Number of observations	Last seen (UTC)	Present status (status as per 17/09/2018)
	Longitude (degrees)	Latitude (degrees)								
RUS-13	62.72	55.28	1 402, 1 406, 1 410, 1 424		162	−16.113 8		201	17/09/2018 13:28	ON
RUS-14	37.47	55.49	1 400-1 424		316	−13.212 1		18	13/09/2018 14:18	ON
RUS-15	49.26	55.63	1 402, 1 415		240	−14.406 8		192	17/09/2018 13:29	ON
RUS-16	37.75	55.66	1 400-1 424		318	−13.184 7		15	7/09/2018 4:21	ON
RUS-17	113.58	54.43	1 402, 1 415, 1 424		480	−11.396 5		14	20/08/2018 22:49	ON
RUS-18	48.78	51.98	1 402, 1 424		136	−16.873 5		73	16/09/2018 14:29	ON
RUS-19	93.6	56.32	1 402, 1 410, 1 415, 1 424		103	−18.080 6		221	17/09/2018 0:39	ON
RUS-20	35.56	52.46	1 406		123	−17.309 9		177	17/09/2018 15:06	ON
RUS-21	44.64	43.7	1 404, 1 412		116	−17.564 3		43	2/08/2018 14:37	ON
RUS-22	132.35	42.86	1 405		106	−17.955 9		144	17/09/2018 22:02	ON
RUS-23	66.43	66.65	1 417-1 422		101	−18.165 7		34	31/08/2018 12:54	ON
RUS-24	66.41	59.51	1 412, 1 418		62	−20.285		144	17/09/2018 2:17	ON
RUS-25	37.26	55.37	1 412, 1 419		290	−13.584 9		14	16/09/2018 14:30	ON

TABLE 10 (*continued*)

Source ID.	**Observed geolocation**		**Centre frequency (MHz)**	**Source detection characteristics**	**Level of interference detected by sensor (K)**	**e.i.r.p. of transmitting source(s) (dBW)**	**City/ State/ Region**	**Number of observations**	**Last seen (UTC)**	**Present status (status as per 17/09/2018)**
	Longitude (degrees)	**Latitude (degrees)**								
RUS-26	37.67	54.23	1 407, 1 412, 1 422		87	−18.813 7		156	17/09/2018 15:07	ON
RUS-27	39.71	59.26	1 404		89	−18.715		29	4/07/2018 14:55	ON
RUS-28	54.26	56.26	1 404, 1 417, 1 422		56	−20.727		152	17/09/2018 13:27	ON
RUS-29	20.59	54.88	1 418		105	−17.997		64	11/09/2018 5:08	ON
RUS-30	51.85	53.95	1 404, 1 412		141	−16.716 7		19	12/07/2018 3:43	ON
RUS-31	61.47	55.1	1 400, 1 424		72	−19.635 6		48	15/09/2018 2:43	ON
RUS-32	57.28	65.24	1 414, 1 420		64	−20.147 1		92	17/09/2018 13:31	ON
RUS-33	38.29	57.55	1 414		101	−18.165 7		13	4/07/2018 14:55	ON
RUS-34	59.81	58.66	1 404		51	−21.133 2		52	16/09/2018 12:51	ON
RUS-35	60.09	57.27	1 400-1 405, 1 424		54	−20.885		51	16/09/2018 12:53	ON
RUS-36	35.81	55.98	1 400, 1 406, 1 410, 1 414		72	−19.635 6		19	17/09/2018 15:07	ON
RUS-37	136.91	50.43	1 400-1 405, 1 424		66	−20.013 5		18	31/08/2018 7:55	ON
RUS-38	75.69	67.94	1 400, 1 415, 1 419		55	−20.805 3		94	17/09/2018 11:54	ON

TABLE 10 (*end*)

Source ID.	Observed geolocation		Centre frequency (MHz)	Source detection characteristics	Level of interference detected by sensor (K)	e.i.r.p. of transmitting source(s) (dBW)	City/ State/ Region	Number of observations	Last seen (UTC)	Present status (status as per 17/09/2018)
	Longitude (degrees)	Latitude (degrees)								
RUS-39	39.36	52.82	1 402, 1 415		109	−17.834 7		11	27/06/2018 4:21	ON
RUS-40	132.04	43.94	1 422		53	−20.966 2		15	11/09/2018 21:38	ON
RUS-41	39.02	45.1	1 410, 1 420		72	−19.635 6		19	11/09/2018 3:34	ON
RUS-42	30.68	59.82	1 424		64	−20.147 1		12	26/08/2018 5:06	ON
RUS-43	38.5	59.22	1 405		448	−11.696 1		12	17/09/2018 3:55	ON
RUS-44	47.48	43.01	1 424		73	−19.575 7		143	16/09/2018 14:27	ON

6.7.6.3 Supporting information

Figure 29 shows the peak hold data over the Russian Federation on a 0.25° × 0.25° grid of horizontally polarized TAs in kelvin before RFI filtering. Figure 30 shows a map of observed RFI on a 0.25° × 0.25° grid of the percentage of observations. Figure 31 shows the location and intensity of RFI sources over the Russian Federation.

FIGURE 29

Peak hold data over the Russian Federation on a 0.25° × 0.25° grid of horizontally polarized TAs in kelvin before RFI filtering for the week of 12/09/2018 to 18/09/2018

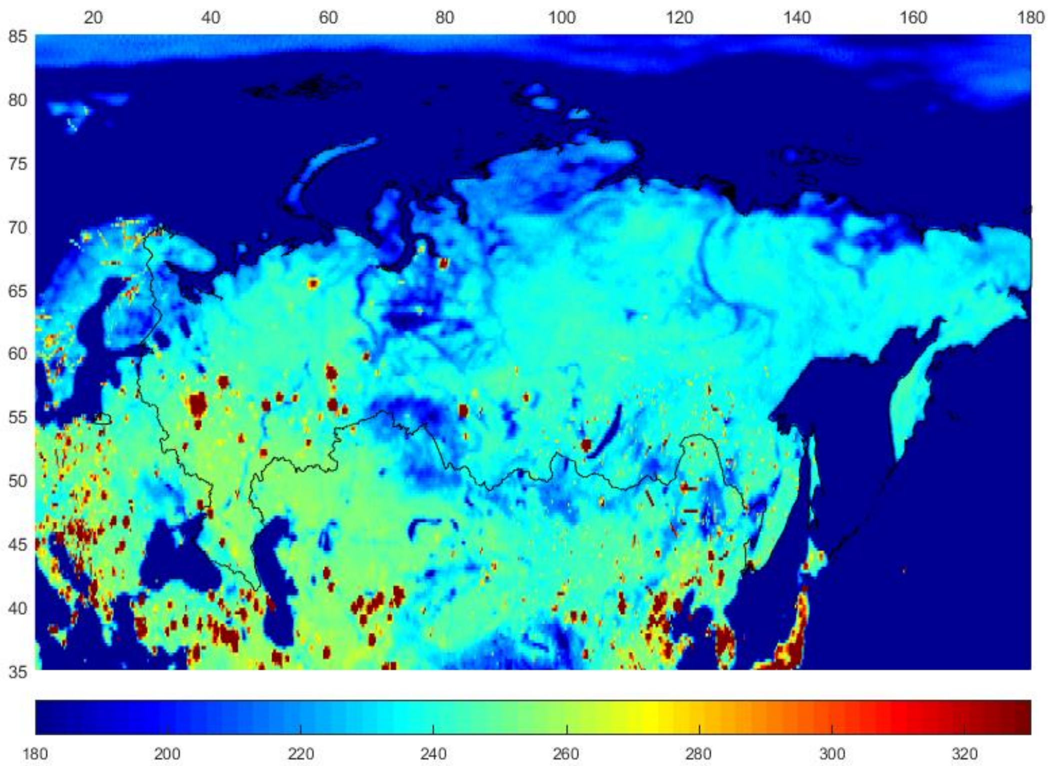

Note to Fig. 29: Similar results were seen in the vertical polarization. A 'peak hold' plot (i.e. the maximum value observed) emphasized large RFI contributions since geophysical contributions to the brightness background were also included. The colour scale was limited to 180 to 330 K. Footprints 180 K and under appear dark blue and those 330 K and above are dark red. Anything greater than 330 K was automatically flagged as RFI since this is the geophysical limit for measurements.

FIGURE 30

Map on a 0.25° × 0.25° grid of the percentage of observations over the period June to August 2018 that obtained a detected RFI level of 5K or more in the horizontal polarization

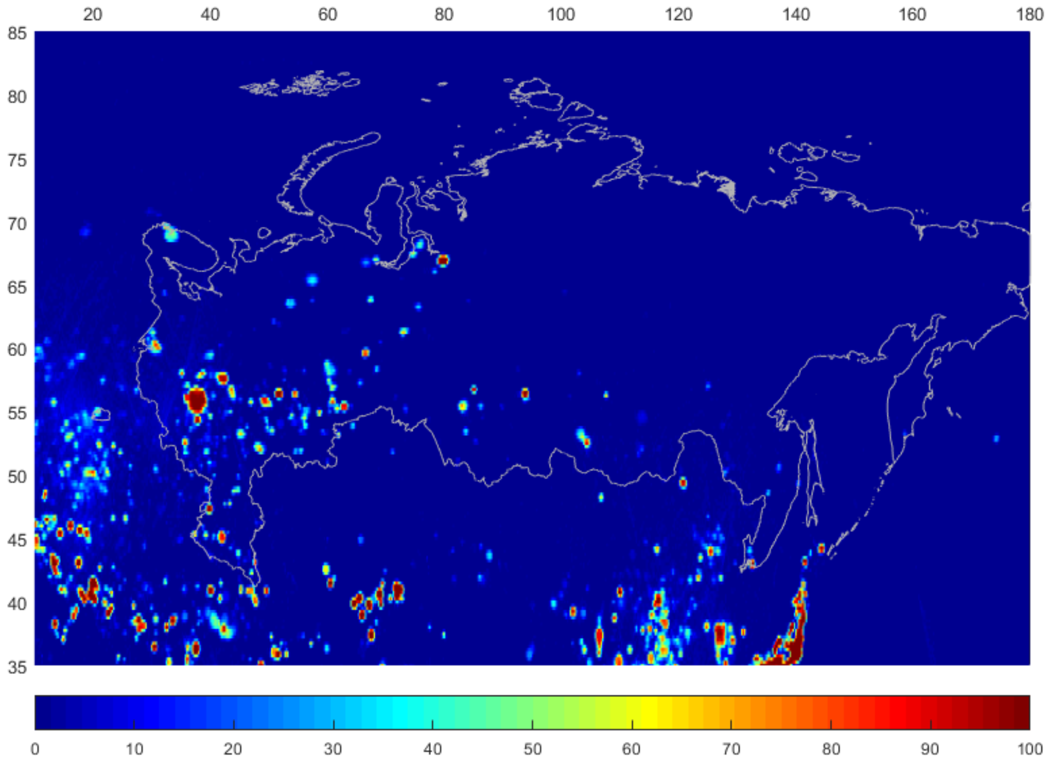

Note to Fig. 30: Vertical polarization showed similar results. Points having values greater than approximately 25 to 30% (i.e. light blue to red) were persistent sources of interference during this period. This plot does not distinguish between large amplitude and small amplitude, but rather highlights the temporal persistence of specific sources.

FIGURE 31

Location and intensity of RFI sources over the Russian Federation

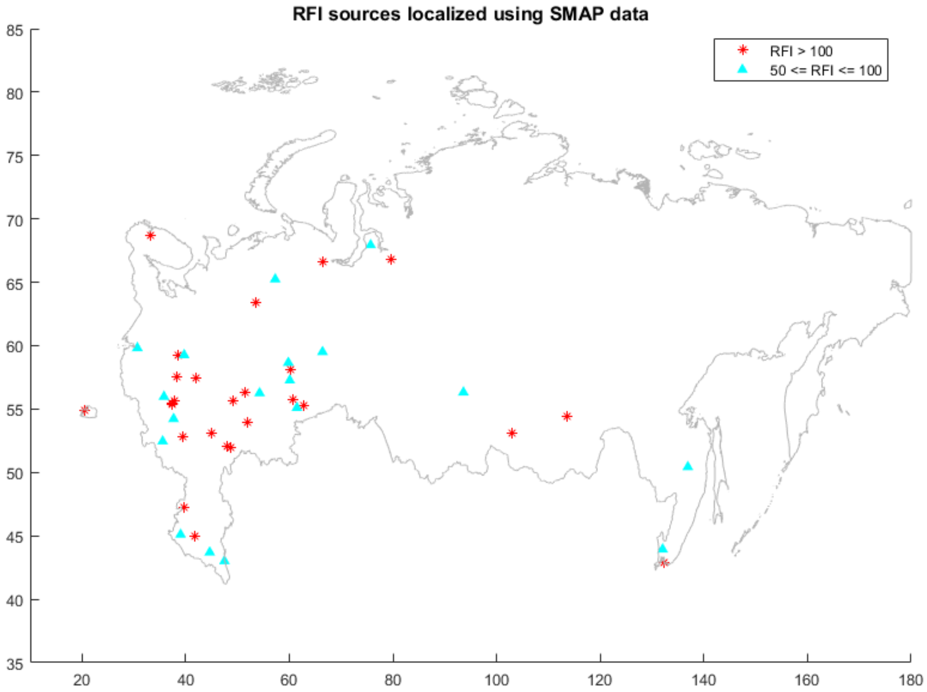

Note to Fig. 31: Colours indicate range of RFI levels in kelvin. These locations can be easily seen in the probability map. The strong and very strong sources are also easily seen in the peak hold map. Some of the moderate level RFI sources are a more difficult to identify on the peak hold map since the peak hold map also includes geophysical contributions.

6.7.6.4 Classification of RFIs per intensity over Russia (status as of 17/09/2018)

A general summary of the prevalence of moderate, strong, and very strong sources over the Russian Federation is summarized from Table 10 as follows:

Very strong RFI (RFI level > 100 K)	26 RFI sources
Strong RFI (50 K ≤ RFI level < 100 K)	18 RFI sources

6.7.7 Report of observed RFI over Italy over a three-month timeframe from 1 August 2018 to 31 October 2018

6.7.7.1 Summary of the RFI sources over Italy

Table 11 defines the fields in the Summary of RFI sources form that was completed by the USA when it reported an RFI event over Italy.

TABLE 11

Summary of RFI sources

Date of this RFI status update	1 August 2018 to 31 October 2018
Total number of RFI cases detected	22
Active RFI sources	22 reported
** **Old RFI active sources**	N/A
** **New RFI active sources**	22 reported, see Table 12 for RFI level and geolocation details
RFI sources OFF	N/A

6.7.7.2 Geolocation and other detailed RFI information

Table 12 includes the following detailed information for the RFI source: latitude and longitude, centre frequency, average RFI level in kelvin, number of observations used to geolocate the source and determine RFI level where the source is located as well as the time the source was last seen as of this writing. There were 44 sources identified over Italy. Data from 1 August 2018 to 31 October 2018 was used to create Table 12 as well as supporting Figures.

The localization of RFI sources was based on the difference between SMAP measurements before and after RFI filtering. This difference corresponds to the effect that RFI has on the data. A machine learning algorithm was then applied to automatically find the points where the effect of RFI is highest (local maxima). These points define the location of RFI sources. Since every RFI source was observed multiple times during the course of the reporting period, the coordinates and RFI level provided in this report were the result of an average of the individual observations from 1 August 2018 to 31 October 2018. SMAP science telemetry includes frequency information thus the RFI centre frequency was also identified for the RFI sources. A range was given if there appeared to be an observable bandwidth in the spectrum for the RFI source. Multiple centre frequencies were given if there were multiple peaks across the 16 sub-bands that were obviously RFI (TA > 330 K).

TABLE 12

Interference source detail log
Number of active sources listed: [22]

Source ID.	Observed geolocation		Centre frequency (MHz)	Source detection characteristics	Level of interference detected by sensor (K)	e.i.r.p. of transmitting source(s) (dBW)	City/ State/ Region	Number of observations	Last seen (UTC)	Present status (status as per 31/10/2018)
	Longitude (degrees)	Latitude (degrees)								
ITA-1	13.34	38.13	1 400, 1 412, 1 424	Point source	207	−15.049 2	Sicily	100	30/10/2018 16:53:42	ON
ITA-2	16.97	39.28	1 414, 1 420	Point source	180	−15.656 2	Calabria	92	29/10/2018 16:15:12	ON
ITA-3	17.7	40.68	1 400, 1 424	Point source	202	−15.155 4	Apulia	97	29/10/2018 16:17:46	ON
ITA-4	14.76	36.93	1 416, 1 422	Point source	127	−17.170 9	Sicily	94	30/10/2018 16:53:09	ON
ITA-5	16.48	38.73	1 415-1 424	Point source	247	−14.282	Calabria	82	29/10/2018 16:15:04	ON
ITA-6	12.59	38.04	1 402	Point source	406	−12.123 7	Sicily	43	24/10/2018 16:29:12	ON
ITA-7	7.93	45.49	1 400, 1 424	Point source	157	−16.249 9	Piedmont	125	30/10/2018 16:56:01	ON
ITA-8	13.63	43.15	1 400, 1 412, 1 424	Point source	120	−17.417 1	Marche	31	30/10/2018 16:53:06	ON
ITA-9	10.16	44.81	1 400, 1 424	Point source	83	−19.018 1	Emilia-Romagna	106	30/10/2018 16:53:19	ON
ITA-10	11.43	46.49	1 400, 1 424	Point source	98	−18.296 7	Trentino-Alto Adige	30	30/10/2018 16:53:55	ON
ITA-11	14.33	40.94	1 400, 1 416, 1 424	Point source	66	−20.013 5	Campania	104	29/10/2018 5:15:01	ON
ITA-12	13.03	42.85	1 400, 1 424	Point source	70	−19.757 9	Umbria	59	30/10/2018 16:54:52	ON

TABLE 12 (*end*)

Source ID.	Observed geolocation		Centre frequency (MHz)	Source detection characteristics	Level of interference detected by sensor (K)	e.i.r.p. of transmitting source(s) (dBW)	City/ State/ Region	Number of observations	Last seen (UTC)	Present status (status as per 31/10/2018)
	Longitude (degrees)	Latitude (degrees)								
ITA-13	13.49	42.26	1 400, 1 424	Point source	53	−20.966 2	Abruzzo	61	30/10/2018 16:52:49	ON
ITA-14	13.19	43.04	1 400, 1 424	Point source	60	−20.427 4	Marche	29	27/10/2018 16:40:33	ON
ITA-15	15.61	41.38	1 400, 1 412, 1 424	Point source	71	−19.696 3	Apulia	30	29/10/2018 5:15:01	ON
ITA-16	7.68	44.65	1 405, 1 424	Point source	95	−18.431 7	Piedmont	11	1/9/2018 16:41:11	ON
ITA-17	9.64	46.03	1 400, 1 424	Point source	50	−21.219 2	Lombardy	44	28/10/2018 6:14:42	ON
ITA-18	18.42	40.15	1 407, 1 414, 1 424	Point source	78	−19.288	Apulia	17	16/10/2018 16:29:40	ON
ITA-19	15.27	40.64	1 407	Point source	59	−20.500 4	Campania	45	27/10/2018 5:39:37	ON
ITA-20	11.49	45.12	1 415, 1 424	Point source	80	−19.178	Veneto	22	17/10/2018 6:00:53	ON
ITA-21	18.41	40.02	1 408, 1 414	Point source	63	−20.215 5	Apulia	19	29/10/2018 5:13:00	ON
ITA-22	11.91	46.69	1 400, 1 424	Point source	75	−19.458 3	Trentino-Alto Adige	17	16/10/2018 16:31:47	ON

6.7.7.3 Supporting information

Figure 32 shows the peak hold plot over Italy on a 0.25° × 0.25° grid of horizontally polarized TAs in kelvin before RFI filtering. Figure 33 shows the map of observed RFI on a 0.25° × 0.25° grid of the percentage of observations. Figure 34 shows the location and intensity of RFI sources over Italy.

FIGURE 32

Peak hold plot over Italy on a 0.25° × 0.25° grid of horizontally polarized TAs in kelvin before RFI filtering over the time period of 24/10/2018 to 30/10/2018

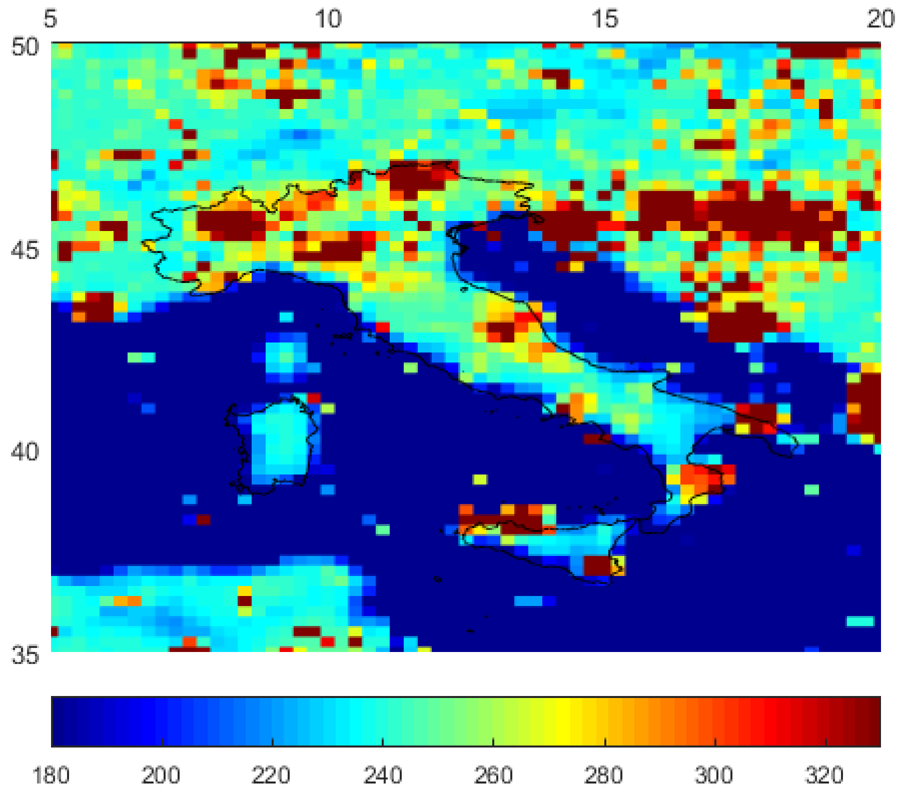

Note to Fig. 32: Similar results were seen in the vertical polarization. A 'peak hold' plot (i.e. the maximum value observed) emphasizes large RFI contributions since geophysical contributions to the brightness background were also included. The colour scale was limited to values from 180 K to 330 K. Footprints with TA equal to or lower than 180 K appear dark blue and those that are 330 K and above are dark red. Any value greater than 330 K is automatically flagged as RFI since this is the geophysical limit for brightness temperature measurements.

FIGURE 33

Map on a 0.25° × 0.25° grid of the percentage of observations over the period August to October 2018 with a detected RFI level of 5 K or more in the horizontal polarization

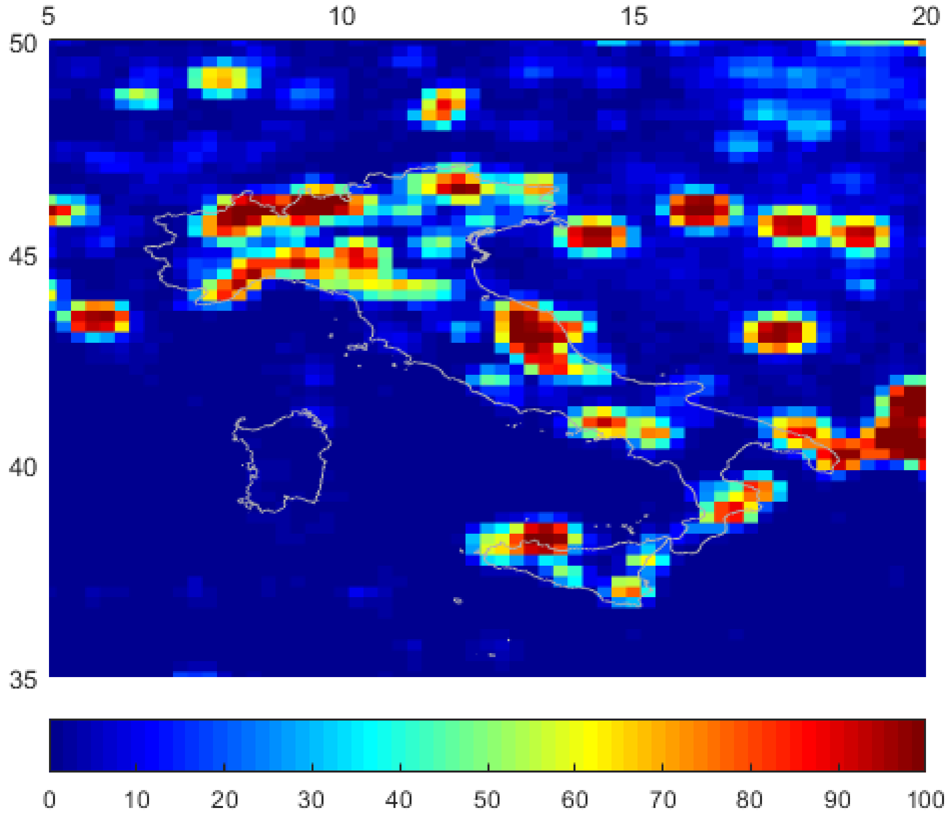

Note to Fig. 33: Vertical polarization showed similar results. Points having values greater than approximately 25 to 30% (i.e. light blue to red) were persistent sources of interference during this period. This plot does not distinguish between large amplitude and small amplitude, but rather highlights the temporal persistence of specific sources.

FIGURE 34

Location and intensity of RFI sources over Italy

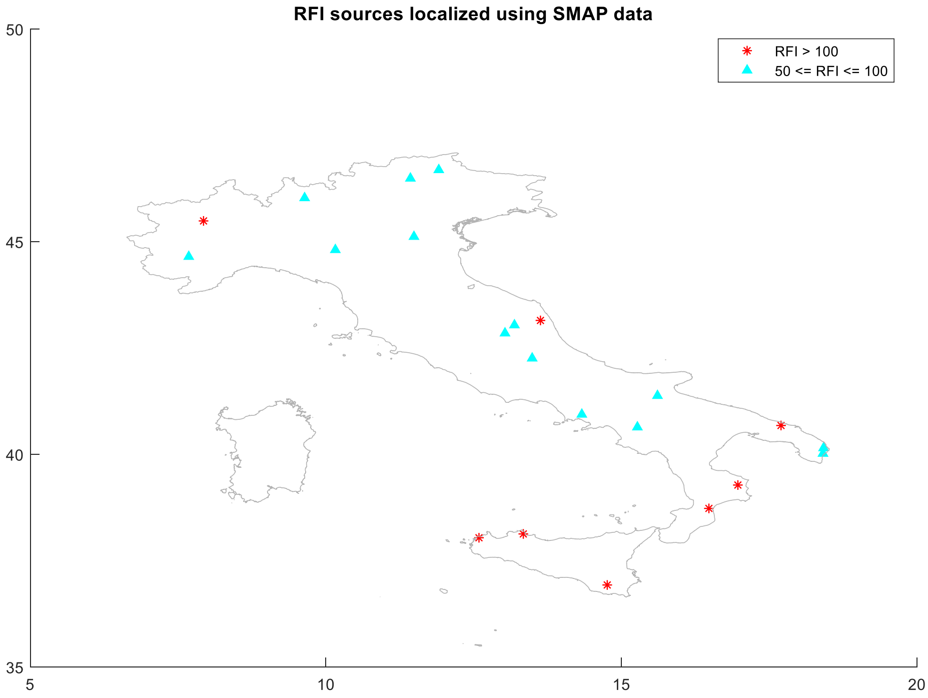

Note to Fig. 34: Colours indicate range of RFI levels in kelvin. These locations can be easily seen in the probability map. The strong and very strong sources were also easily noticeable in the peak hold map. Some of the moderate level RFI sources were a more difficult to identify on the peak hold map since the peak hold map also included geophysical contributions.

6.7.7.4 Classification of RFI sources per intensity over Italy (status as of 09/11/2018)

A general summary of the prevalence of strong and very strong sources over Italy is summarized from Table 12 as follows:

Very strong RFI (RFI level > 100 K) 8 RFI sources

Strong RFI (50 K ≤ RFI level < 100 K) 14 RFI sources

6.7.8 Report of observed RFI over Kuwait over a three-month timeframe from 16 September 2018 to 16 December 2018

6.7.8.1 Summary of the RFI sources over Kuwait

Table 13 defines the fields in the Summary of RFI sources form that was completed by the USA when it reported an RFI event over Kuwait.

TABLE 13

Summary of RFI sources

Date of this RFI status update	16 September 2018 to 16 December 2018
Total number of RFI cases detected	1
Active RFI sources	1 reported
** **Old RFI active sources**	N/A
** **New RFI active sources**	1 reported, see Table 14 for RFI level and geolocation details
RFI sources OFF	N/A

6.7.8.2 Geolocation and other detailed RFI information

Table 14 includes the following detailed information for the RFI source: latitude and longitude, centre frequency, average RFI level in kelvin, number of observations used to geolocate the source and determine RFI level where the source was located as well as the time the source was last seen as of this writing. There was one (1) source identified over Kuwait. Data from 16 September 2018 to 16 December 2018 was used to create Table 14 as well as supporting Figures.

The localization of RFI sources was based on the difference between SMAP measurements before and after RFI filtering. This difference corresponds to the effect that RFI has on the data. A machine learning algorithm is then applied to automatically find the points where the effect of RFI is highest (local maxima). These points define the location of RFI sources. Since every RFI source was observed multiple times during the course of the reporting period, the coordinates and RFI level provided in this report were the result of an average of the individual observations from 16 September 2018 to 16 December 2018. SMAP science telemetry includes frequency information thus the RFI centre frequency was also identified for the RFI sources. A range was given if there appeared to be an observable bandwidth in the spectrum for the RFI source. Multiple centre frequencies were given if there were multiple peaks across the 16 sub-bands that were obviously RFI (TA > 330 K).

TABLE 14

Interference source detail log
Number of active sources listed: [1]

Source ID.	Observed geolocation		Centre frequency (MHz)	Source detection characteristics	Level of interference detected by sensor (K)	e.i.r.p. of transmitting source(s) (dBW)	City/ State/ Region	Number of observations	Last seen (UTC)	Present status (status as per 16/12/2018)
	Longitude (degrees)	Latitude (degrees)								
KWT-1	48.06	29.25	1 424	Point source	95	−18.43		52	15/12/2018 3:00	ON

6.7.8.3 Supporting information

Figure 35 shows the peak hold plot over Kuwait on a 0.25° × 0.25° grid of horizontally polarized TAs in kelvin before RFI filtering. Figure 36 shows the map of observed RFI on a 0.25° × 0.25° grid of the percentage of observations. Figure 37 shows the location and intensity of the RFI source over Kuwait.

FIGURE 35

Peak hold plot over Kuwait on a 0.25° × 0.25° grid of horizontally polarized TAs in kelvin before RFI filtering over the time period of 05/12/2018 to 11/12/2018

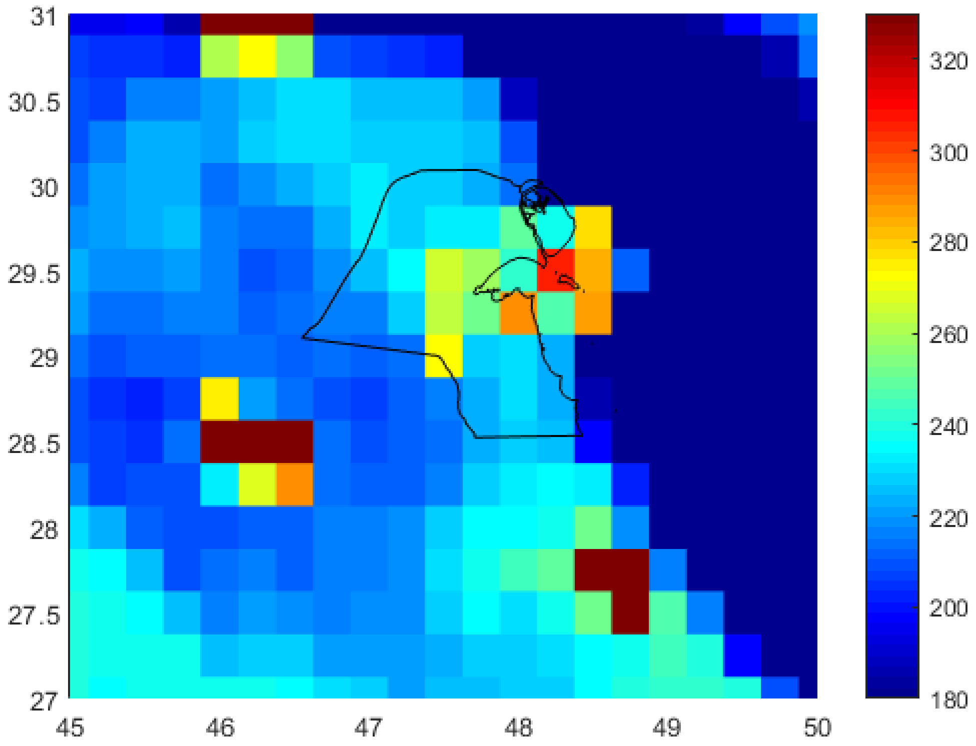

Note to Fig. 35: Similar results were seen in the vertical polarization. A 'peak hold' plot (i.e. the maximum value observed) emphasized large RFI contributions since geophysical contributions to the brightness background are also included. The colour scale is limited to values from 180 K to 330 K. Footprints with TA equal to or lower than 180 K appear dark blue and those that are 330 K and above are dark red. Any value greater than 330 K was automatically flagged as RFI since this is the geophysical limit for brightness temperature measurements.

FIGURE 36

Map on a 0.25° × 0.25° grid of the percentage of observations over the period September to November 2018 with a detected RFI level of 5 K or more in the horizontal polarization

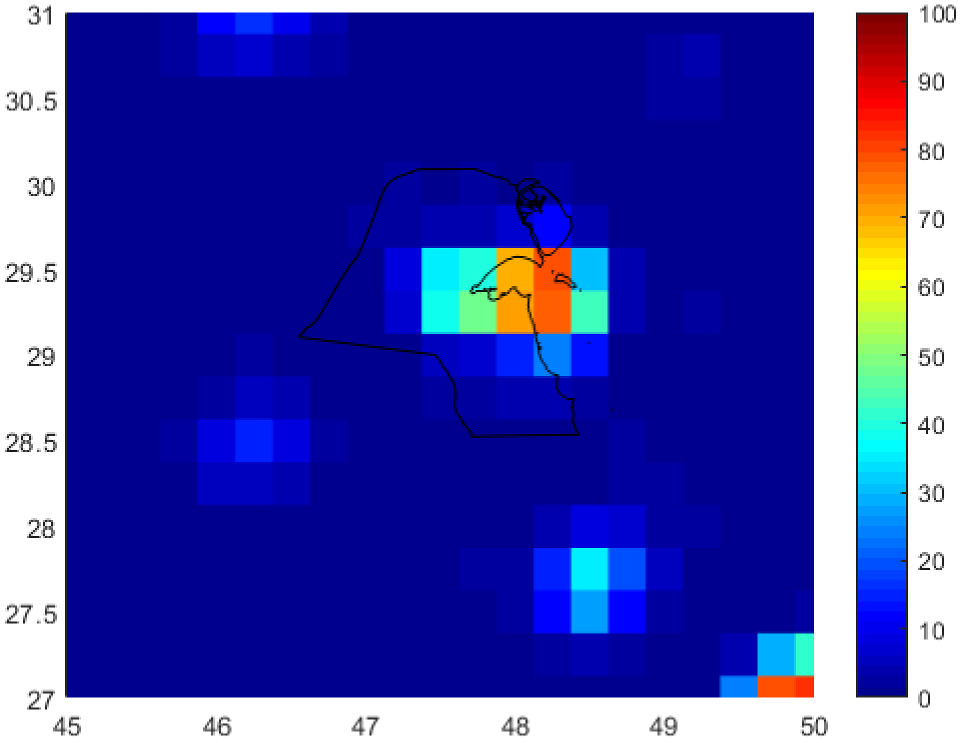

Note to Fig. 36: Vertical polarization showed similar results. Points having values greater than approximately 25-30% (i.e. light blue to red) are persistent sources of interference during this period. This plot does not distinguish between large amplitude and small amplitude, but rather highlights the temporal persistence of specific sources.

FIGURE 37

Location and intensity of the RFI source over Kuwait

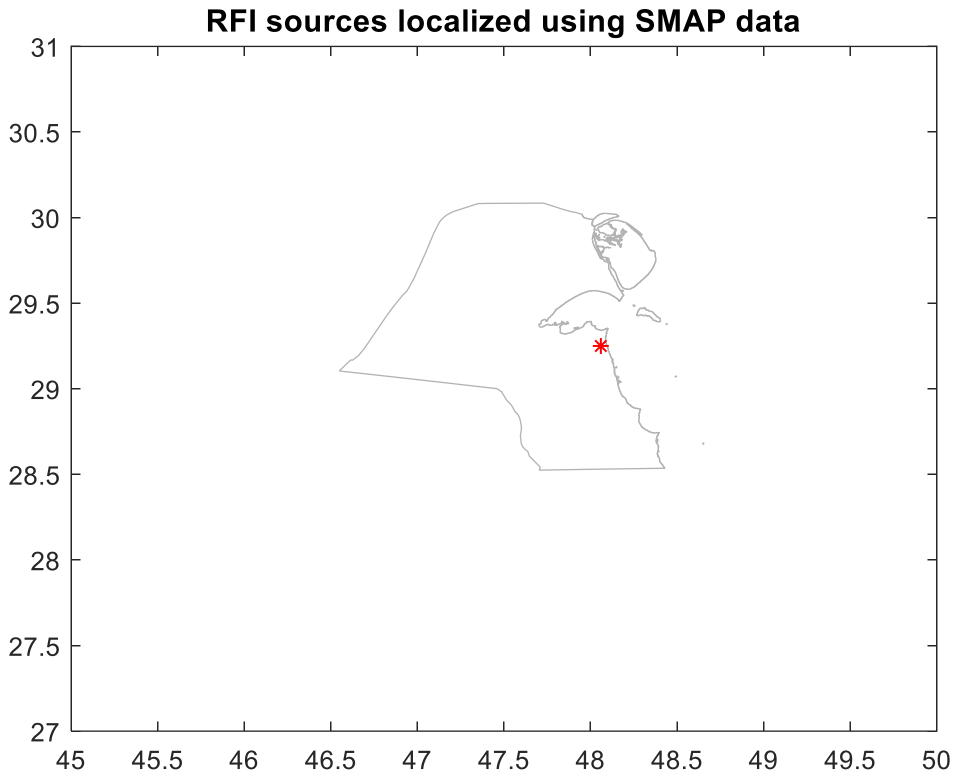

Note to Fig. 37: The source is 95 K. The source location can be easily seen in the probability map and is also noticeable in the peak hold map.

6.7.8.4 Classification of RFI sources per intensity over Kuwait (status as of 16/12/2018)

A general summary of the prevalence of RFI sources over Kuwait is summarized from Table 14 as follows:

Strong RFI (RFI level ≥ 50 K) 1 RFI source

6.7.9 Report of observed RFI over the United Arab Emirates over a three-month timeframe from 16 September 2018 to 16 December 2018

6.7.9.1 Summary of the RFI sources over the United Arab Emirates

Table 15 defines the fields in the Summary of RFI Sources form that were completed by the USA reported an RFI event over the United Arab Emirates.

TABLE 15

Summary of RFI sources

Date of this RFI status update	16 September 2018 to 16 December 2018
Total number of RFI cases detected	5
Active RFI sources	5 reported
** **Old RFI active sources**	N/A
** **New RFI active sources**	5 reported, see Table 16 for RFI level and geolocation details
RFI sources OFF	N/A

6.7.9.2 Geolocation and other detailed RFI information

Table 16 includes the following detailed information for the RFI source: latitude and longitude, centre frequency, average RFI level in kelvin, number of observations used to geolocate the source and determine RFI level where the source is located as well as the time the source was last seen as of this writing. There were five sources identified over the United Arab Emirates. Data from 16 September 2018 to 16 December 2018 was used to create Table 16 as well as supporting Figures.

The localization of RFI sources was based on the difference between SMAP measurements before and after RFI filtering. This difference corresponds to the effect that RFI has on the data. A machine learning algorithm was then applied to automatically find the points where the effect of RFI is highest (local maxima). These points define the location of RFI sources. Since every RFI source was observed multiple times during the course of the reporting period, the coordinates and RFI level provided in this Report were the result of an average of the individual observations from 16 September 2018 to 16 December 2018. SMAP science telemetry includes frequency information thus the RFI centre frequency was also identified for the RFI sources. A range is given if there appeared to be an observable bandwidth in the spectrum for the RFI source. Multiple centre frequencies were given if there were multiple peaks across the 16 sub-bands that were obviously RFI (TA > 330 K).

TABLE 16

Interference source detail log
Number of active sources listed: [5]

Source ID.	Observed geolocation		Centre frequency (MHz)	Source detection characteristics	Level of interference detected by sensor (K)	e.i.r.p. of transmitting source(s) (dBW)	City/ State/ Region	Number of observations	Last seen (UTC)	Present status (status as per 16/12/2018)
	Longitude (degrees)	Latitude (degrees)								
UAE-1	52.6	24.15	1 409	Point source	187	−15.49		88	16/12/2018 14:32	ON
UAE-2	55.47	24.94	1 409	Point source	166	−16.01		129	14/12/2018 2:27	ON
UAE-3	53.87	24.18	1 409	Point source	156	−16.28		50	2/11/2018 2:51	ON
UAE-4	54.65	24.68	1 409	Point source	100	−18.21		55	13/12/2018 14:20	ON
UAE-5	54.31	25.49	1 409, 1 424	Point source	146	−16.57		120	14/12/2018 2:26	ON

6.7.9.3 Supporting information

Figure 38 shows the peak hold plot over the United Arab Emirates on a 0.25° × 0.25° grid of horizontally polarized TAs in kelvin before RFI filtering. Figure 39 shows the map of observed RFI on a 0.25° × 0.25° grid of the percentage of observations. Figure 40 shows the location and intensity of RFI sources over the United Arab Emirates.

FIGURE 38

Peak hold plot over the United Arab Emirates on a 0.25° × 0.25° grid of horizontally polarized TAs in kelvin before RFI filtering over the time period of 05/12/2018 to 11/12/2018

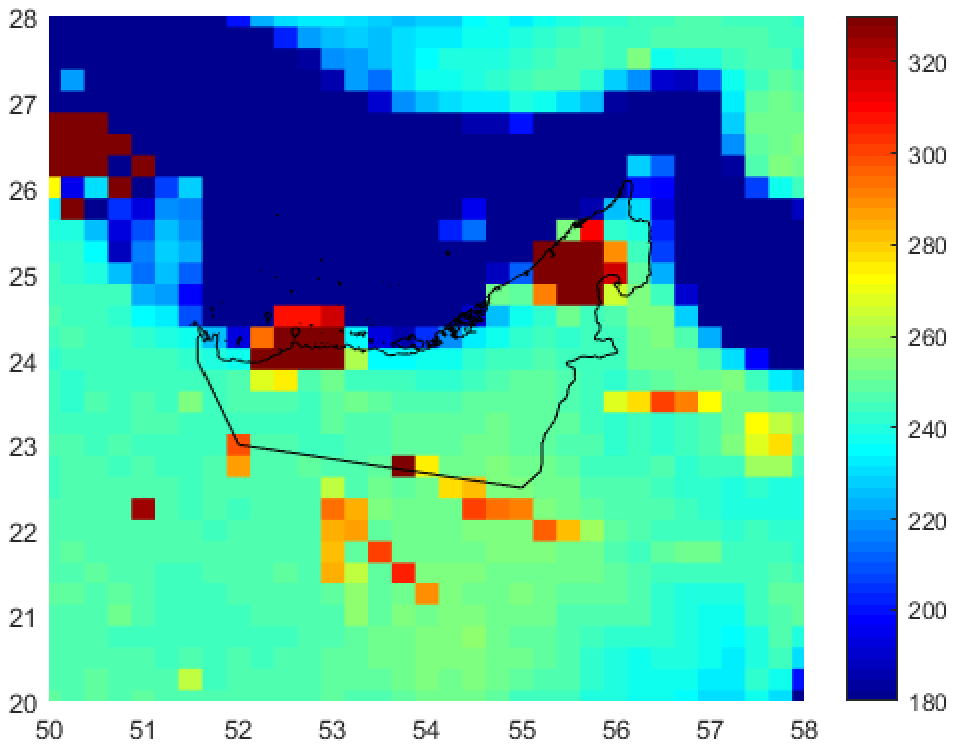

Note to Fig. 38: Similar results were seen in the vertical polarization. A 'peak hold' plot (i.e. the maximum value observed) emphasized large RFI contributions since geophysical contributions to the brightness background were also included. The colour scale was limited to values from 180 K to 330 K. Footprints with TA equal to or lower than 180 K appear dark blue and those that are 330 K and above are dark red. Any value greater than 330 K is automatically flagged as RFI since this is the geophysical limit for brightness temperature measurements.

FIGURE 39

Map on a 0.25° × 0.25° grid of the percentage of observations over the period September to November 2018 with a detected RFI level of 5 K or more in the horizontal polarization

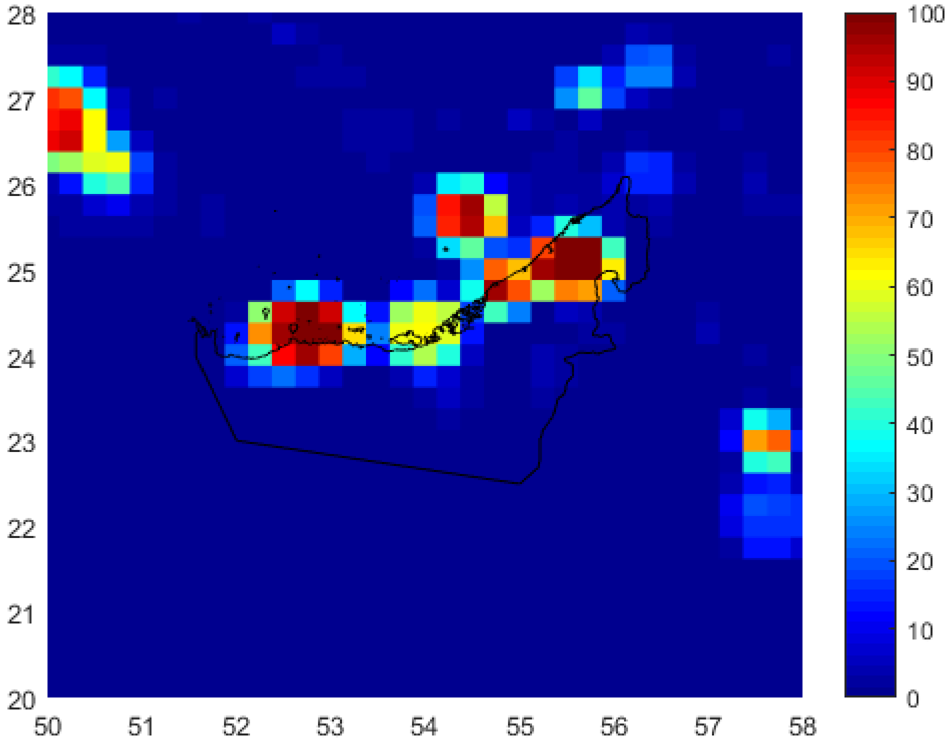

Note to Fig. 39: Vertical polarization showed similar results. Points having values greater than approximately 25 to 30% (i.e. light blue to red) were persistent sources of interference during this period. This plot does not distinguish between large amplitude and small amplitude, but rather highlights the temporal persistence of specific sources.

FIGURE 40

Location and intensity of RFI sources over the United Arab Emirates

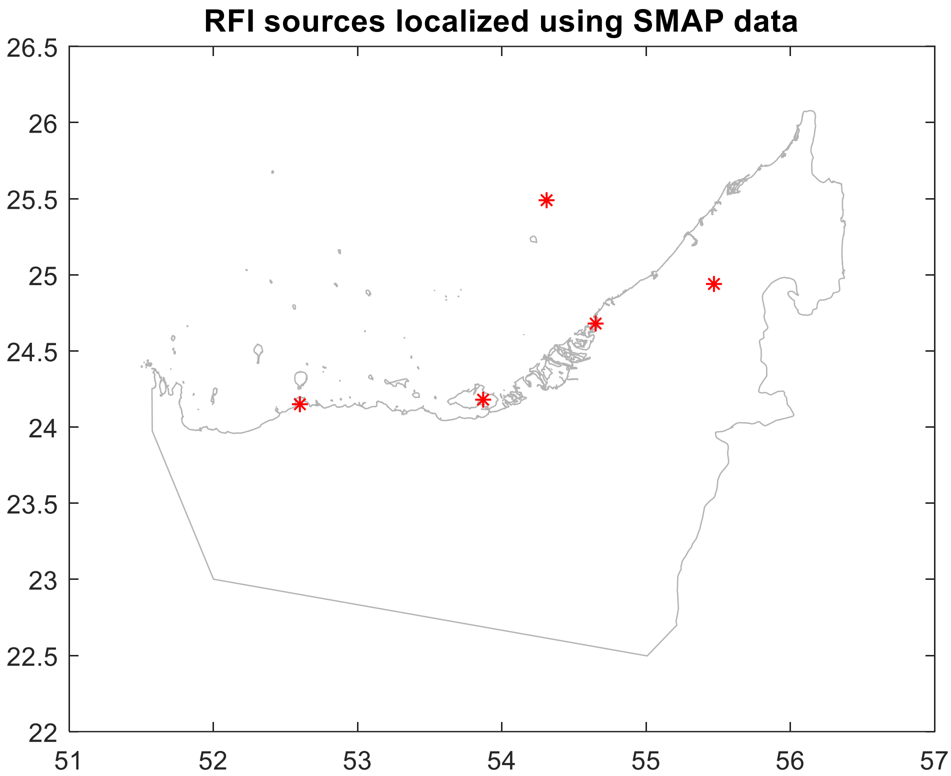

Note to Fig. 40: All sources are 100 K or greater. These locations can be easily seen in the probability map. The sources are also easily noticeable in the peak hold map. UAE-5 was a persistent source at a location in the United Arab Emirates' waters of the Persian Gulf.

6.7.9.4 Classification of RFI sources per intensity over a three-month timeframe from 16 September 2018 to 16 December 2018 (status as of 16/12/2018)

A general summary of the prevalence of RFI sources over the United Arab Emirates is summarized from Table 16 as follows:

Very strong RFI (RFI level ≥ 100 K) 5 RFI sources

6.7.10 Report of observed RFI over Uzbekistan over a three-month timeframe from 16 September 2018 to 16 December 2018

6.7.10.1 Summary of the RFI sources over Uzbekistan

Table 17 defines the fields in the Summary of RFI sources form that was completed by the USA reporting an RFI event over Uzbekistan.

TABLE 17

Summary of RFI sources

Date of this RFI status update	18 December 2018 to 17 February 2019
Total number of RFI cases detected	11
Active RFI sources	11 reported
** **Old RFI active sources**	N/A
** **New RFI active sources**	11 reported, see Table 18 for RFI level and geolocation details
RFI sources OFF	N/A

6.7.10.2 Geolocation and other detailed RFI information

Table 18 includes the following detailed information for the RFI source: latitude and longitude, centre frequency, average RFI level in kelvin, number of observations used to geolocate the source and determine RFI level where the source is located as well as the time the source was last seen as of this writing. There were 11 sources identified over Uzbekistan. Data from 18 December 2018 to 17 February 2019 was used to create Table 19 as well as supporting Figures.

The localization of RFI sources was based on the difference between SMAP measurements before and after RFI filtering. This difference corresponds to the effect that RFI has on the data. A machine learning algorithm was then applied to automatically find the points where the effect of RFI is highest (local maxima). These points defined the location of RFI sources. Since every RFI source was observed multiple times during the course of the reporting period, the coordinates and RFI level provided in this Report were the result of an average of the individual observations from 18 December 2018 to 17 February 2019. SMAP science telemetry includes frequency information thus the RFI centre frequency was also identified for the RFI sources. A range was given if there appeared to be an observable bandwidth in the spectrum for the RFI source. Multiple centre frequencies were given if there were multiple peaks across the 16 sub-bands that were obviously RFI (TA > 330 K).

TABLE 18

Interference source detail log
Number of active sources listed: [11]

Source ID.	Observed geolocation		Centre frequency (MHz)	Source detection characteristics	Level of interference detected by sensor (K)	e.i.r.p. of transmitting source(s) (dBW)	City/ State/Region	Number of observations	Last seen (UTC)	Present status (status as per 17/02/2019)
	Longitude (degrees)	Latitude (degrees)								
UZB-1	68.76	40.48	1 407-1 409	Point source	206	−15.070 3		103	15/2/2019 12:47	ON
UZB-2	66.94	39.69	1 407-1 409	Point source	202	−15.155 4		106	16/2/2019 13:23	ON
UZB-3	67.33	37.28	1 407-1 409	Point source	184	−15.560 7		107	16/2/2019 13:23	ON
UZB-4	71.97	40.92	1 407-1 409	Point source	196	−15.286 4		15	10/2/2019 12:57	ON
UZB-5	65.75	38.83	1 407-1 409	Point source	177	−15.729 2		99	16/2/2019 13:23	ON
UZB-6	65.34	40.15	1 407-1 409	Point source	139	−16.778 8		83	16/2/2019 13:24	ON
UZB-7	60.36	41.34	1 407-1 409	Point source	149	−16.477 1		111	16/2/2019 13:24	ON
UZB-8	64.38	39.72	1 407-1 409	Point source	181	−15.632 1		96	16/2/2019 13:24	ON
UZB-9	59.62	42.44	1 407-1 409	Point source	186	−15.513 8		97	16/2/2019 13:25	ON
UZB-10	71.72	40.99	1 407-1 409	Point source	191	−15.398 6		31	17/2/2019 1:19	ON
UZB-11	69.28	41.32	1 407-1 409	Point source	70	−19.757 9		64	15/2/2019 12:45	ON

6.7.10.3 Supporting information

Figure 41 shows the peak hold plot over Uzbekistan on a 0.25° × 0.25° grid of horizontally polarized TA in kelvin before RFI filtering. Figure 42 shows the map of observed RFI on a 0.25° × 0.25° grid of the percentage of observations. Figure 43 shows the location and intensity of RFI sources over Uzbekistan.

FIGURE 41

Peak hold plot over Uzbekistan on a 0.25° × 0.25° grid of horizontally polarized TAs in kelvin before RFI filtering over the time period of 06/02/2019 to 12/02/2019

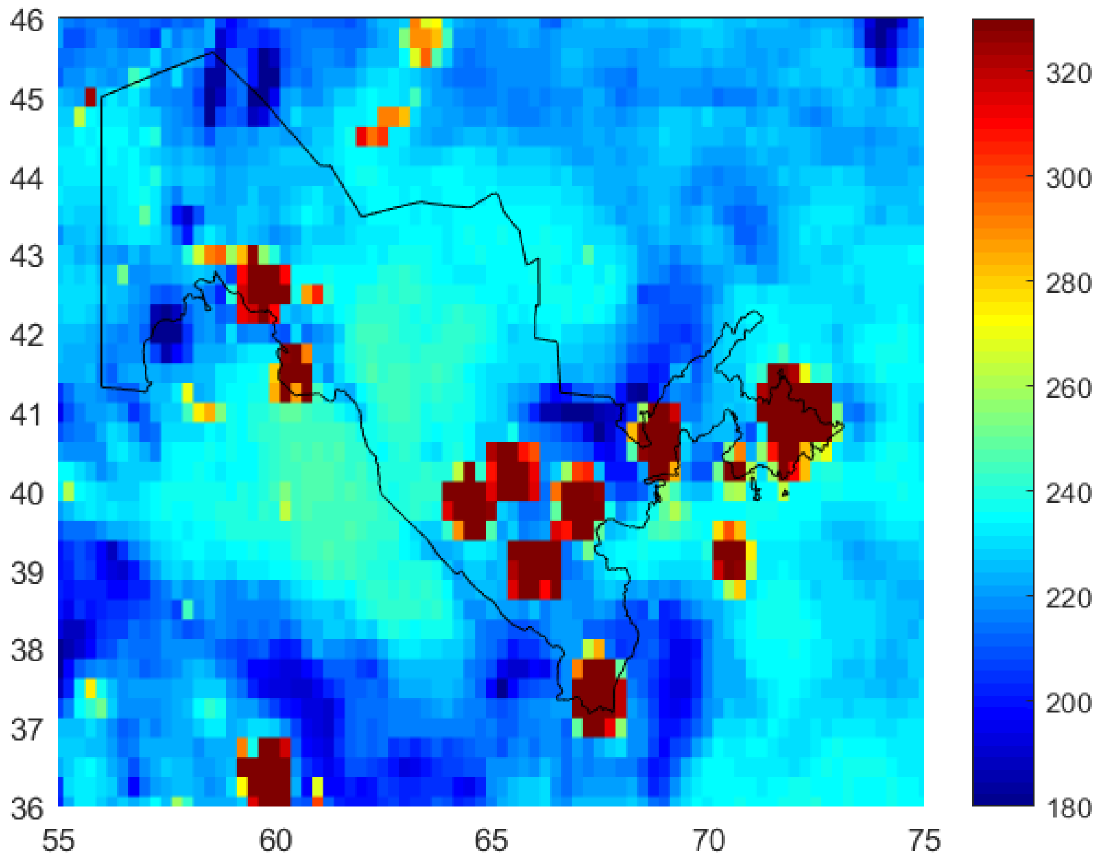

Note to Fig. 41: Similar results were seen in the vertical polarization. A 'peak hold' plot (i.e. the maximum value observed) emphasized large RFI contributions since geophysical contributions to the brightness background were also included. The colour scale was limited to values from 180 K to 330 K. Footprints with TA equal to or lower than 180 K appear dark blue and those that are 330 K and above are dark red. Any value greater than 330 K was automatically flagged as RFI since this is the geophysical limit for brightness temperature measurements.

FIGURE 42

Map on a 0.25° × 0.25° grid of the percentage of observations over the period December 2018 to February 2019 with a detected RFI level of 5 K or more in the horizontal polarization

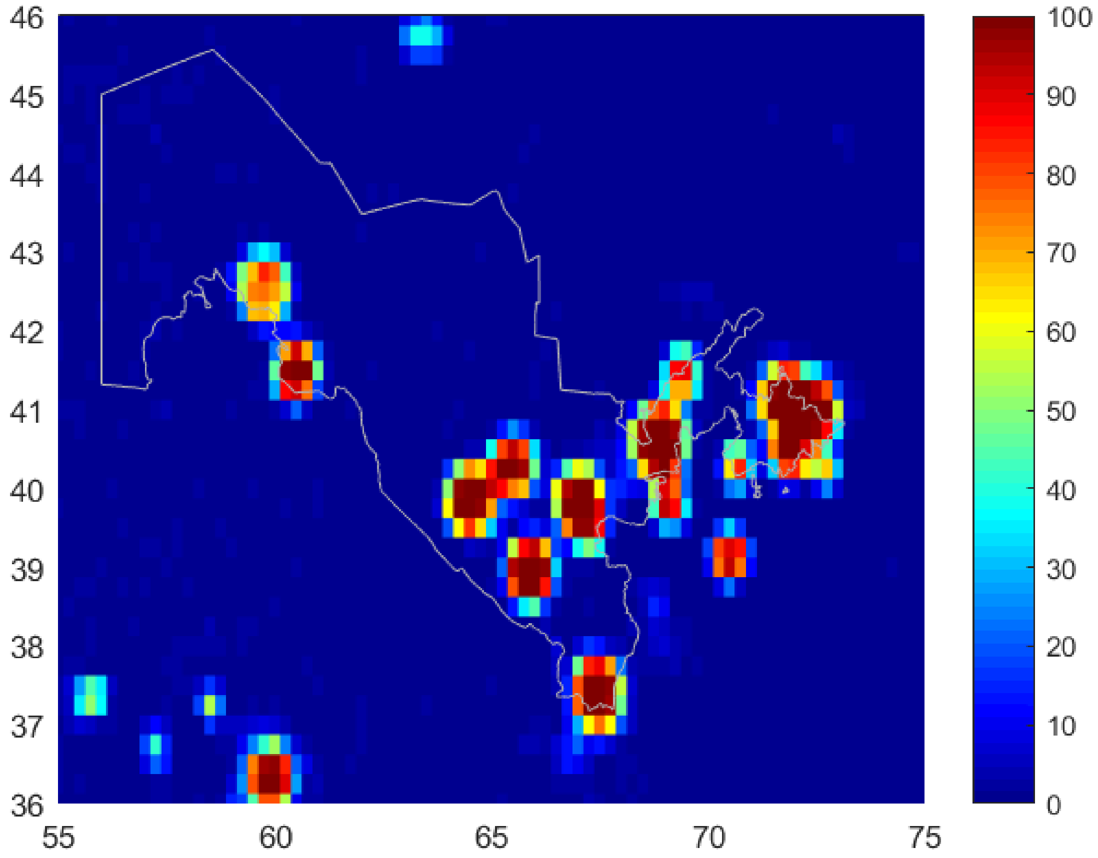

Note to Fig. 42: Vertical polarization showed similar results. Points having values greater than approximately 25-30% (i.e. light blue to red) were persistent sources of interference during this period. This plot does not distinguish between large amplitude and small amplitude, but rather highlights the temporal persistence of specific sources.

FIGURE 43

Location and intensity of RFI sources over Uzbekistan

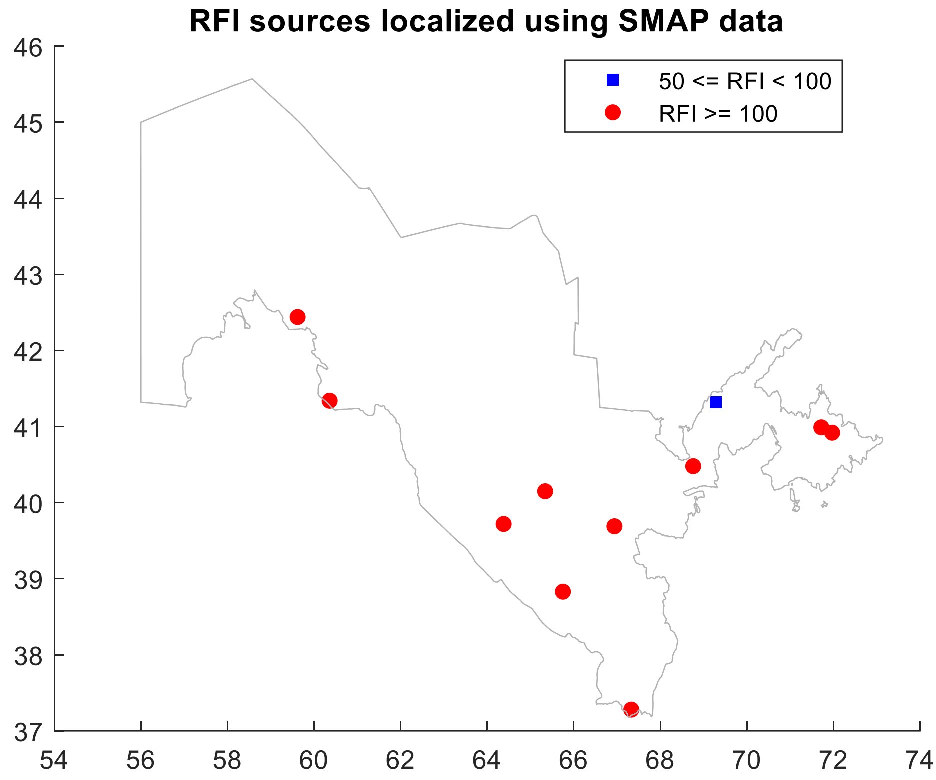

Note to Fig. 43: These locations can be easily seen in the probability and peak hold maps. The colours indicate range of RFI level in kelvin.

6.7.10.4 Classification of RFI sources per intensity over Uzbekistan (status as of 17/02/2019)

A general summary of the prevalence of RFI sources over Uzbekistan is summarized from Table 18 as follows:

Very strong RFI (RFI level ≥ 100 K) 10 RFI sources

Strong RFI (50 K ≤ RFI level < 100 K) 1 RFI sources

6.7.11 Report of observed RFI over Turkey over a two-month timeframe from 18 December 2018 to 17 February 2019

6.7.11.1 Summary of the RFI sources over Turkey

Table 19 defines the fields in the Summary of RFI sources form that was completed by the USA reporting an RFI event over Turkey.

TABLE 19

Summary of RFI sources

Date of this RFI status update	18 December 2018 to 17 February 2019
Total number of RFI cases detected	18
Active RFI sources	18 reported
** **Old RFI active sources**	N/A
** **New RFI active sources**	18 reported, see Table 20 for RFI level and geolocation details
RFI sources OFF	N/A

6.7.11.2 Geolocation and other detailed RFI information

Table 20 includes the following detailed information for the RFI source: latitude and longitude, centre frequency, average RFI level in kelvin, number of observations used to geolocate the source and determine RFI level where the source is located as well as the time the source was last seen as of this writing. There were 18 sources identified over Turkey. Data from 18 December 2018 to 17 February 2019 was used to create Table 20 as well as supporting Figures.

The localization of RFI sources was based on the difference between SMAP measurements before and after RFI filtering. This difference corresponded to the effect that RFI has on the data. A machine learning algorithm was then applied to automatically find the points where the effect of RFI is highest (local maxima). These points defined the location of RFI sources. Since every RFI source was observed multiple times during the course of the reporting period, the coordinates and RFI level provided in this report were the result of an average of the individual observations from 18 December 2018 to 17 February 2019. SMAP science telemetry includes frequency information thus the RFI centre frequency was also identified for the RFI sources. A range was given if there appeared to be an observable bandwidth in the spectrum for the RFI source. Multiple centre frequencies were given if there were multiple peaks across the 16 sub-bands that were obviously RFI (TA > 330 K).

TABLE 20

Interference source detail log
Number of active sources listed: [18]

Source ID.	Observed geolocation		Centre frequency (MHz)	Source detection characteristics	Level of interference detected by sensor (K)	e.i.r.p. of transmitting source(s) (dBW)	City/ State/ Region	Number of observations	Last seen (UTC)	Present status (status as per 17/02/2019)
	Longitude (degrees)	Latitude (degrees)								
TUR-1	27.95	40.33	1 412	Point source	1136	−7.655 1		24	12/02/2019 4:49	ON
TUR-2	43.72	37.56	1 403, 1 421	Point source	1479	−6.509 2		17	13/02/2019 3:48	ON
TUR-3	29.35	40.83	1 403, 1 421	Point source	1512	−6.413 4		16	14/02/2019 4:25	ON
TUR-4	42.17	37.75	1 414	Point source	201	−15.177		45	16/02/2019 15:01	ON
TUR-5	39.89	40.8	1 407, 1 412	Point source	200	−15.198 6		89	16/02/2019 15:02	ON
TUR-6	33.41	38.4	1 402, 1 407	Point source	227	−14.648 7		84	16/02/2019 15:02	ON
TUR-7	28.45	37.98	1 418-1 420	Point source	221	−14.765		25	17/02/2019 4:38	ON
TUR-8	27.65	38.5	1 413-1 415	Point source	208	−15.028 3		40	15/02/2019 16:01	ON
TUR-9	26.75	39.59	1 400, 1 414, 1 424	Point source	113	−17.678 1		75	17/02/2019 4:35	ON
TUR-10	36.92	37.58	1 414	Point source	96	−18.386 2		49	14/02/2019 15:26	ON
TUR-11	40.22	37.91	1 407, 1 414	Point source	256	−14.126 5		45	16/02/2019 15:02	ON
TUR-12	32.4	37.87	1 421	Point source	90	−18.666 5		48	23/01/2019 4:01	ON

TABLE 20 (*end*)

Source ID.	Observed geolocation		Centre frequency (MHz)	Source detection characteristics	Level of interference detected by sensor (K)	e.i.r.p. of transmitting source(s) (dBW)	City/ State/ Region	Number of observations	Last seen (UTC)	Present status (status as per 17/02/2019)
	Longitude (degrees)	Latitude (degrees)								
TUR-13	27.74	37.75	1 421	Point source	136	−16.873 5		18	4/02/2019 4:50	ON
TUR-14	27.27	37.05	1 404, 1 411	Point source	92	−18.571		32	14/02/2019 4:24	ON
TUR-15	30.56	37.46	1 404, 1 421	Point source	34	−22.894 1		23	17/02/2019 4:35	ON
TUR-16	36.02	36.3	1 404	Point source	76	−19.400 8		29	14/02/2019 15:24	ON
TUR-17	34.04	37.53	1 404	Point source	29	−23.584 9		20	9/02/2019 15:38	ON
TUR-18	32.09	41.46	1 404, 1 412	Point source	22	−24.784 7		22	14/02/2019 15:27	ON

6.7.11.3 Supporting information

Figure 44 shows the peak hold plot over Turkey on a 0.25° × 0.25° grid of horizontally polarized TAs in kelvin before RFI filtering. Figure 45 shows a map on a 0.25° × 0.25° grid of the percentage of observations. Figure 46 shows the location and intensity of RFI sources over Turkey.

FIGURE 44

Peak hold plot over Turkey on a 0.25° × 0.25° grid of horizontally polarized TAs in kelvin before RFI filtering over the time period of 06/02/2019 to 12/02/2019

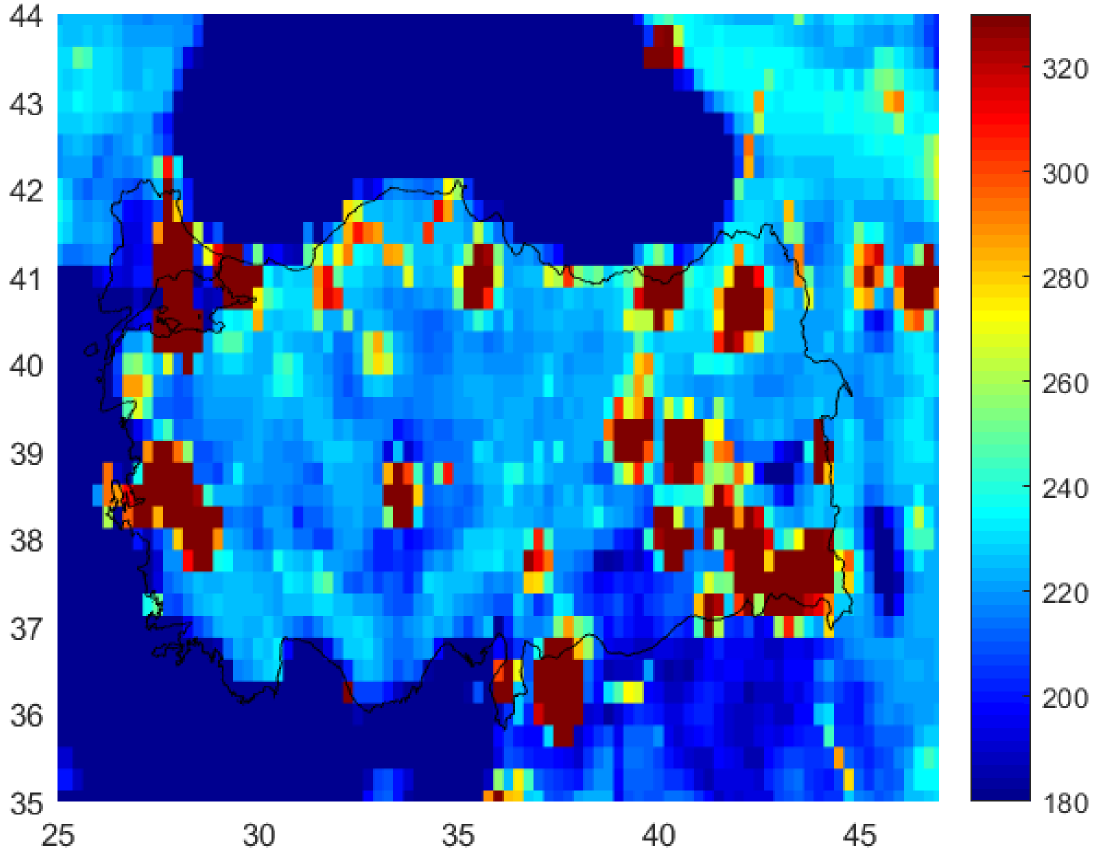

Note to Fig. 44: Similar results were seen in the vertical polarization. A 'peak hold' plot (i.e. the maximum value observed) emphasized large RFI contributions since geophysical contributions to the brightness background were also included. The colour scale was limited to values from 180 K to 330 K. Footprints with TA equal to or lower than 180 K appear dark blue and those that are 330 K and above are dark red. Any value greater than 330 K was automatically flagged as RFI since this is the geophysical limit for brightness temperature measurements.

FIGURE 45

Map on a 0.25° × 0.25° grid of the percentage of observations over the period December 2018 to February 2019 with a detected RFI level of 5 K or more in the horizontal polarization

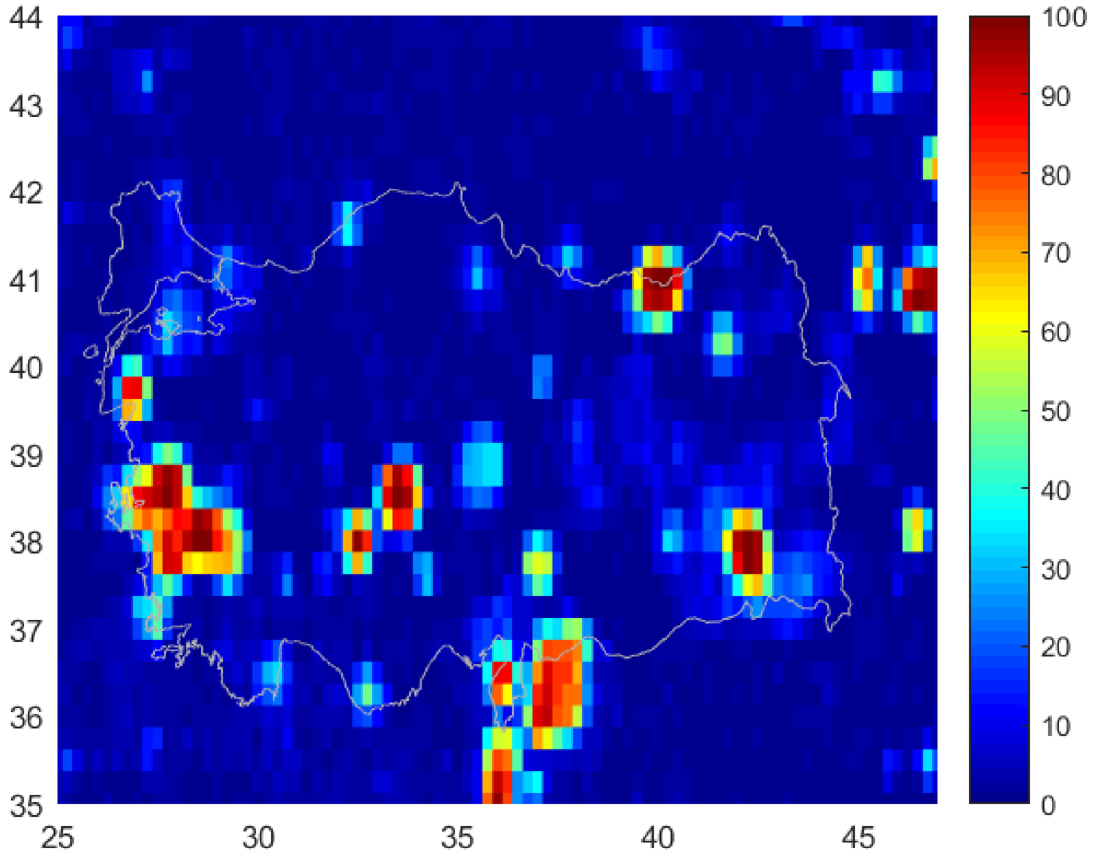

Note to Fig. 45: Vertical polarization showed similar results. Points having values greater than approximately 25-30% (i.e. light blue to red) were persistent sources of interference during this period. This plot does not distinguish between large amplitude and small amplitude, but rather highlights the temporal persistence of specific sources.

FIGURE 46

Location and intensity of RFI sources over Turkey

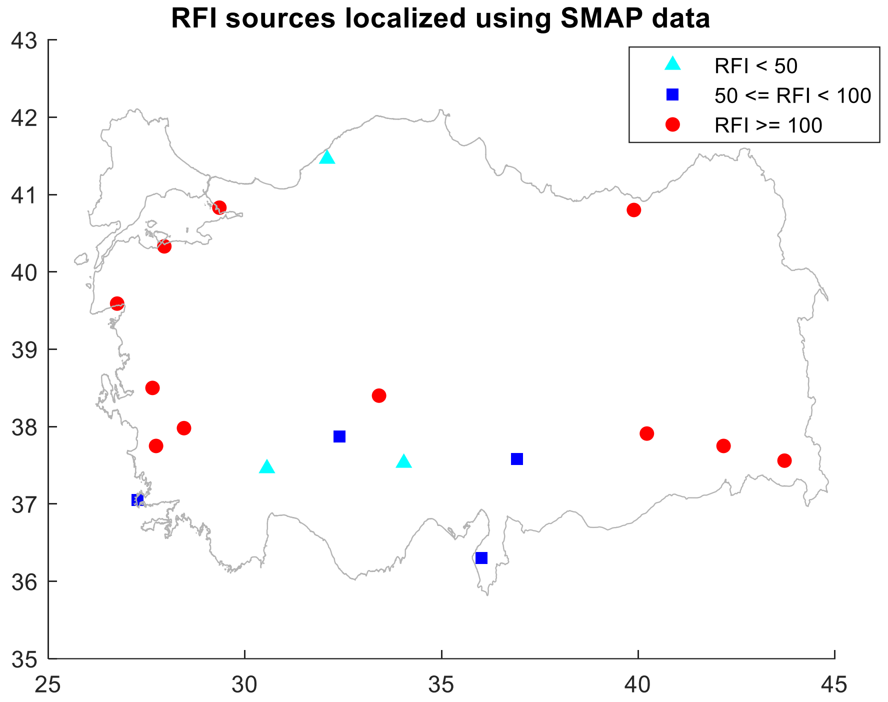

Note to Fig. 46: These locations can be easily seen in the probability and peak hold maps. The colours indicate range of RFI level in kelvin.

6.7.11.4 Classification of RFI sources per intensity over Turkey (status as of 17/02/2019)

A general summary of the prevalence of RFI sources over Turkey is summarized from Table 20 as follows:

Very strong RFI (RFI level ≥ 100 K)	11 RFI sources
Strong RFI (50 K ≤ RFI level < 100 K)	4 RFI sources
Moderate RFI (RFI level < 50 K)	3 RFI sources

6.7.12 Report of observed RFI over Democratic Republic of the Congo over a two-month timeframe from 18 December 2018 to 17 February 2018

6.7.12.1 Summary of the RFI sources over the Democratic Republic of the Congo

Table 21 defines the fields in the Summary of RFI sources form that were completed by the USA reporting an RFI event over the Democratic Republic of the Congo.

TABLE 21

Summary of RFI sources

Date of this RFI status update	18 December 2018 to 17 February 2019
Total number of RFI cases detected	5
Active RFI sources	5 reported
** **Old RFI active sources**	N/A
** **New RFI active sources**	5 reported, see Table 22 for RFI level and geolocation details
RFI sources OFF	N/A

6.7.12.2 Geolocation and other detailed RFI information

Table 22 includes the following detailed information for the RFI source: latitude and longitude, centre frequency, average RFI level in kelvin, number of observations used to geolocate the source and determine RFI level where the source was located as well as the time the source was last seen as of this writing. There were five sources identified over the Democratic Republic of the Congo. Data from 18 December 2018 to 17 February 2019 was used to create Table 22 as well as supporting Figures.

The localization of RFI sources was based on the difference between SMAP measurements before and after RFI filtering. This difference corresponded to the effect that RFI has on the data. A machine learning algorithm was then applied to automatically find the points where the effect of RFI is highest (local maxima). These points define the location of RFI sources. Since every RFI source was observed multiple times during the course of the reporting period, the coordinates and RFI level provided in this report were the result of an average of the individual observations from 18 December 2018 to 17 February 2019. SMAP science telemetry includes frequency information thus the RFI centre frequency was also identified for the RFI sources. A range was given if there appeared to be an observable bandwidth in the spectrum for the RFI source. Multiple centre frequencies were given if there were multiple peaks across the 16 sub-bands that were obviously RFI (TA > 330 K).

TABLE 22

Interference source detail log
Number of active sources listed: [5]

Source ID.	Observed geolocation		Centre frequency (MHz)	Source detection characteristics	Level of interference detected by sensor (K)	e.i.r.p. of transmitting source(s) (dBW)	City/ State/ Region	Number of observations	Last seen (UTC)	Present status (status as per 17/02/2019)
	Longitude (degrees)	Latitude (degrees)								
DRC-1	28.83	−2.46	1 403, 1 408-1 412, 1 424	Point source	766	−9.366 6		71	15/02/2019 15:52	ON
DRC-2	15.31	−4.31	1 402-1 404, 1 407-1 411, 1 413-1 417	Point source	245	−14.317 3		67	17/02/2019 17:05	ON
DRC-3	29.48	0.57	1 400, 1 407-1 412, 1 424	Point source	288	−13.615		71	15/02/2019 15:53	ON
DRC-4	29.26	−1.59	1 424	Point source	129	−17.103		46	15/02/2019 15:52	ON
DRC-5	25	−8.72	1 424	Point source	64	−20.147 1		62	13/02/2019 4:00	ON

6.7.12.3 Supporting information

Figure 47 shows the peak hold plot over the Democratic Republic of the Congo on a 0.25° × 0.25° grid of horizontally polarized TA in kelvin before RFI filtering. Figure 48 shows a map of observed RFI on a 0.25° × 0.25° grid of the percentage of observations with a detected RFI level of 5 K or more in the horizontal polarization. Figure 49 shows the location and intensity of RFI sources over the Democratic Republic of the Congo.

FIGURE 47

Peak hold plot over the Democratic Republic of the Congo on a 0.25° × 0.25° grid of horizontally polarized TAs in kelvin before RFI filtering over the time period of 06/02/2019 to 12/02/2019

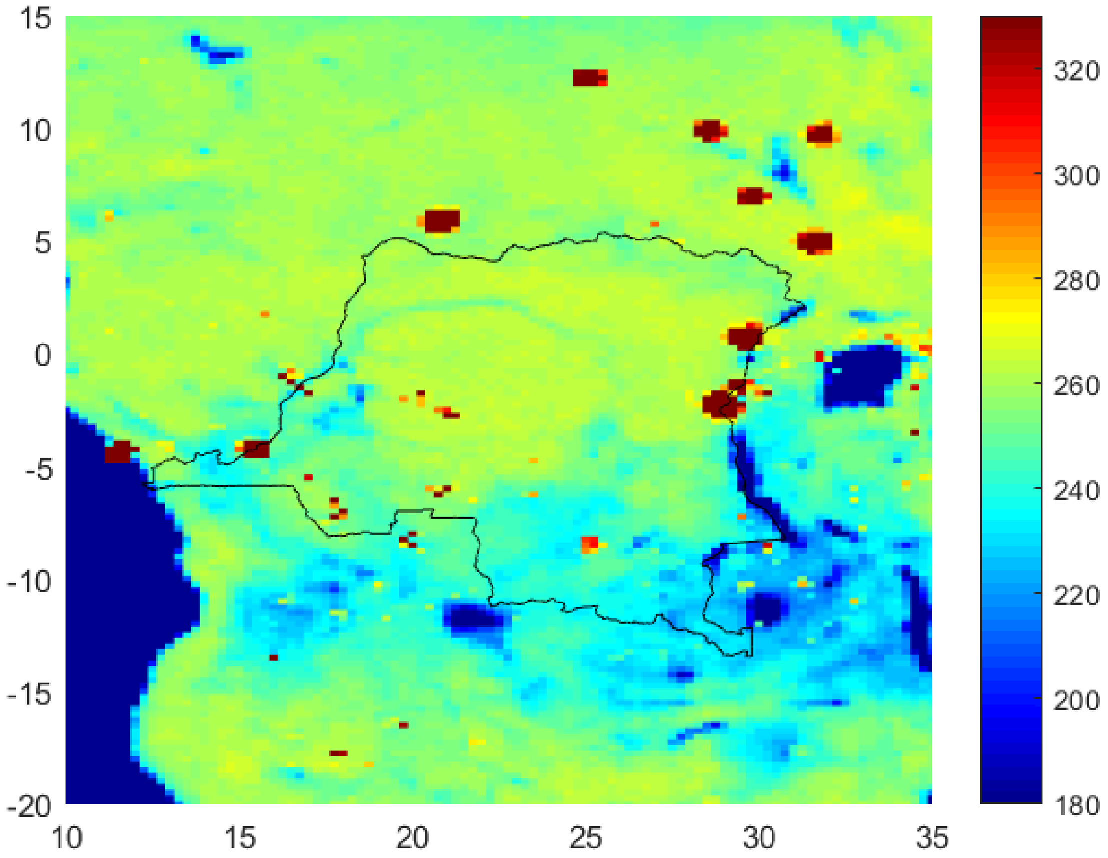

Note to Fig. 47: Similar results were seen in the vertical polarization. A ‘peak hold’ plot (i.e. the maximum value observed) emphasized large RFI contributions since geophysical contributions to the brightness background were also included. The colour scale was limited to values from 180 K to 330 K. Footprints with TA equal to or lower than 180 K appear dark blue and those that are 330 K and above are dark red. Any value greater than 330 K was automatically flagged as RFI since this is the geophysical limit for brightness temperature measurements.

FIGURE 48

Map on a 0.25° × 0.25° grid of the percentage of observations over the period December 2018 to February 2019 with a detected RFI level of 5 K or more in the horizontal polarization

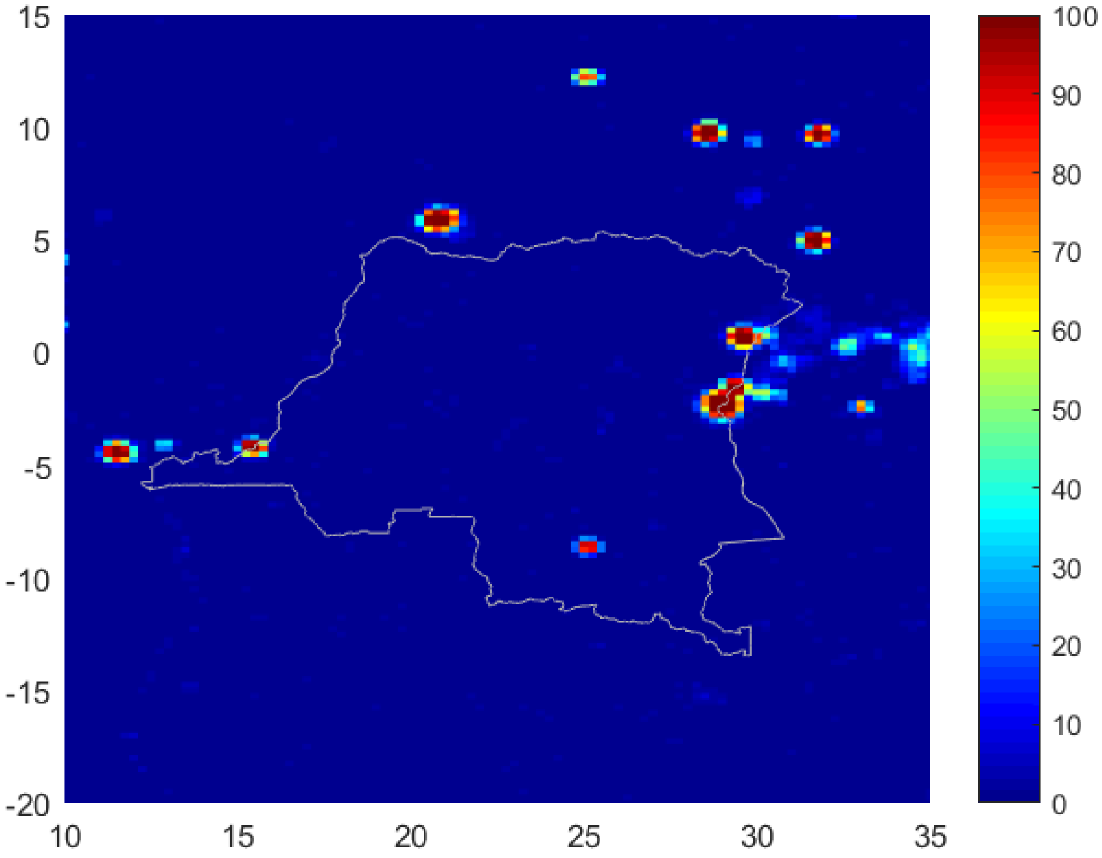

Note to Fig. 48: Vertical polarization showed similar results. Points having values greater than approximately 25 to 30% (i.e. light blue to red) were persistent sources of interference during this period. This plot does not distinguish between large amplitude and small amplitude, but rather highlights the temporal persistence of specific sources.

FIGURE 49

Location and intensity of RFI sources over the Democratic Republic of the Congo

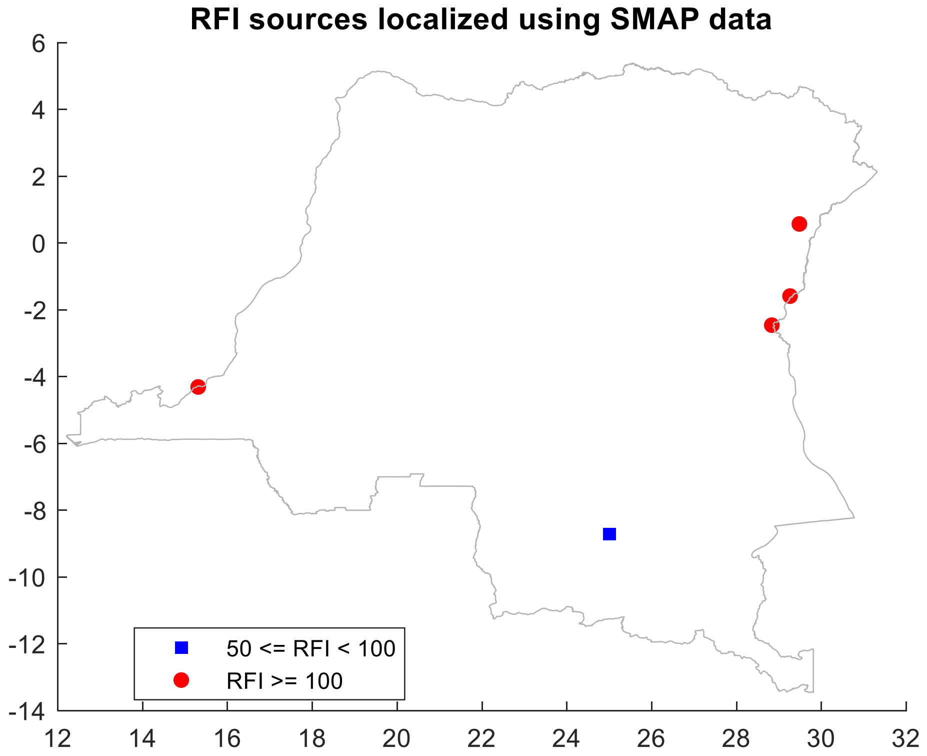

Note to Fig. 49: These locations can be easily seen in the probability and peak hold maps. The colours indicate range of RFI level in kelvin.

6.7.12.4 Classification of RFI sources per intensity over the Democratic Republic of the Congo (status as of 17/02/2019)

A general summary of the prevalence of RFI sources over the Democratic Republic of the Congo is summarized from Table 22 as follows:

Very strong RFI (RFI level ≥ 100 K) 4 RFI sources

Strong RFI (50 K ≤ RFI level < 100 K) 1 RFI sources

6.7.13 Report of observed RFI over the Republic of Azerbaijan over a three-month timeframe from 2 January 2019 to 1 April 2019

6.7.13.1 Summary of the RFI sources over the Republic of Azerbaijan

Table 23 defines the fields in the Summary of RFI sources form that should be completed by the administration reporting an RFI event.

TABLE 23

Summary of RFI sources

Date of this RFI status update	2 January 2019 to 1 April 2019
Total number of RFI cases detected	6
Active RFI sources	6 reported
** **Old RFI active sources**	N/A
** **New RFI active sources**	6 reported, see Table 24 for RFI level and geolocation details
RFI sources OFF	N/A

6.7.13.2 Geolocation and other detailed RFI information

Table 24 includes the following detailed information for the RFI source: latitude and longitude, centre frequency, average RFI level in kelvin, number of observations used to geolocate the source and determine RFI level where the source is located as well as the time the source was last seen as of this writing. There are six sources identified over the Republic of Azerbaijan. Data from 2 January 2019 to 1 April 2019 was used to create Table 24 as well as supporting Figures.

The localization of RFI sources is based on the difference between SMAP measurements before and after RFI filtering. This difference corresponds to the effect that RFI has on the data. A machine learning algorithm is then applied to automatically find the points where the effect of RFI is highest (local maxima). These points define the location of RFI sources. Since every RFI source is observed multiple times during the course of the reporting period, the coordinates and RFI level provided in this report are the result of an average of the individual observations from 2 January 2019 to 1 April 2019. SMAP science telemetry includes frequency information thus the RFI centre frequency was also identified for the RFI sources. See appendix for spectral plots. A range is given if there appeared to be an observable bandwidth in the spectrum for the RFI source. Multiple centre frequencies were given if there were multiple peaks across the 16 sub-bands that were obviously RFI (TA > 330 K).

TABLE 24

Interference source detail log
Number of active sources listed: [6]

Source ID.	Observed geolocation		Centre frequency (MHz)	Source detection characteristics	Level of interference detected by sensor in kelvin	e.i.r.p. of transmitting source(s) (dBW)	City/ State/ Region	Number of observations	Last seen (UTC)	Present status
	Longitude (degrees)	Latitude (degrees)								
AZE-1	47.62	39.9	1 400-1 418, 1 424	Point source	444	−11.735 1		149	1/04/2019 14:13	ON
AZE-2	47.64	39.84	1 400-1 418, 1 424	Point source	480	−11.396 5		98	1/04/2019 14:13	ON
AZE-3	46.31	40.73	1 400-1 409, 1 424	Point source	170	−15.904 4		110	1/04/2019 14:14	ON
AZE-4	48.26	38.77	1 400-1 409, 1 424	Point source	113	−17.678 1		132	1/04/2019 14:13	ON
AZE-5	47.05	40.76	1 400-1 409, 1 424	Point source	157	−16.249 9		39	30/03/2019 3:35	ON
AZE-6	49.4	40.79	1 400, 1 424	Point source	68	−19.883 8		34	4/02/2019 14:14	ON

6.7.13.3 Supporting information

Figure 50 shows the peak hold plot over the Republic of Azerbaijan on a 0.25° × 0.25° grid of horizontally polarized TAs in kelvin before RFI filtering. Figure 51 shows a map on a 0.25° × 0.25° grid of the percentage of observations over the period 2 January 2019 to 1 April 2019 with a detected RFI level of 5 K or more in the horizontal polarization. Figure 52 shows location and intensity of RFI sources over the Republic of Azerbaijan.

FIGURE 50

Peak hold plot over the Republic of Azerbaijan on a 0.25° × 0.25° grid of horizontally polarized TAs in kelvin before RFI filtering over the time period of 02/01/2019 to 01/04/2019

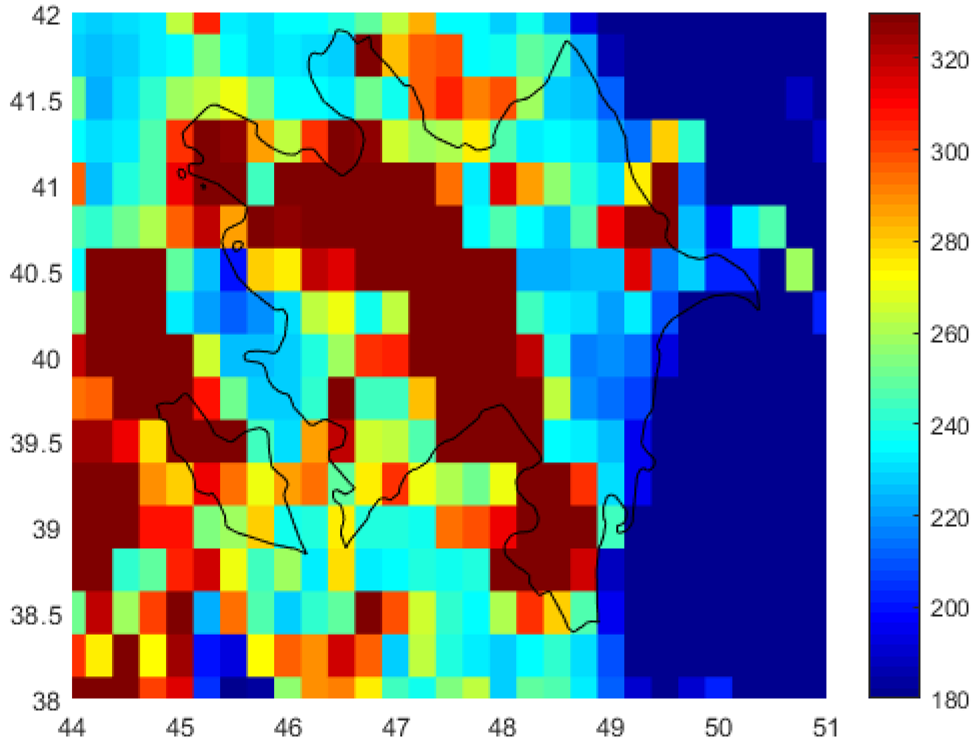

Note to Fig. 50: Similar results are seen in the vertical polarization. A 'peak hold' plot (i.e. the maximum value observed) emphasizes large RFI contributions since geophysical contributions to the brightness background are also included. The colour scale is limited to values from 180 K to 330 K. Footprints with TA equal to or lower than 180 K appear dark blue and those that are 330 K and above are dark red. Any value greater than 330 K is automatically flagged as RFI since this is the geophysical limit for brightness temperature measurements.

FIGURE 51

Map on a 0.25° × 0.25° grid of the percentage of observations over the period 02/01/2019 to 01/04/2019 with a detected RFI level of 5 K or more in the horizontal polarization

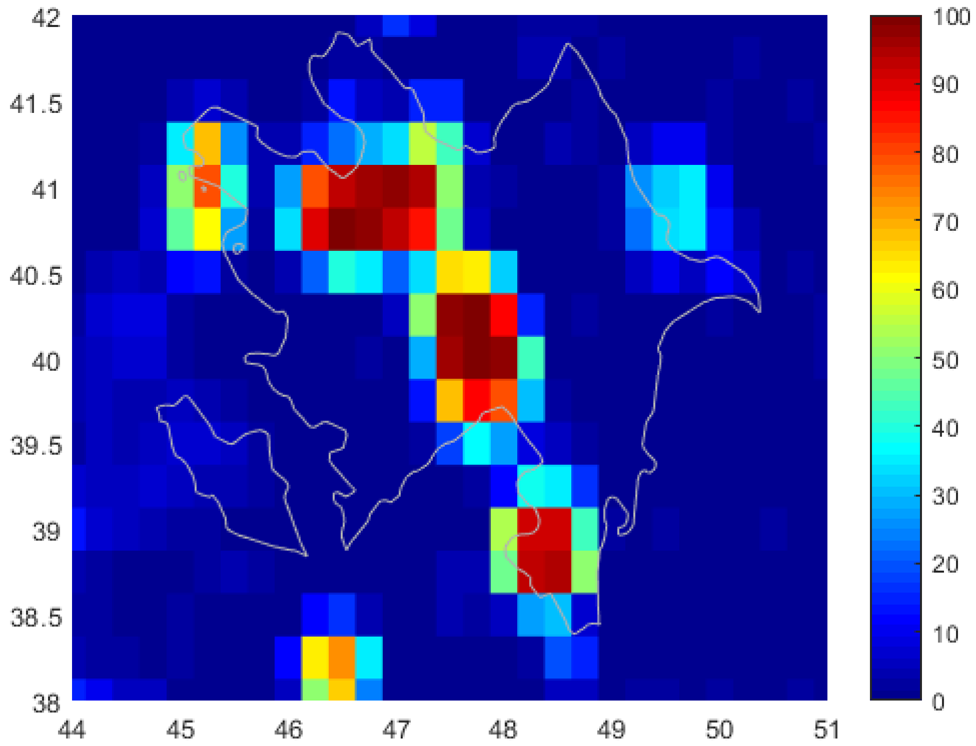

Note to Fig. 51: Vertical polarization shows similar results. Points having values greater than approximately 25 to 30% (i.e. light blue to red) are persistent sources of interference during this period. This plot does not distinguish between large amplitude and small amplitude, but rather highlights the temporal persistence of specific sources.

FIGURE 52

Location and intensity of RFI sources over the Republic of Azerbaijan

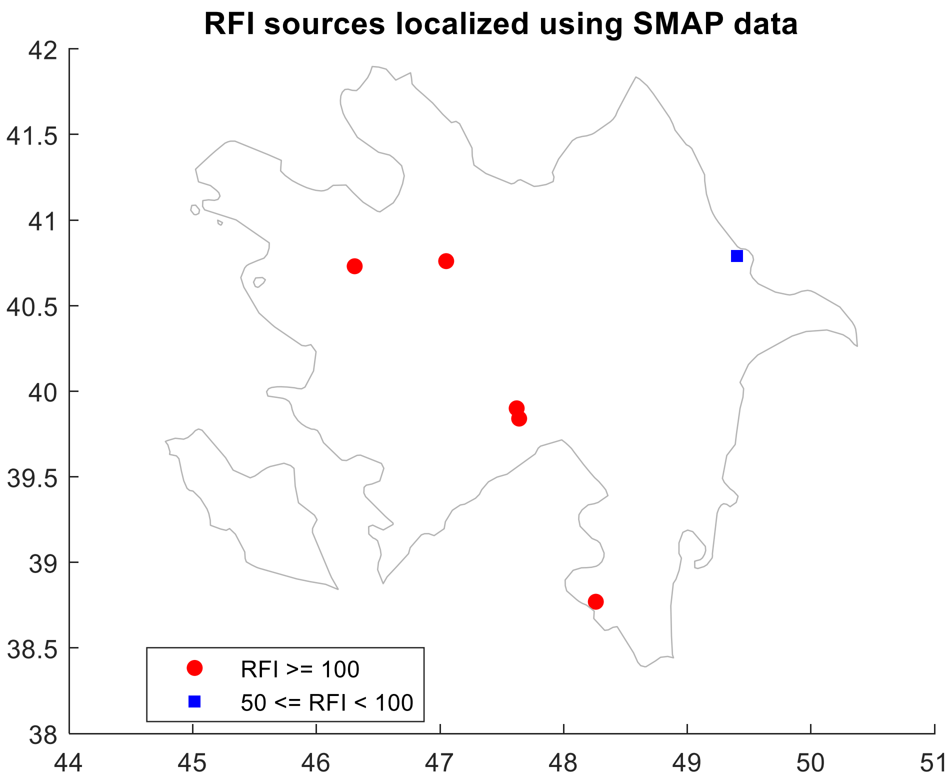

Note to Fig. 52: These locations can be easily seen in the probability and peak hold maps. The colours indicate range of RFI level in kelvin.

6.7.13.4 Classification of RFI sources per intensity (status as of 01/04/2019)

A general summary of the prevalence of RFI sources over the Republic of Azerbaijan is summarized from Table 24 as follows:

Very strong RFI (RFI level ≥ 100 K)	5 RFI sources
Strong RFI (50 K ≤ RFI level < 100 K)	1 RFI source

6.7.14 Report of observed RFI over the United Republic of Tanzania over a three-month timeframe from 2 January 2019 to 1 April 2019

6.7.14.1 Summary of the RFI sources over the United Republic of Tanzania

Table 25 defines the fields in the Summary of RFI sources form that should be completed by the administration reporting an RFI event.

TABLE 25

Summary of RFI sources

Date of this RFI status update	2 January 2019 to 1 April 2019
Total number of RFI cases detected	2
Active RFI sources	2 reported
** **Old RFI active sources**	N/A
** **New RFI active sources**	2 reported, see Table 26 for RFI level and geolocation details
RFI sources OFF	N/A

6.7.14.2 Geolocation and other detailed RFI information

Table 26 includes the following detailed information for the RFI source: latitude and longitude, centre frequency, average RFI level in kelvin, number of observations used to geolocate the source and determine RFI level where the source is located as well as the time the source was last seen as of this writing. There are 2 sources identified over the United Republic of Tanzania. Data from 2 January 2019 to 1 April 2019 was used to create Table 26 as well as supporting Figures.

The localization of RFI sources is based on the difference between SMAP measurements before and after RFI filtering. This difference corresponds to the effect that RFI has on the data. A machine learning algorithm is then applied to automatically find the points where the effect of RFI is highest (local maxima). These points define the location of RFI sources. Since every RFI source is observed multiple times during the course of the reporting period, the coordinates and RFI level provided in this Report are the result of an average of the individual observations from 2 January 2019 to 1 April 2019. SMAP science telemetry includes frequency information thus the RFI centre frequency was also identified for the RFI sources. See appendix for spectral plots. A range is given if there appeared to be an observable bandwidth in the spectrum for the RFI source. Multiple centre frequencies were given if there were multiple peaks across the 16 sub-bands that were obviously RFI (TA > 330 K).

TABLE 26

Interference source detail log
Number of active sources listed: [2]

Source ID.	Observed geolocation		Centre frequency (MHz)	Source detection characteristics	Level of interference detected by sensor (K)	e.i.r.p. of transmitting source(s) (dBW)	City/ State/Region	Number of observations	Last seen (UTC)	Present status
	Longitude (degrees)	Latitude (degrees)								
TZA-1	39.26	−6.8	1 400-1 424	Point source	1 271	−7.17		121	1/04/2019 15:39	ON
TZA-2	32.92	−2.53	1 424	Point source	32	−23.16		80	1/04/2019 15:38	ON

6.7.14.3 Supporting information

Figure 53 shows the peak hold plot over the United Republic of Tanzania on a 0.25° × 0.25° grid of horizontally polarized TAs in kelvin before RFI filtering. Figure 54 shows a map on a 0.25° × 0.25° grid of the percentage of observations over the period 2 January 2019 to 1 April 2019 with a detected RFI level of 5 K or more in the horizontal polarization. Figure 55 shows location and intensity of RFI sources over the United Republic of Tanzania.

FIGURE 53

Peak hold plot over the United Republic of Tanzania on a 0.25° × 0.25° grid of horizontally polarized TAs in kelvin before RFI filtering over the time period of 02/01/2019 to 01/04/2019

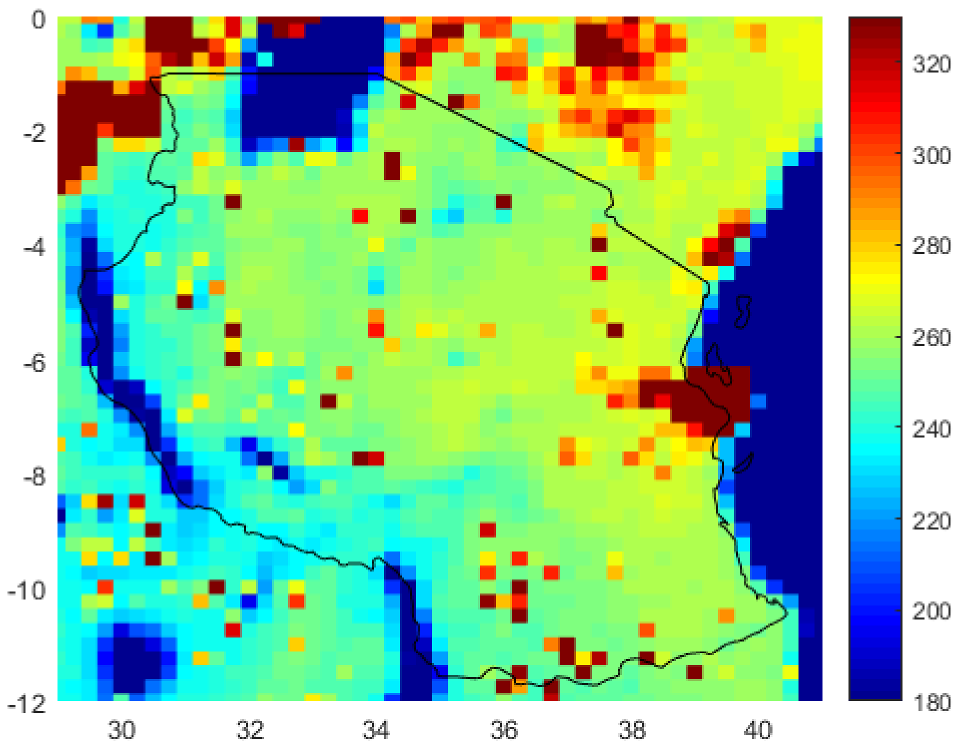

Note to Fig. 53: Similar results are seen in the vertical polarization. A 'peak hold' plot (i.e. the maximum value observed) emphasizes large RFI contributions since geophysical contributions to the brightness background are also included. The colour scale is limited to values from 180 K to 330 K. Footprints with TA equal to or lower than 180 K appear dark blue and those that are 330 K and above are dark red. Any value greater than 330 K is automatically flagged as RFI since this is the geophysical limit for brightness temperature measurements.

FIGURE 54

Map on a 0.25° × 0.25° grid of the percentage of observations over the period 02/01/2019 to 01/04/2019 with a detected RFI level of 5 K or more in the horizontal polarization

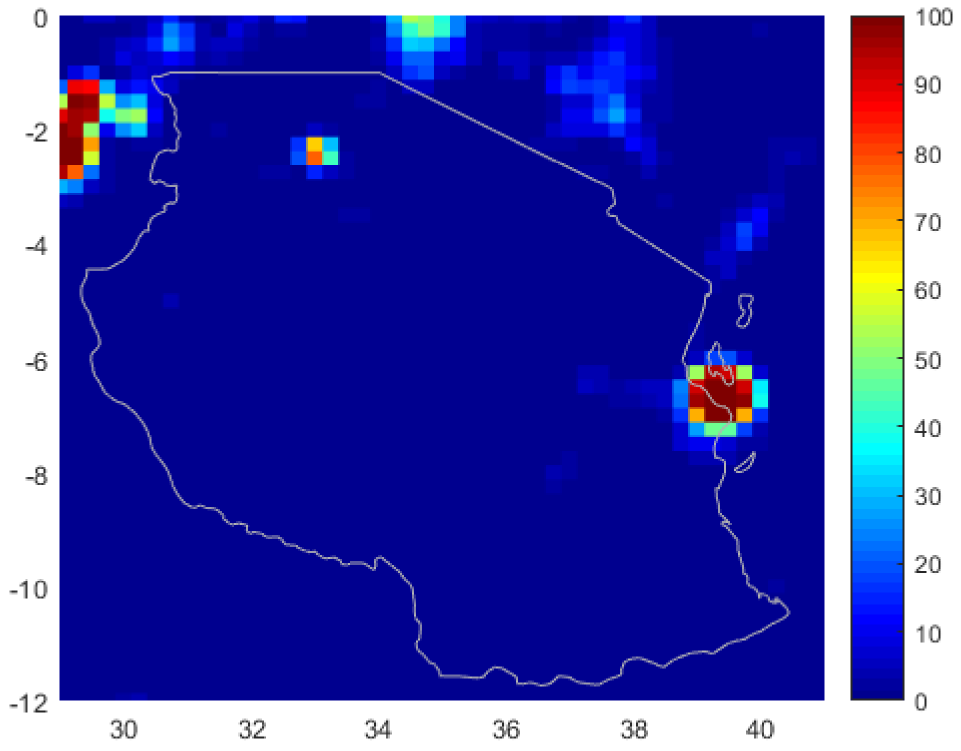

Note to Fig. 54: Vertical polarization shows similar results. Points having values greater than approximately 25 to 30% (i.e. light blue to red) are persistent sources of interference during this period. This plot does not distinguish between large amplitude and small amplitude, but rather highlights the temporal persistence of specific sources.

FIGURE 55

Location and intensity of RFI sources over the United Republic of Tanzania

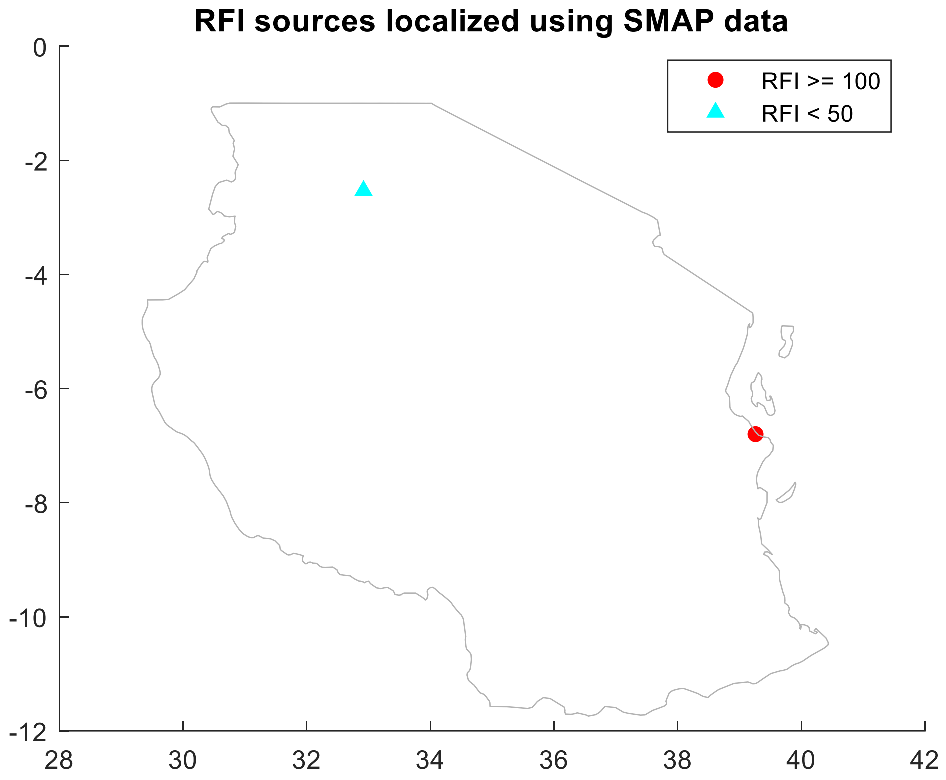

Note to Fig. 55: These locations can be easily seen in the probability and peak hold maps. The colours indicate range of RFI level in kelvin.

6.7.14.4 Classification of RFI sources per intensity (status as of 01/04/2019)

A general summary of the prevalence of RFI sources over the United Republic of Tanzania is summarized from Table 26 as follows:

Very strong RFI (RFI level ≥ 100 K)	1 RFI source
Moderate RFI (RFI level < 50 K)	1 RFI source

6.7.15 Report of observed RFI over the Republic of Croatia over a three-month timeframe from 26 February 2019 to 27 May 2019

6.7.15.1 Summary of the RFI sources over the Republic of Croatia

Table 27 defines the fields in the Summary of RFI sources form that should be completed by the administration reporting an RFI event.

TABLE 27

Summary of RFI sources

Date of this RFI status update	26 February 2019 to 27 May 2019
Total number of RFI cases detected	5
Active RFI sources	5 reported
** **Old RFI active sources**	N/A
** **New RFI active sources**	5 reported, see Table 28 for RFI level and geolocation details
RFI sources OFF	N/A

6.7.15.2 Geolocation and other detailed RFI information

Table 28 includes the following detailed information for the RFI source: latitude and longitude, centre frequency, average RFI level in kelvin, number of observations used to geolocate the source and determine RFI level where the source is located as well as the time the source was last seen as of this writing. There are five sources identified over the Republic of Croatia. Data from 26 February 2019 to 27 May 2019 was used to create Table 28 as well as supporting Figures.

The localization of RFI sources is based on the difference between SMAP measurements before and after RFI filtering. This difference corresponds to the effect that RFI has on the data. A machine learning algorithm is then applied to automatically find the points where the effect of RFI is highest (local maxima). These points define the location of RFI sources. Since every RFI source is observed multiple times during the course of the reporting period, the coordinates and RFI level provided in this report are the result of an average of the individual observations from 26 February 2019 to 27 May 2019. SMAP science telemetry includes frequency information thus the RFI centre frequency was also identified for the RFI sources. See appendix for spectral plots. A range is given if there appeared to be an observable bandwidth in the spectrum for the RFI source. Multiple centre frequencies were given if there were multiple peaks across the 16 sub-bands that were obviously RFI (TA > 330 K).

TABLE 28

Interference source detail log
Number of active sources listed: [5]

Source ID.	Observed geolocation		Centre frequency (MHz)	Source detection characteristics	Level of interference detected by sensor (K)	e.i.r.p. of transmitting source(s) (dBW)	City/ State/Region	Number of observations	Last seen (UTC)	Present status
	Longitude (degrees)	Latitude (degrees)								
HRV-1	16.03	45.87	1 400, 1 412, 1 424	Point source	268	−13.93		151	25/05/2019 16:19	ON
HRV-2	17.6	45.53	1 410, 1 422	Point source	207	−15.05		99	27/05/2019 15:52	ON
HRV-3	17.37	42.97	1 406, 1 420	Point source	399	−12.20		125	25/05/2019 16:18	ON
HRV-4	14.19	45.29	1 406, 1 410, 1 422	Point source	285	−13.66		117	25/05/2019 16:18	ON
HRV-5	18.76	45.32	1 407, 1 422	Point source	174	−15.80		85	27/05/2019 15:52	ON

6.7.15.3 Supporting information

Figure 56 shows the peak hold plot over the United Republic of Croatia on a 0.25° × 0.25° grid of horizontally polarized TAs in kelvin before RFI filtering. Figure 57 shows a map on a 0.25° × 0.25° grid of the percentage of observations over the period 26 February 2019 to 27 May 2019 with a detected RFI level of 5 K or more in the horizontal polarization. Figure 58 shows location and intensity of RFI sources over the United Republic of Croatia.

FIGURE 56

Peak hold plot over the Republic of Croatia on a 0.25° × 0.25° grid of horizontally polarized TAs in kelvin before RFI filtering over the time period of 26/02/2019 to 27/05/2019

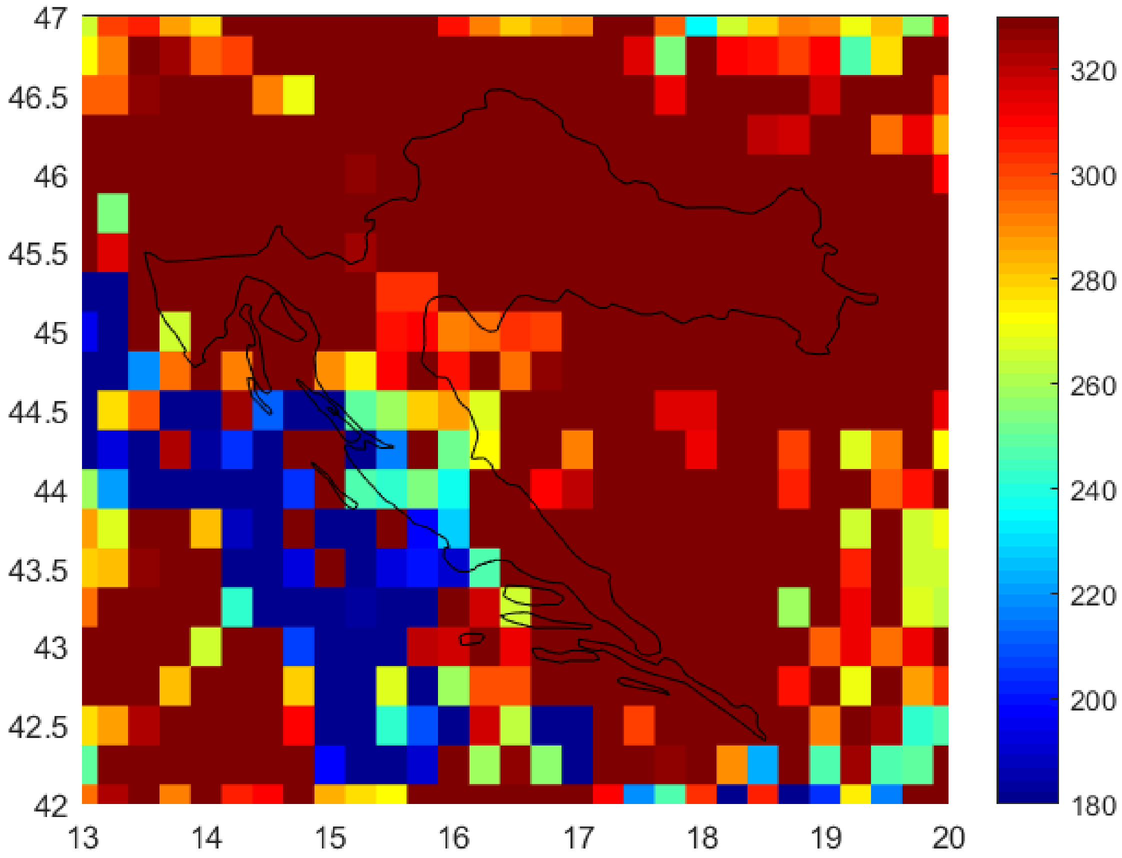

Note to Fig. 56: Similar results are seen in the vertical polarization. A 'peak hold' plot (i.e. the maximum value observed) emphasizes large RFI contributions since geophysical contributions to the brightness background are also included. The colour scale is limited to values from 180 K to 330 K. Footprints with TA equal to or lower than 180 K appear dark blue and those that are 330 K and above are dark red. Any value greater than 330 K is automatically flagged as RFI since this is the geophysical limit for brightness temperature measurements.

FIGURE 57

Map on a 0.25° × 0.25° grid of the percentage of observations over the period 26/02/2019 to 27/05/2019 with a detected RFI level of 5 K or more in the horizontal polarization

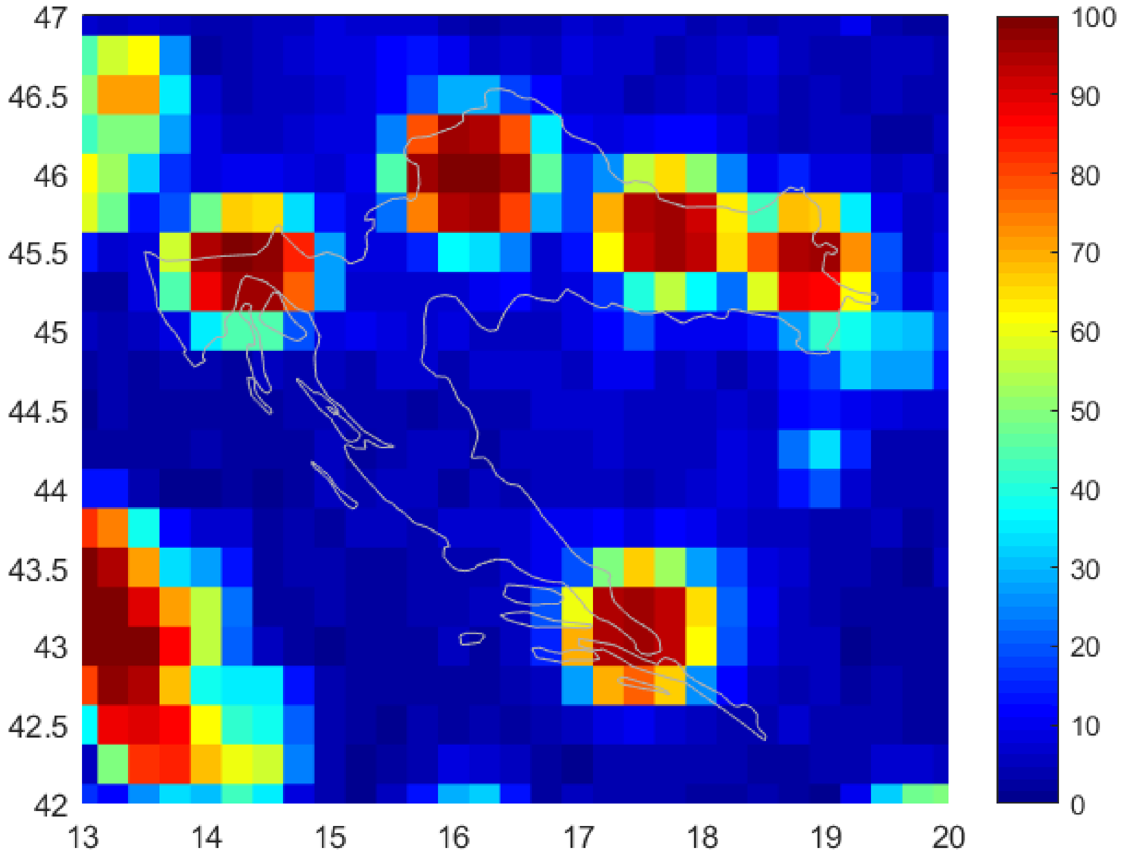

Note to Fig. 57: Vertical polarization shows similar results. Points having values greater than approximately 25 to 30% (i.e. light blue to red) are persistent sources of interference during this period. This plot does not distinguish between large amplitude and small amplitude, but rather highlights the temporal persistence of specific sources.

FIGURE 58

Location and intensity of RFI sources over the Republic of Croatia

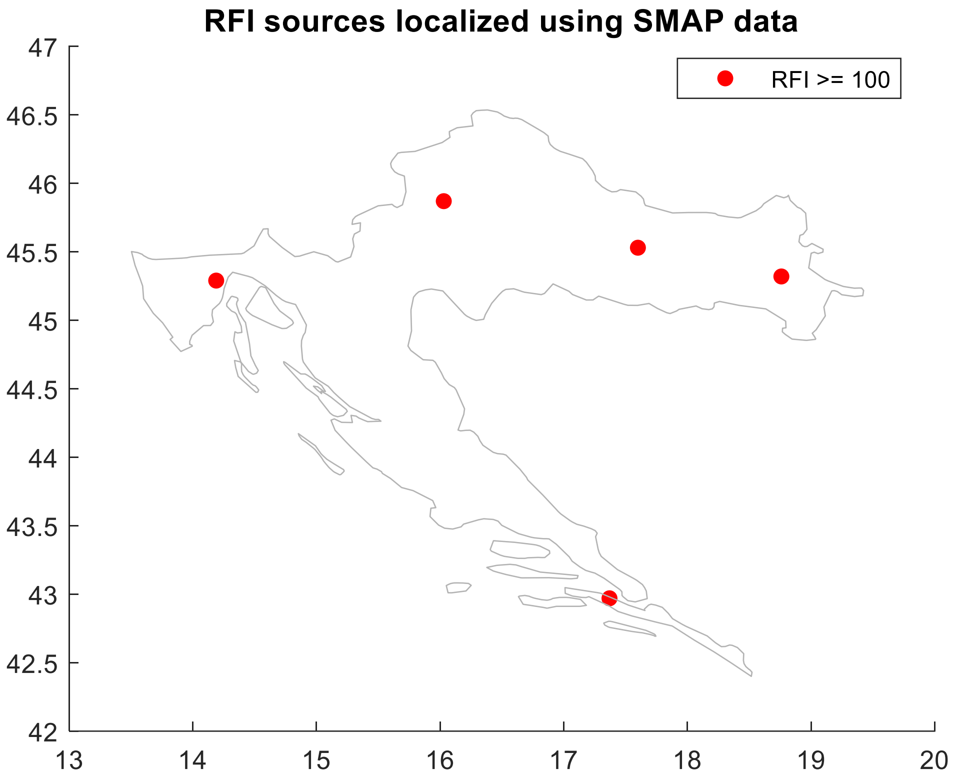

Note to Fig. 58: These locations can be easily seen in the probability and peak hold maps. The colour indicates range of RFI level in kelvin.

6.7.15.4 Classification of RFI sources per intensity (status as of 27/05/2019)

A general summary of the prevalence of RFI sources over the Republic of Croatia is summarized from Table 28 as follows:

Very strong RFI (RFI level ≥ 100 K) 5 RFI sources

6.7.16 Report of observed RFI over the Syrian Arab Republic over a three-month timeframe from 26 February 2019 to 27 May 2019

6.7.16.1 Summary of the RFI sources over the Syrian Arab Republic

Table 29 defines the fields in the Summary of RFI sources form that should be completed by the administration reporting an RFI event.

TABLE 29

Summary of RFI sources

Date of this RFI status update	26 February 2019 to 27 May 2019
Total number of RFI cases detected	5
Active RFI sources	5 reported
** **Old RFI active sources**	N/A
** **New RFI active sources**	5 reported, see Table 30 for RFI level and geolocation details
RFI sources OFF	N/A

6.7.16.2 Geolocation and other detailed RFI information

Table 30 includes the following detailed information for the RFI source: latitude and longitude, centre frequency, average RFI level in kelvin, number of observations used to geolocate the source and determine RFI level where the source is located as well as the time the source was last seen as of this writing. There are five sources identified over the Syrian Arab Republic. Data from 26 February 2019 to 27 May 2019 was used to create Table 30 as well as supporting Figures.

The localization of RFI sources is based on the difference between SMAP measurements before and after RFI filtering. This difference corresponds to the effect that RFI has on the data. A machine learning algorithm is then applied to automatically find the points where the effect of RFI is highest (local maxima). These points define the location of RFI sources. Since every RFI source is observed multiple times during the course of the reporting period, the coordinates and RFI level provided in this Report are the result of an average of the individual observations from 26 February 2019 to 27 May 2019. SMAP science telemetry includes frequency information thus the RFI centre frequency was also identified for the RFI sources. See appendix for spectral plots. A range is given if there appeared to be an observable bandwidth in the spectrum for the RFI source. Multiple centre frequencies were given if there were multiple peaks across the 16 sub-bands that were obviously RFI (TA > 330 K).

TABLE 30

Interference source detail log
Number of active sources listed: [5]

Source ID.	Observed geolocation		Centre frequency (MHz)	Source detection characteristics	Level of interference detected by sensor (K)	e.i.r.p. of transmitting source(s) (dBW)	City/ State/Region	Number of observations	Last seen (UTC)	Present status
	Longitude (degrees)	Latitude (degrees)								
SYR-1	37.42	36.18	1 400, 1 410, 1 421	Point source	666	−9.97		155	25/05/2019 3:37	ON
SYR-2	37.36	33.63	1 421	Point source	545	−10.85		54	20/05/2019 3:50	ON
SYR-3	36.32	33.34	1 408-1 420	Point source	532	−10.95		72	25/05/2019 3:36	ON
SYR-4	36.77	35.19	1 421	Point source	665	−9.98		19	23/05/2019 4:00	ON
SYR-5	40.17	35.32	1 420	Point source	563	−10.70		13	23/05/2019 4:00	ON

6.7.16.3 Supporting information

Figure 59 shows the peak hold plot over the Syrian Arabic Republic on a 0.25° × 0.25° grid of horizontally polarized TAs in kelvin before RFI filtering. Figure 60 shows a map on a 0.25° × 0.25° grid of the percentage of observations over the period 26 February 2019 to 27 May 2019 with a detected RFI level of 5 K or more in the horizontal polarization. Figure 61 shows location and intensity of RFI sources over the Syrian Arabic Republic.

FIGURE 59

Peak hold plot over the Syrian Arab Republic on a 0.25° × 0.25° grid of horizontally polarized TAs in kelvin before RFI filtering over the time period of 26/02/2019 to 27/05/2019

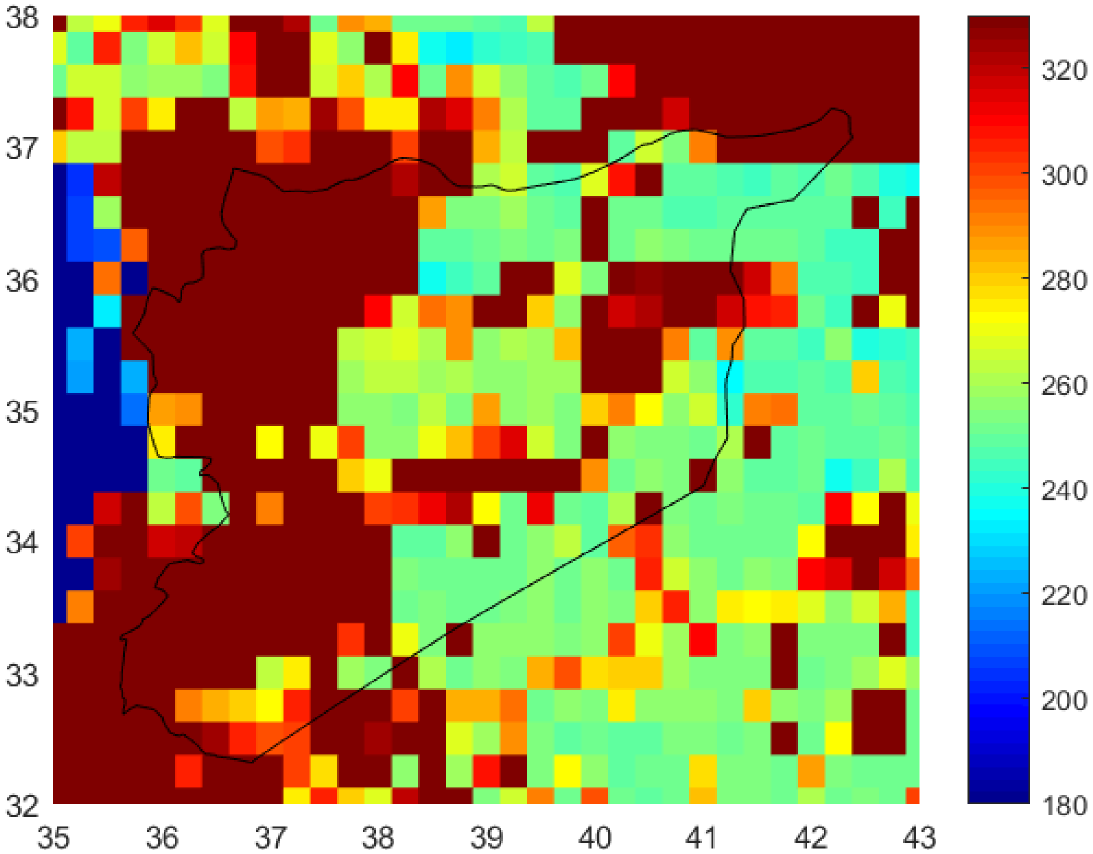

Note to Fig. 59: Similar results are seen in the vertical polarization. A ‘peak hold’ plot (i.e. the maximum value observed) emphasizes large RFI contributions since geophysical contributions to the brightness background are also included. The colour scale is limited to values from 180 K to 330 K. Footprints with TA equal to or lower than 180 K appear dark blue and those that are 330 K and above are dark red. Any value greater than 330 K is automatically flagged as RFI since this is the geophysical limit for brightness temperature measurements.

FIGURE 60

Map on a 0.25° × 0.25° grid of the percentage of observations over the period 26/02/2019 to 27/05/2019 with a detected RFI level of 5 K or more in the horizontal polarization

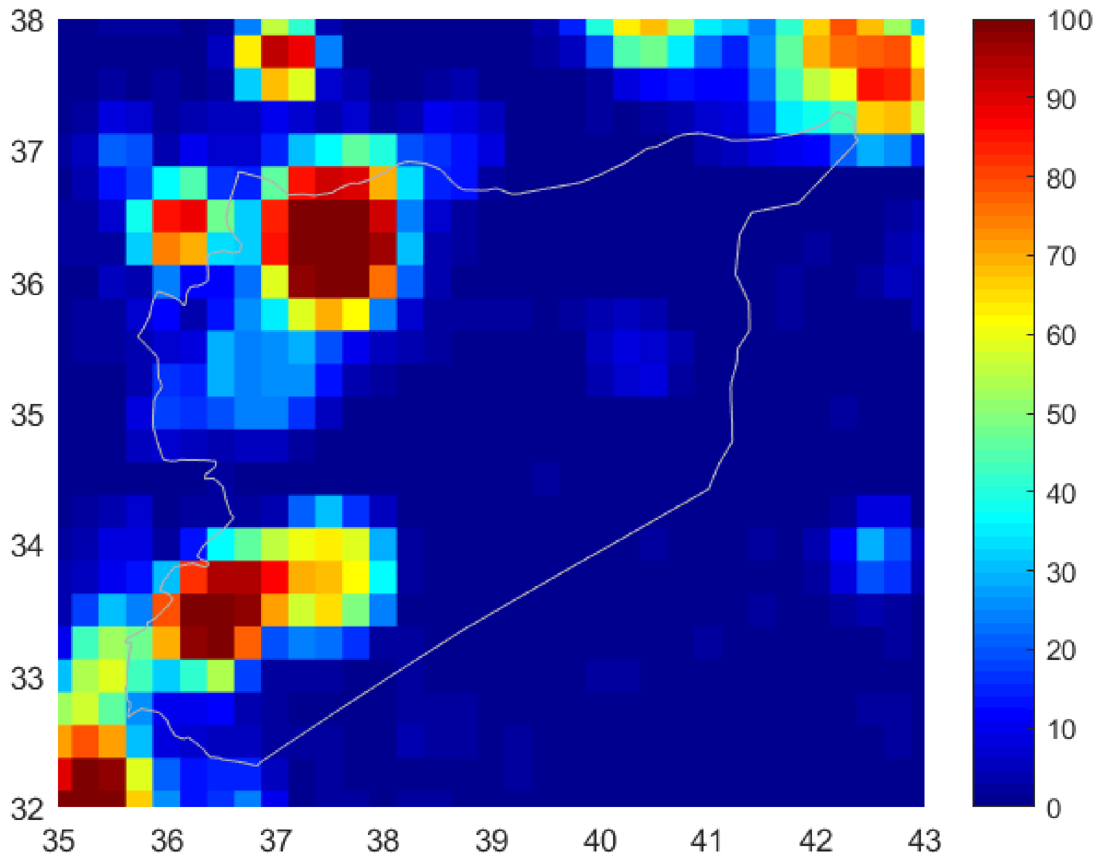

Note to Fig. 60: Vertical polarization shows similar results. Points having values greater than approximately 25 to 30% (i.e. light blue to red) are persistent sources of interference during this period. This plot does not distinguish between large amplitude and small amplitude, but rather highlights the temporal persistence of specific sources.

FIGURE 61

Location and intensity of RFI sources over the Syrian Arab Republic

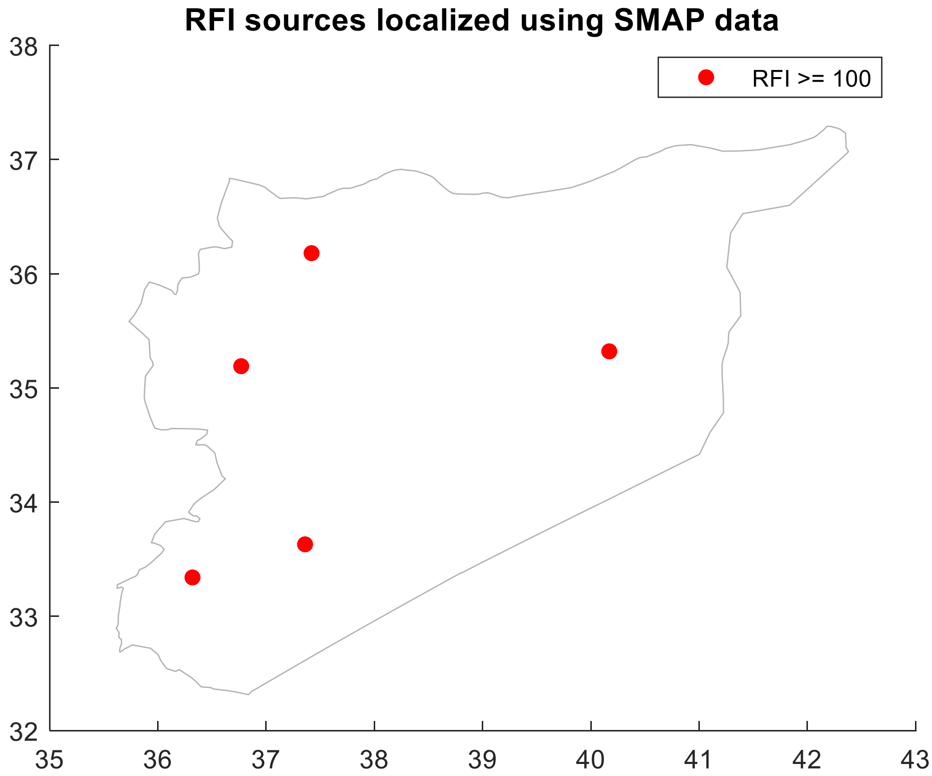

Note to Fig. 61: These locations can be easily seen in the probability and peak hold maps. The colour indicates range of RFI level in kelvin.

6.7.16.4 Classification of RFI sources per intensity (status as of 27/05/2019)

A general summary of the prevalence of RFI sources over the Syrian Arab Republic is summarized from Table 30 as follows:

Very strong RFI (RFI level ≥ 100 K) 5 RFI sources

6.7.17 Report of observed RFI over Albania over a three-month timeframe from 19 March 2019 to 18 June 2019

6.7.17.1 Summary of the RFI sources over Albania

Table 31 defines the fields in the Summary of RFI sources form that should be completed by the administration reporting an RFI event.

TABLE 31

Summary of RFI sources

Date of this RFI status update	19 March 2019 to 18 June 2019
Total number of RFI cases detected	2
Active RFI sources	2 reported
** **Old RFI active sources**	N/A
** **New RFI active sources**	2 reported, see Table 32 for RFI level and geolocation details
RFI sources OFF	N/A

6.7.17.2 Geolocation and other detailed RFI information

Table 32 includes the following detailed information for the RFI source: latitude and longitude, centre frequency, average RFI level in kelvin, number of observations used to geolocate the source and determine RFI level where the source is located as well as the time the source was last seen as of this writing. There are two sources identified over the Republic of Albania. Data from 19 March 2019 to 18 June 2019 was used to create Table 32 as well as supporting Figures.

The localization of RFI sources is based on the difference between SMAP measurements before and after RFI filtering. This difference corresponds to the effect that RFI has on the data. A machine learning algorithm is then applied to automatically find the points where the effect of RFI is highest (local maxima). These points define the location of RFI sources. Since every RFI source is observed multiple times during the course of the reporting period, the coordinates and RFI level provided in this report are the result of an average of the individual observations from 19 March 2019 to 18 June 2019. SMAP science telemetry includes frequency information thus the RFI centre frequency was also identified for the RFI sources. See appendix for spectral plots. A range is given if there appeared to be an observable bandwidth in the spectrum for the RFI source. Multiple centre frequencies were given if there were multiple peaks across the 16 sub-bands that were obviously RFI (TA > 330 K).

TABLE 32

Interference source detail log
Number of active sources listed: [2]

Source ID.	Observed geolocation		Centre frequency (MHz)	Source detection characteristics	Level of interference detected by sensor (K)	e.i.r.p. of transmitting source(s) (dBW)	City/ State/Region	Number of observations	Last seen (UTC)	Present status
	Longitude (degrees)	Latitude (degrees)								
ALB-1	20.12	40.09	1 402, 1 406, 1 422	Point source	229	−14.610 6		163	15/06/2019 16:05	ON
ALB-2	19.78	41.32	1 402, 1 422	Point source	295	−13.510 7		175	18/06/2019 16:17	ON

6.7.17.3 Supporting information

Figure 62 shows the peak hold plot over the Republic of Albania on a 0.25° × 0.25° grid of horizontally polarized TAs in kelvin before RFI filtering. Figure 63 shows a map on a 0.25° × 0.25° grid of the percentage of observations over the period 19 March 2019 to 18 June 2019 with a detected RFI level of 5 K or more in the horizontal polarization. Figure 64 shows location and intensity of RFI sources over the Republic of Albania.

FIGURE 62

Peak hold plot over the Republic of Albania on a 0.25° × 0.25° grid of horizontally polarized TAs in kelvin before RFI filtering over the time period of 19/03/2019 to 18/06/2019

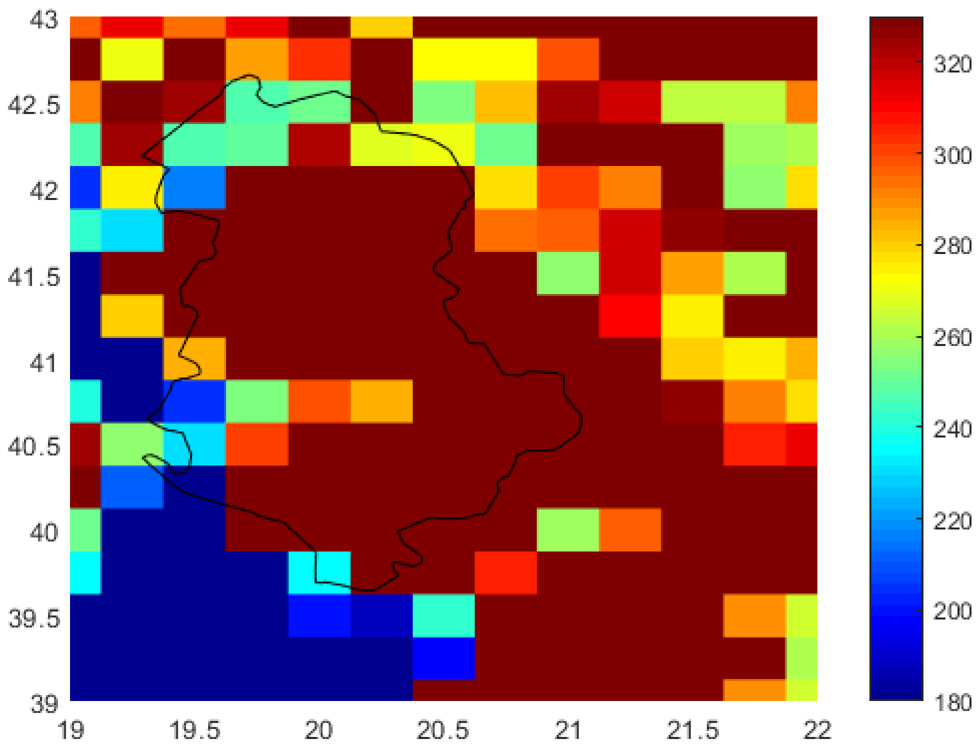

Note to Fig. 62: Similar results are seen in the vertical polarization. A "peak hold" plot (i.e. the maximum value observed) emphasizes large RFI contributions since geophysical contributions to the brightness background are also included. The colour scale is limited to values from 180 K to 330 K. Footprints with TA equal to or lower than 180 K appear dark blue and those that are 330 K and above are dark red. Any value greater than 330 K is automatically flagged as RFI since this is the geophysical limit for brightness temperature measurements.

FIGURE 63

Map on a 0.25° × 0.25° grid of the percentage of observations over the period 19/03/2019 to 18/06/2019 with a detected RFI level of 5 K or more in the horizontal polarization

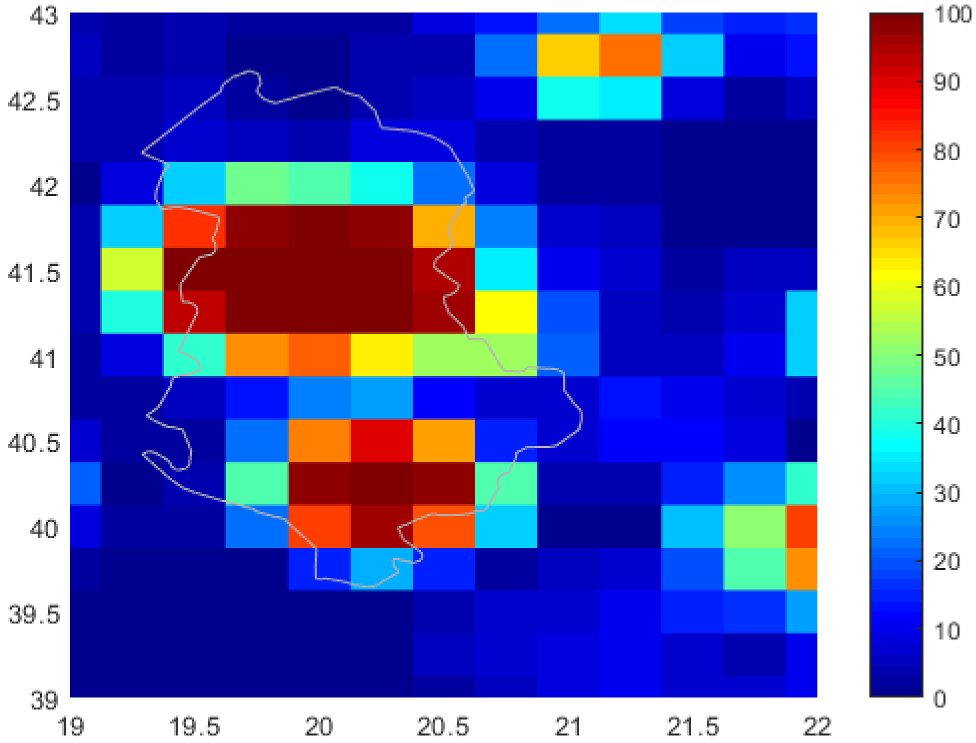

Note to Fig. 63: Vertical polarization shows similar results. Points having values greater than approximately 25 to 30% (i.e. light blue to red) are persistent sources of interference during this period. This plot does not distinguish between large amplitude and small amplitude, but rather highlights the temporal persistence of specific sources.

FIGURE 64

Location and intensity of RFI sources over the Republic of Albania

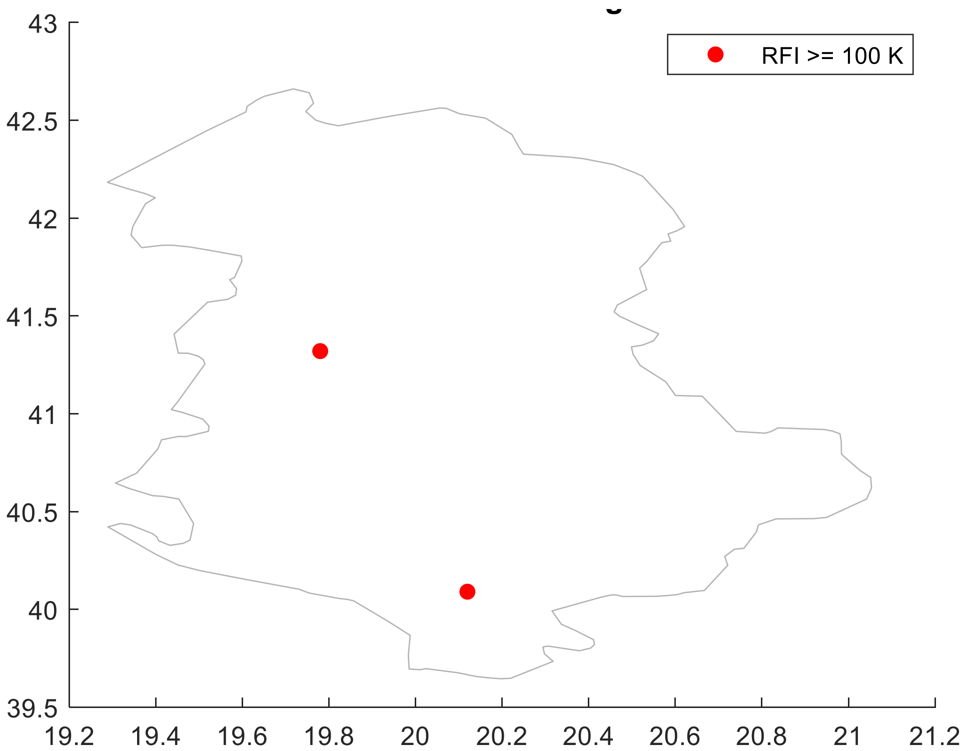

Note to Fig. 64: These locations can be easily seen in the probability and peak hold maps. The colour indicates range of RFI level in kelvin.

6.7.17.4 Classification of RFI sources per intensity (status as of 18/06/2019)

A general summary of the prevalence of RFI sources over the Republic of Albania is summarized from Table 32 as follows:

Very strong RFI (RFI level ≥ 100 K) 2 RFI sources

6.7.18 Report of observed RFI over the Republic of India over a three-month timeframe from 22 May 2019 to 21 August 2019

6.7.18.1 Summary of the RFI sources over the Republic of India

Table 33 defines the fields in the Summary of RFI sources form that should be completed by the administration reporting an RFI event.

TABLE 33

Summary of RFI sources

Date of this RFI status update	22 May 2019 to 21 August 2019
Total number of RFI cases detected	6
Active RFI sources	6 reported
** **Old RFI active sources**	N/A
** **New RFI active sources**	6 reported, see Table 34 for RFI level and geolocation details
RFI sources OFF	N/A

6.7.18.2 Geolocation and other detailed RFI information

Table 34 includes the following detailed information for the RFI source: latitude and longitude, centre frequency, average RFI level in kelvin, number of observations used to geolocate the source and determine RFI level where the source is located as well as the time the source was last seen as of this writing. There are six sources identified over the Republic of India. Data from 22 May 2019 to 21 August 2019 was used to create Table 34 as well as supporting Figures.

The localization of RFI sources is based on the difference between SMAP measurements before and after RFI filtering. This difference corresponds to the effect that RFI has on the data. A machine learning algorithm is then applied to automatically find the points where the effect of RFI is highest (local maxima). These points define the location of RFI sources. Since every RFI source is observed multiple times during the course of the reporting period, the coordinates and RFI level provided in this Report are the result of an average of the individual observations from 22 May 2019 to 21 August 2019. SMAP science telemetry includes frequency information thus the RFI centre frequency was also identified for the RFI sources. See appendix for spectral plots. A range is given if there appeared to be an observable bandwidth in the spectrum for the RFI source. Multiple centre frequencies were given if there were multiple peaks across the 16 sub-bands that were obviously RFI (TA > 330 K).

TABLE 34

Interference source detail log
Number of active sources listed: [6]

Source ID.	Observed geolocation		Centre frequency (MHz)	Source detection characteristics	Level of interference detected by sensor (K)	e.i.r.p. of transmitting source(s) (dBW)	City/ State/Region	Number of observations	Last seen (UTC)	Present status
	Longitude (degrees)	Latitude (degrees)								
IND-1	79.51	29.44	1 402, 1 412, 1 424	Point source	374	−12.48		15	17/08/2019 1:11	ON
IND-2	78.66	30.85	1 419	Point source	372	−12.50		27	11/08/2019 0:46	ON
IND-3	74.95	33.83	1 412-1 415, 1 417	Point source	504	−11.18		23	17/08/2019 1:10	ON
IND-4	93.7	24.39	1 412-1 415, 1 417	Point source	314	−13.24		11	2/08/2019 0:11	ON
IND-5	77.27	28.64	1 412-1 415, 1 417, 1 424	Point source	112	−17.72		16	20/08/2019 12:20	ON
IND-6	73.87	18.5	1 412-1 415, 1 417	Point source	111	−17.76		15	17/08/2019 1:14	ON

6.7.18.3 Supporting information

Figure 65 shows the peak hold plot over the Republic of India on a 0.25° × 0.25° grid of horizontally polarized TAs in kelvin before RFI filtering. Figure 66 shows a map on a 0.25° × 0.25° grid of the percentage of observations over the period 22 May 2019 to 21 August 2019 with a detected RFI level of 5 K or more in the horizontal polarization. Figure 67 shows location and intensity of RFI sources over the Republic of India.

FIGURE 65

Peak hold plot over the Republic of India on a 0.25° × 0.25° grid of horizontally polarized TAs in kelvin before RFI filtering over the time period of 22/05/2019 to 21/08/2019

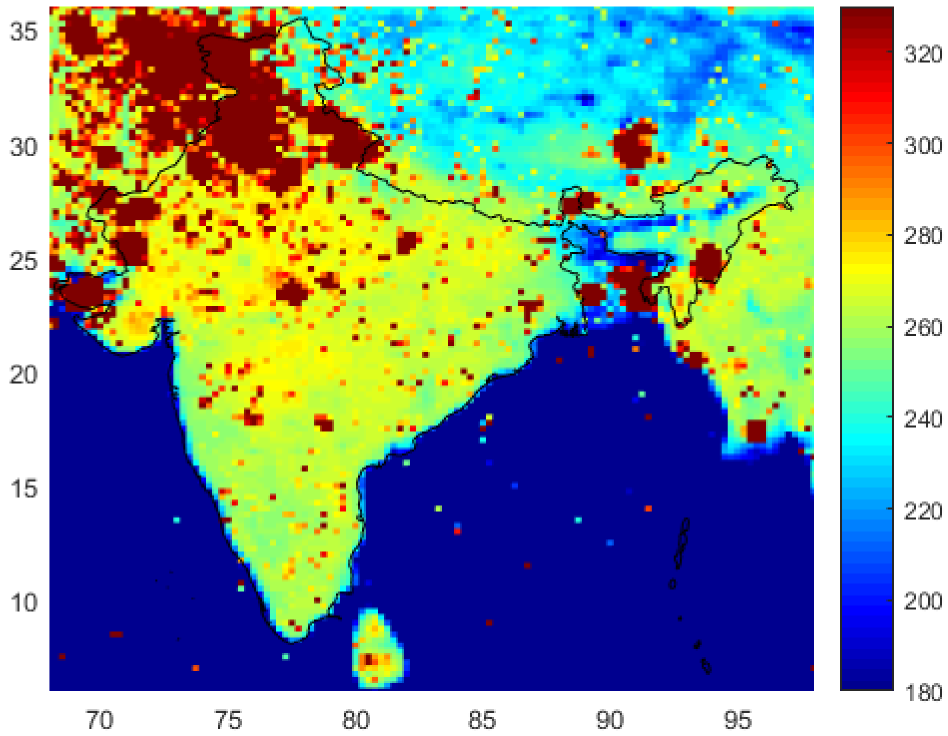

Note to Fig. 65: Similar results are seen in the vertical polarization. A 'peak hold' plot (i.e. the maximum value observed) emphasizes large RFI contributions since geophysical contributions to the brightness background are also included. The colour scale is limited to values from 180 K to 330 K. Footprints with TA equal to or lower than 180 K appear dark blue and those that are 330 K and above are dark red. Any value greater than 330 K is automatically flagged as RFI since this is the geophysical limit for brightness temperature measurements.

FIGURE 66

Map on a 0.25° × 0.25° grid of the percentage of observations over the period 22/05/2019 to 21/08/2019 with a detected RFI level of 5 K or more in the horizontal polarization

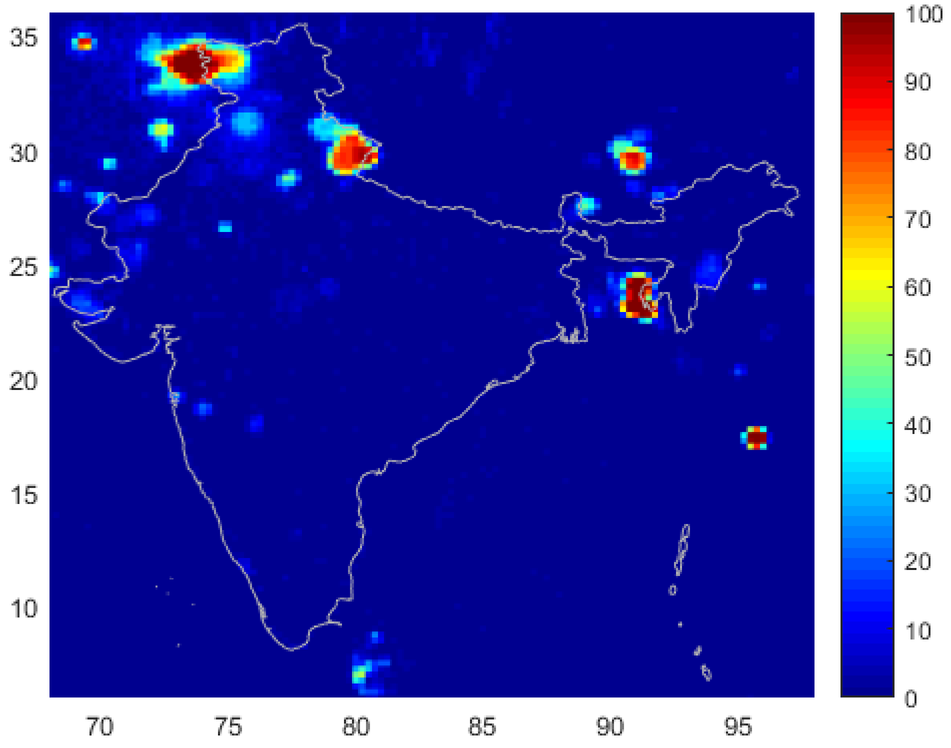

Note to Fig. 66: Vertical polarization shows similar results. Points having values greater than approximately 25 to 30% (i.e. light blue to red) are persistent sources of interference during this period. This plot does not distinguish between large amplitude and small amplitude, but rather highlights the temporal persistence of specific sources.

FIGURE 67

Location and intensity of RFI sources over the Republic of India

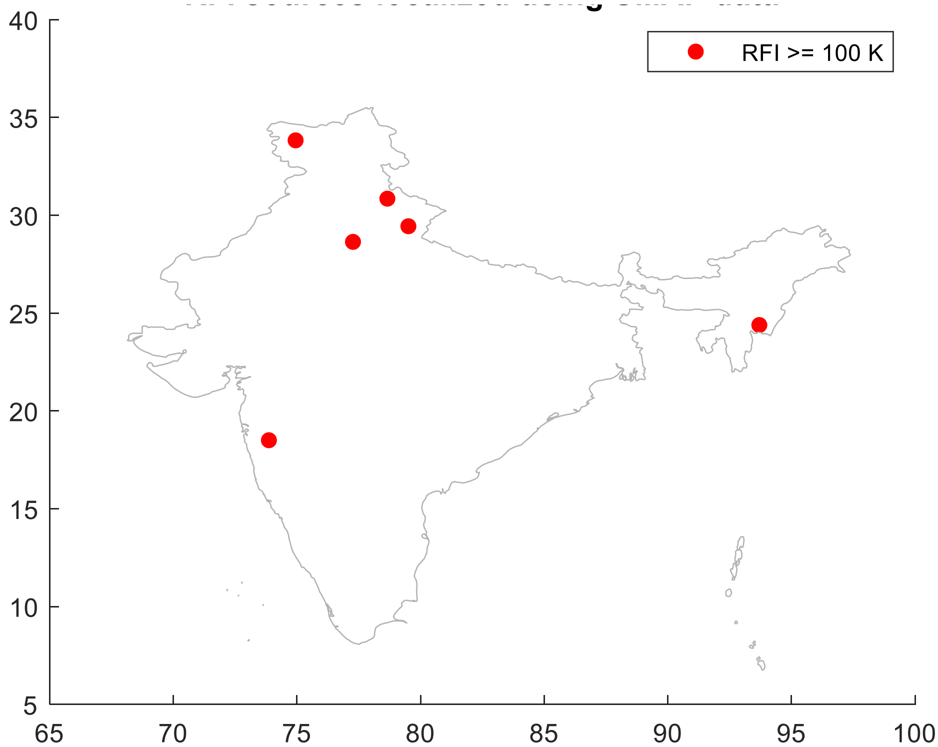

Note to Fig. 67: These locations can be easily seen in the probability and peak hold maps. The colour indicates range of RFI level in kelvin.

6.7.18.4 Classification of RFI sources per intensity (status as of 21/08/2019)

A general summary of the prevalence of RFI sources over the Republic of India is summarized from Table 34 as follows:

Very strong RFI (RFI level ≥ 100 K) 6 RFI sources

6.7.19 Report of observed RFI over Republic of Indonesia over a three-month timeframe from 29 July 2019 to 28 October 2019

6.7.19.1 Summary of the RFI sources over the Republic of Indonesia

Table 35 defines the fields in the Summary of RFI sources form that should be completed by the Administration reporting an RFI event.

TABLE 35

Summary of RFI sources

Date of this RFI status update	29 July 2019 to 28 October 2019
Total number of RFI cases detected	24
Active RFI sources	24 reported
** **Old RFI active sources**	N/A
** **New RFI active sources**	24 reported, see Table 36 for RFI level and geolocation details
RFI sources OFF	N/A

6.7.19.2 Geolocation and other detailed RFI information

Table 36 includes the following detailed information for the RFI source: latitude and longitude, centre frequency, average RFI level in kelvin, number of observations used to geolocate the source and determine RFI level where the source is located as well as the time the source was last seen as of this writing. There are 24 sources identified over the Republic of Indonesia. Data from 29 July 2019 to 28 October 2019 was used to create Table 36 as well as supporting Figures.

The localization of RFI sources is based on the difference between SMAP measurements before and after RFI filtering. This difference corresponds to the effect that RFI has on the data. A machine learning algorithm is then applied to automatically find the points where the effect of RFI is highest (local maxima). These points define the location of RFI sources. Since every RFI source is observed multiple times during the course of the reporting period, the coordinates and RFI level provided in this report are the result of an average of the individual observations from 29 July 2019 to 28 October 2019. SMAP science telemetry includes frequency information thus the RFI centre frequency was also identified for the RFI sources. See appendix for spectral plots. A range is given if there appeared to be an observable bandwidth in the spectrum for the RFI source. Multiple centre frequencies were given if there were multiple peaks across the 16 sub-bands that were obviously RFI (TA > 330 K).

TABLE 36

Interference source detail log
Number of active sources listed: [24]

Source ID.	Observed geolocation		Centre frequency (MHz)	Source detection characteristics	Level of interference detected by sensor (K)	e.i.r.p. of transmitting source(s) (dBW)	City/ State/Region	Number of observations	Last seen (UTC)	Present status
	Longitude (degrees)	Latitude (degrees)								
INS-1	114.596 7	−3.328 5	1 413	Point source	151.144 9	−16.415	Indonesia	104	28/10/2019 10:19	ON
INS-2	106.387 3	−6.198 2	1 413	Point source	79.781 4	−19.189 9	Indonesia	75	26/10/2019 23:04	ON
INS-3	119.880 4	−0.907 5	1 413	Point source	42.723 4	−21.902 3	Indonesia	95	27/10/2019 22:02	ON
INS-4	119.654 3	−5.499 3	1 413	Point source	40.677 7	−22.115 4	Indonesia	83	28/10/2019 10:18	ON
INS-5	124.878	1.503 6	1 413	Point source	45.218 2	−21.655 8	Indonesia	51	22/10/2019 9:54	ON
INS-6	116.214 7	−8.633 8	1 413	Point source	41.5	−22.028 4	Indonesia	83	28/10/2019 10:15	ON
INS-7	113.281 2	−7.861 7	1 413	Point source	59.152 1	−20.489 2	Indonesia	42	26/10/2019 10:42	ON
INS-8	102.7126	−2.297 1	1 413	Point source	52.9848	−20.967 4	Indonesia	93	27/10/2019 11:21	ON
INS-9	111.3515	−7.626 7	1 413	Point source	49.9161	−21.226 5	Indonesia	40	28/10/2019 22:40	ON
INS-10	112.6587	−7.269 2	1 413	Point source	70.9797	−19.697 6	Indonesia	22	28/10/2019 22:40	ON
INS-11	123.632	−10.180 6	1 413	Point source	31.7385	−23.193 1	Indonesia	85	27/10/2019 9:40	ON
INS-12	116.9128	−1.179 4	1 413	Point source	30.3298	−23.390 2	Indonesia	51	28/10/2019 10:17	ON

TABLE 36 (*end*)

Source ID.	Observed geolocation		Centre frequency (MHz)	Source detection characteristics	Level of interference detected by sensor (K)	e.i.r.p. of transmitting source(s) (dBW)	City/ State/Region	Number of observations	Last seen (UTC)	Present status
	Longitude (degrees)	Latitude (degrees)								
INS-13	113.916 7	−2.237 3	1 413	Point source	26.885 3	−23.913 8	Indonesia	60	28/10/2019 22:38	ON
INS-14	103.640 1	−1.615	1 413	Point source	29.730 9	−23.476 8	Indonesia	49	24/10/2019 11:07	ON
INS-15	113.460 2	−7.038 1	1 413	Point source	34.186 4	−22.870 4	Indonesia	16	7/10/2019 10:28	ON
INS-16	109.359 4	−0.068 7	1 413	Point source	26.739 6	−23.937 4	Indonesia	24	28/10/2019 22:36	ON
INS-17	95.357	5.548 3	1 413	Point source	21.786	−24.827 2	Indonesia	34	27/10/2019 11:21	ON
INS-18	113.862 4	−8.095 4	1 413	Point source	45.519 8	−21.626 9	Indonesia	21	28/10/2019 10:18	ON
INS-19	112.569 7	−7.348 2	1 413	Point source	58.895 6	−20.508 1	Indonesia	34	23/10/2019 10:31	ON
INS-20	117.177 3	−0.436 8	1 413	Point source	35.569 7	−22.698 1	Indonesia	28	28/10/2019 10:20	ON
INS-21	110.223 9	−7.574	1 413	Point source	32.566 9	−23.081 2	Indonesia	10	28/10/2019 22:40	ON
INS-22	101.414 1	0.477 4	1 413	Point source	20.051 6	−25.187 4	Indonesia	10	26/10/2019 23:01	ON
INS-23	104.792 5	−2.995 6	1 413	Point source	26.469 4	−23.981 5	Indonesia	12	21/10/2019 23:14	ON
INS-24	123.068	0.603 7	1 413	Point source	25.526 2	−24.139 1	Indonesia	10	16/10/2019 9:31	ON

6.7.19.3 Supporting information

Figure 68 shows the peak hold plot over the Republic of Indonesia on a 0.25° × 0.25° grid of horizontally polarized TAs in kelvin before RFI filtering. Figure 69 shows a map on a 0.25° × 0.25° grid of the percentage of observations over the period 29 July 2019 to 28 October 2019 with a detected RFI level of 5 K or more in the horizontal polarization. Figure 70 shows location and intensity of RFI sources over the Republic of Indonesia.

FIGURE 68

Peak hold plot over the Republic of Indonesia on a 0.25° × 0.25° grid of horizontally polarized TAs in kelvin before RFI filtering over the time period of 29/07/2019 to 28/10/201

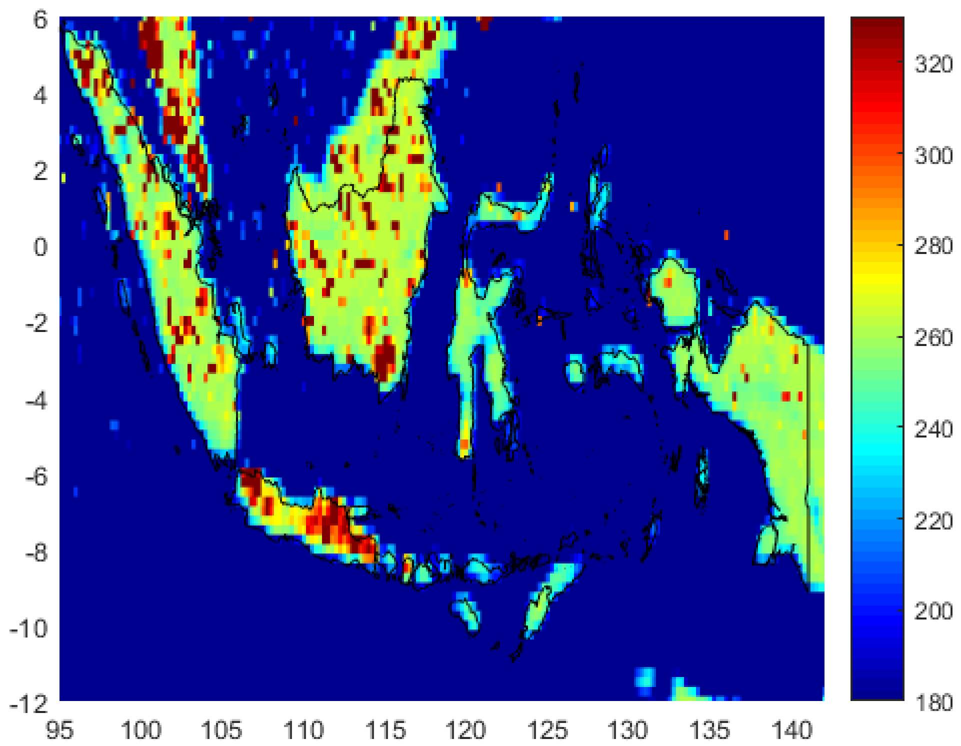

Note to Fig. 68: Similar results are seen in the vertical polarization. A 'peak hold' plot (i.e. the maximum value observed) emphasizes large RFI contributions since geophysical contributions to the brightness background are also included. The colour scale is limited to values from 180 K to 330 K. Footprints with TA equal to or lower than 180 K appear dark blue and those that are 330 K and above are dark red. Any value greater than 330 K is automatically flagged as RFI since this is the geophysical limit for brightness temperature measurements.

FIGURE 69

Map on a 0.25° × 0.25° grid of the percentage of observations over the period 29/07/2019 to 28/10/2019 with a detected RFI level of 5 K or more in the horizontal polarization

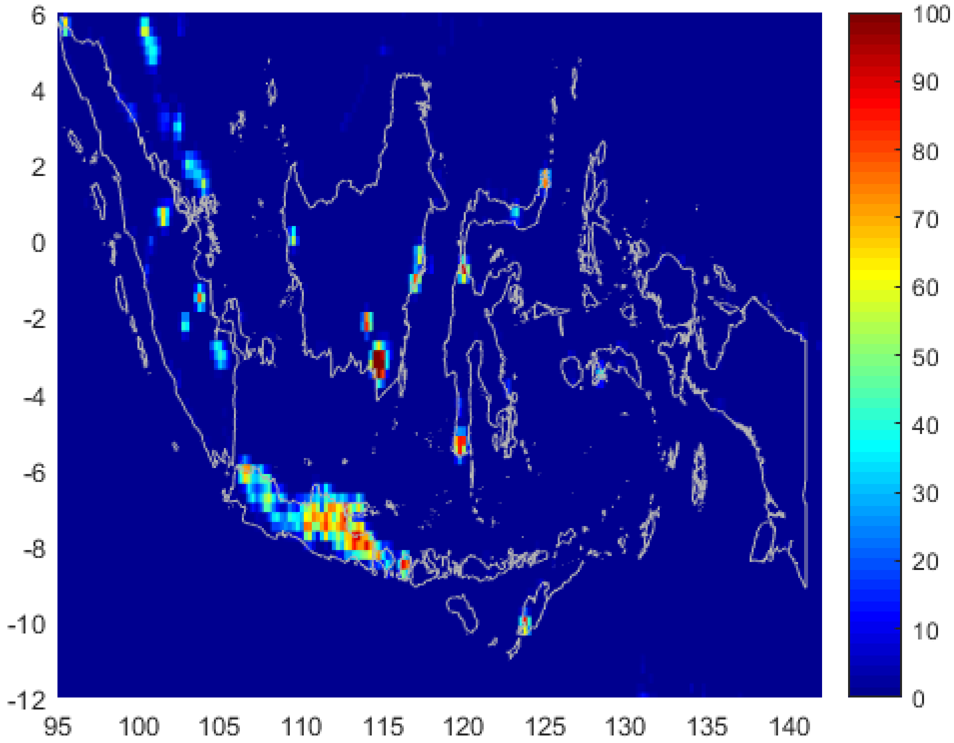

Note to Fig. 69: Vertical polarization shows similar results. Points having values greater than approximately 25 to 30% (i.e. light blue to red) are persistent sources of interference during this period. This plot does not distinguish between large amplitude and small amplitude, but rather highlights the temporal persistence of specific sources.

FIGURE 70

Location and intensity of RFI sources over the Republic of Indonesia

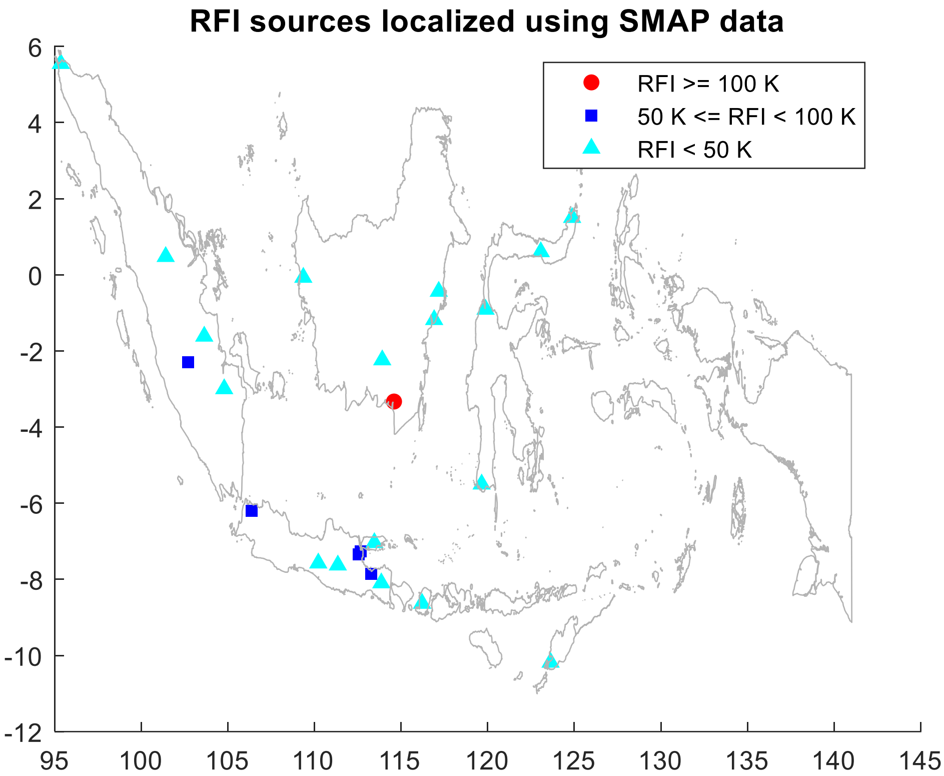

Note to Fig. 70: These locations can be easily seen in the probability and peak hold maps. The colours indicate ranges of RFI level in kelvin.

6.7.19.4 Classification of RFI sources per intensity (status as of 28/10/2019)

A general summary of the prevalence of RFI sources over the Republic of Indonesia is summarized from Table 36 as follows:

Very strong RFI (RFI level >= 100 K)	1 RFI source
Strong RFI (50 K ≤ RFI level < 100 K)	5 RFI sources
Moderate RFI (RFI level < 50 K)	18 RFI sources

6.7.20 Report of observed RFI over Republic of Korea (South Korea) over a three-month timeframe from 1 September 2019 to 30 November 2019

6.7.20.1 Summary of the RFI sources

Table 37 defines the fields in the Summary of RFI sources form that should be completed by the administration reporting an RFI event.

TABLE 37

Summary of RFI sources

Date of this RFI status update	1 September 2019 to 30 November 2019
Total number of RFI cases detected	8
Active RFI sources	8 reported
** **Old RFI active sources**	N/A
** **New RFI active sources**	8 reported, see Table 38 for RFI level and geolocation details
RFI sources OFF	N/A

6.7.20.2 Geolocation and other detailed RFI information

Table 38 includes the following detailed information for the RFI source: latitude and longitude, centre frequency, average RFI level in kelvin, number of observations used to geolocate the source and determine RFI level where the source is located as well as the time the source was last seen as of this writing. There are eight sources identified over the Republic of Korea. Data from 1 September 2019 to 30 November 2019 was used to create Table 38 as well as supporting Figures.

The localization of RFI sources is based on the difference between SMAP measurements before and after RFI filtering. This difference corresponds to the effect that RFI has on the data. A machine learning algorithm is then applied to automatically find the points where the effect of RFI is highest (local maxima). These points define the location of RFI sources. Since every RFI source is observed multiple times during the course of the reporting period, the coordinates and RFI level provided in this report are the result of an average of the individual observations from 1 September 2019 to 30 November 2019. SMAP science telemetry includes frequency information thus the RFI centre frequency was also identified for the RFI sources. See appendix for spectral plots. A range is given if there appeared to be an observable bandwidth in the spectrum for the RFI source. Multiple centre frequencies were given if there were multiple peaks across the 16 sub-bands that were obviously RFI (TA > 330 K).

TABLE 38

Interference source detail log
Number of active sources listed: [8]

Source ID.	Observed geolocation		Centre frequency (MHz)	Source detection characteristics	Level of interference detected by sensor (K)	e.i.r.p. of transmitting source(s) (dBW)	City/ State/Region	Number of observations	Last seen (UTC)	Present status
	Longitude (degrees)	Latitude (degrees)								
KOR-1	128.02	38.13	1 413	Point source	363	−12.61	South Korea	108	29/11/2019 8:52	ON
KOR-2	124.63	37.94	1 413	Point source	181	−15.63	South Korea	81	30/11/2019 9:29	ON
KOR-3	127.85	35	1 413	Point source	127	−17.17	South Korea	75	29/11/2019 8:51	ON
KOR-4	130.88	37.48	1 413	Point source	95	−18.43	South Korea	50	29/11/2019 8:52	ON
KOR-5	126.28	33.25	1 413	Point source	82	−19.07	South Korea	37	30/11/2019 9:28	ON
KOR-6	128.64	35.94	1 413	Point source	85	−18.91	South Korea	28	20/11/2019 21:52	ON
KOR-7	128.9	37.09	1 413	Point source	277	−13.78	South Korea	13	29/11/2019 8:52	ON
KOR-8	126.67	37.7	1 413	Point source	500	−11.22	South Korea	24	5/11/2019 8:50	ON

6.7.20.3 Supporting information

Figure 71 shows the peak hold plot over the Republic of Korea on a 0.25° × 0.25° grid of horizontally polarized TAs in kelvin before RFI filtering. Figure 72 shows a map on a 0.25° × 0.25° grid of the percentage of observations over the period 1 September 2019 to 30 November 2019 with a detected RFI level of 5 K or more in the horizontal polarization. Figure 73 shows location and intensity of RFI sources over the Republic of Korea.

FIGURE 71

Peak hold plot over the Republic of Korea on a 0.25° × 0.25° grid of horizontally polarized TAs in kelvin before RFI filtering over the time period of 01/09/2019 to 30/11/2019

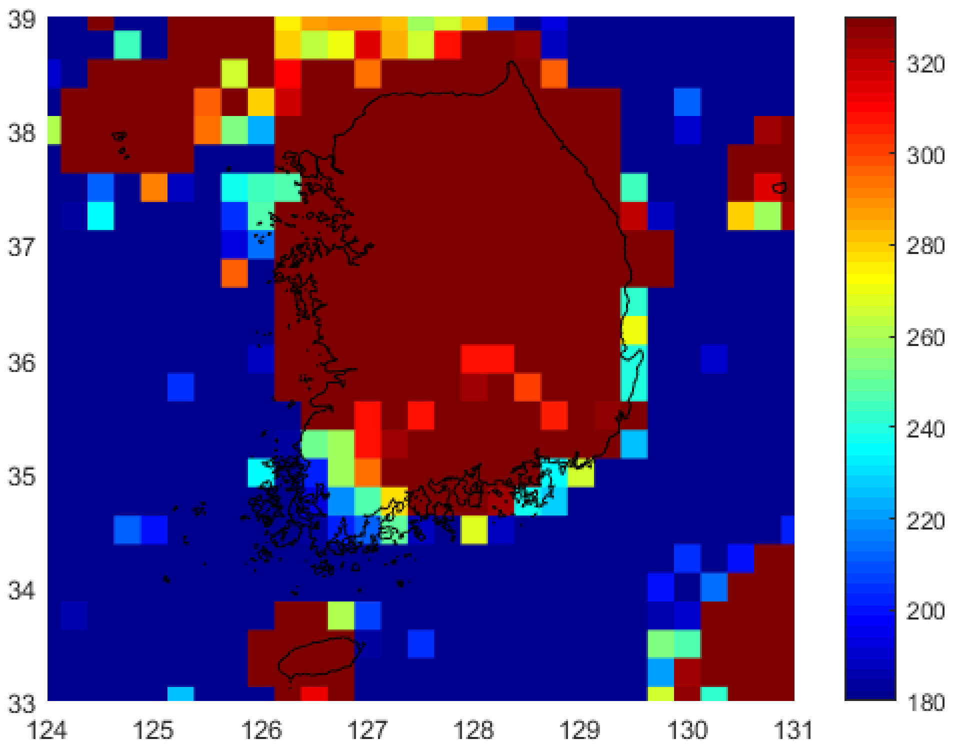

Note to Fig. 71: Similar results are seen in the vertical polarization. A 'peak hold' plot (i.e. the maximum value observed) emphasizes large RFI contributions since geophysical contributions to the brightness background are also included. The colour scale is limited to values from 180 K to 330 K. Footprints with TA equal to or lower than 180 K appear dark blue and those that are 330 K and above are dark red. Any value greater than 330 K is automatically flagged as RFI since this is the geophysical limit for brightness temperature measurements.

FIGURE 72

Map on a 0.25° × 0.25° grid of the percentage of observations over the period 01/09/2019 to 30/11/2019 with a detected RFI level of 5 K or more in the horizontal polarization

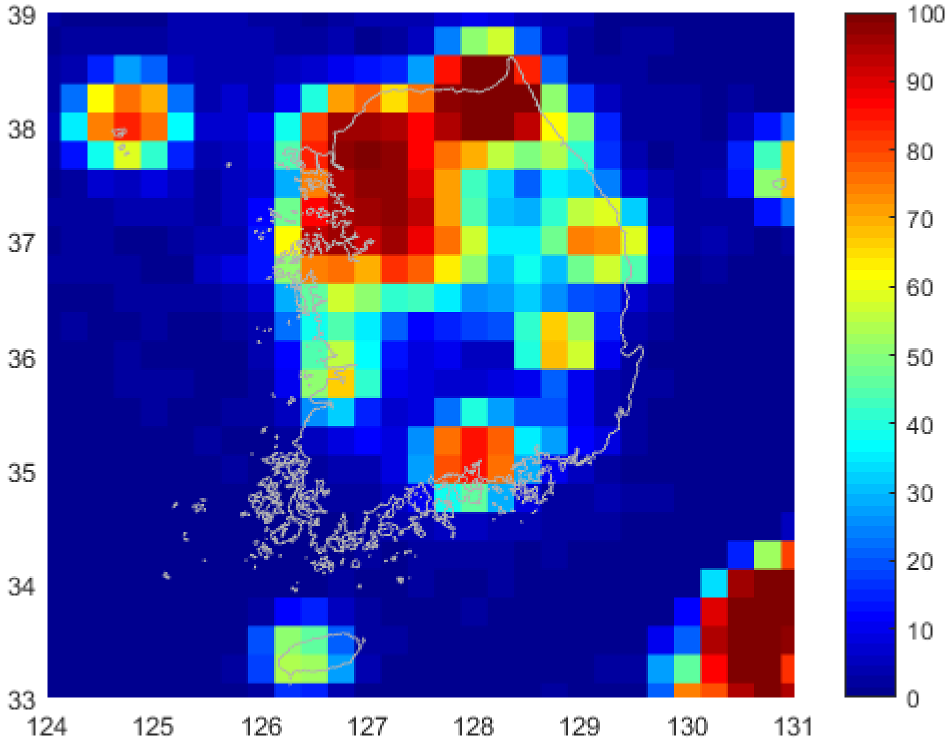

Note to Fig. 72: Vertical polarization shows similar results. Points having values greater than approximately 25-30% (i.e. light blue to red) are persistent sources of interference during this period. This plot does not distinguish between large amplitude and small amplitude, but rather highlights the temporal persistence of specific sources.

FIGURE 73

Location and intensity of RFI sources over the Republic of Korea

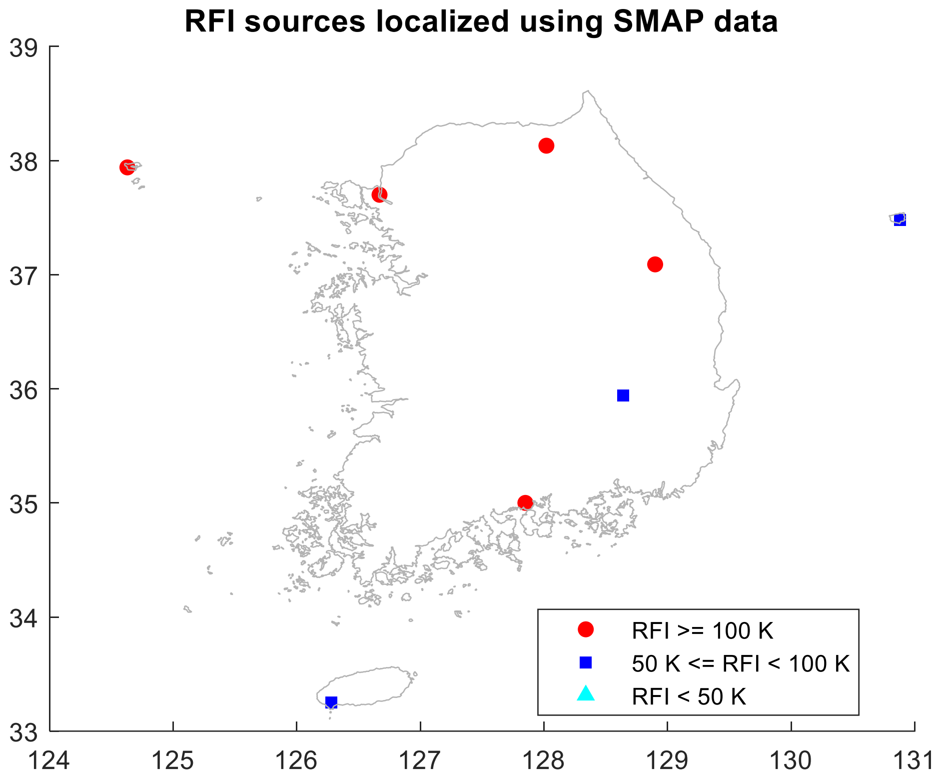

Note to Fig. 73: These locations can be easily seen in the probability and peak hold maps. The colours indicate ranges of RFI level in kelvin.

6.7.20.4 Classification of RFI sources per intensity (status as of 30/11/2019)

A general summary of the prevalence of RFI sources over the Republic of Korea is summarized from Table 38 as follows:

Very strong RFI (RFI level >= 100 K)	5 RFI source
Strong RFI (50 K ≤ RFI level < 100 K)	3 RFI sources
Moderate RFI (RFI level < 50 K)	0 RFI sources

6.7.21 Report of observed RFI over Republic of Sudan over a three-month timeframe from 1 October 2019 to 31 December 2019

6.7.21.1 Summary of the RFI sources over the Republic of Sudan

Table 39 defines the fields in the Summary of RFI sources form that should be completed by the administration reporting an RFI event.

TABLE 39

Summary of RFI sources

Date of this RFI status update	1 October 2019 to 31 December 2019
Total number of RFI cases detected	7
Active RFI sources	7 reported
** **Old RFI active sources**	N/A
** **New RFI active sources**	7 reported, see Table 40 for RFI level and geolocation details
RFI sources OFF	N/A

6.7.21.2 Geolocation and other detailed RFI information

Table 40 includes the following detailed information for the RFI source: latitude and longitude, centre frequency, average RFI level in kelvin, number of observations used to geolocate the source and determine RFI level where the source is located as well as the time the source was last seen as of this writing. There are seven sources identified over the Republic of Sudan. Data from 1 October 2019 to 31 December 2019 was used to create Table 40 as well as supporting Figures.

The localization of RFI sources is based on the difference between SMAP measurements before and after RFI filtering. This difference corresponds to the effect that RFI has on the data. A machine learning algorithm is then applied to automatically find the points where the effect of RFI is highest (local maxima). These points define the location of RFI sources. Since every RFI source is observed multiple times during the course of the reporting period, the coordinates and RFI level provided in this report are the result of an average of the individual observations from 1 October 2019 to 31 December 2019. SMAP science telemetry includes frequency information thus the RFI centre frequency was also identified for the RFI sources. See appendix for spectral plots. A range is given if there appeared to be an observable bandwidth in the spectrum for the RFI source. Multiple centre frequencies were given if there were multiple peaks across the 16 sub-bands that were obviously RFI (TA > 330 K).

TABLE 40

Interference source detail log
Number of active sources listed: [7]

Source ID.	Observed geolocation		Centre frequency (MHz)	Source detection characteristics	Level of interference detected by sensor (K)	e.i.r.p. of transmitting source(s) (dBW)	City/ State/Region	Number of observations	Last seen (UTC)	Present status
	Longitude (degrees)	Latitude (degrees)								
SDN-1	28.45	9.68	1 413	Point source	569	−10.657 8	Sudan	112	30/12/2019 3:56	ON
SDN-2	31.65	9.59	1 413	Point source	261	−14.042 5	Sudan	107	30/12/2019 3:56	ON
SDN-3	31.56	4.86	1 413	Point source	170	−15.904 4	Sudan	132	30/12/2019 3:58	ON
SDN-4	32.56	15.57	1 413	Point source	147	−16.535 8	Sudan	111	30/12/2019 3:55	ON
SDN-5	28.4	4.56	1 413	Point source	77	−19.344	Sudan	95	30/12/2019 16:18	ON
SDN-6	29.69	6.82	1 413	Point source	151	−16.419 2	Sudan	29	28/12/2019 4:20	ON
SDN-7	29.79	9.33	1 413	Point source	55	−20.805 3	Sudan	55	30/12/2019 3:56	ON

6.7.21.3 Supporting information

Figure 74 shows the peak hold plot over the Republic of Sudan on a 0.25° × 0.25° grid of horizontally polarized TAs in kelvin before RFI filtering. Figure 75 shows a map on a 0.25° × 0.25° grid of the percentage of observations over the period 1 October 2019 to 31 December 2019 with a detected RFI level of 5 K or more in the horizontal polarization. Figure 76 shows location and intensity of RFI sources over the Republic of Sudan.

FIGURE 74

Peak hold plot over the Republic of Sudan on a 0.25° × 0.25° grid of horizontally polarized TAs in kelvin before RFI filtering over the time period of 01/10/2019 to 31/12/2019

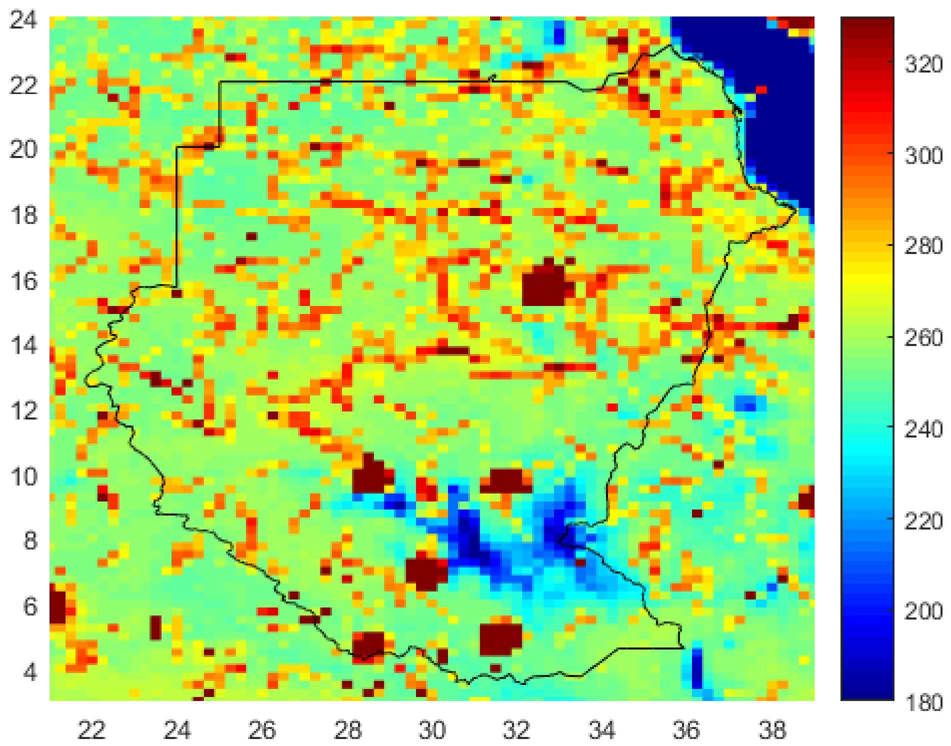

Note to Fig. 74: Similar results are seen in the vertical polarization. A 'peak hold' plot (i.e. the maximum value observed) emphasizes large RFI contributions since geophysical contributions to the brightness background are also included. The colour scale is limited to values from 180 K to 330 K. Footprints with TA equal to or lower than 180 K appear dark blue and those that are 330 K and above are dark red. Any value greater than 330 K is automatically flagged as RFI since this is the geophysical limit for brightness temperature measurements.

FIGURE 75

Map on a 0.25° × 0.25° grid of the percentage of observations over the period 01/10/2019 to 31/12/2019 with a detected RFI level of 5 K or more in the horizontal polarization

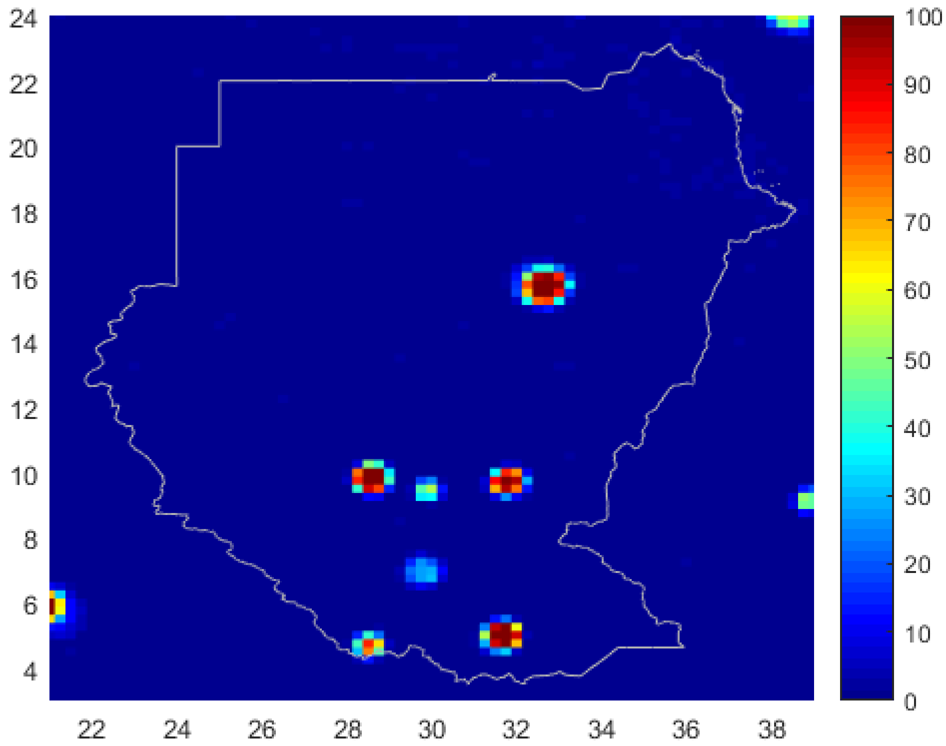

Note to Fig. 75: Vertical polarization shows similar results. Points having values greater than approximately 25 to 30% (i.e. light blue to red) are persistent sources of interference during this period. This plot does not distinguish between large amplitude and small amplitude, but rather highlights the temporal persistence of specific sources.

FIGURE 76

Location and intensity of RFI sources over the Republic of Sudan

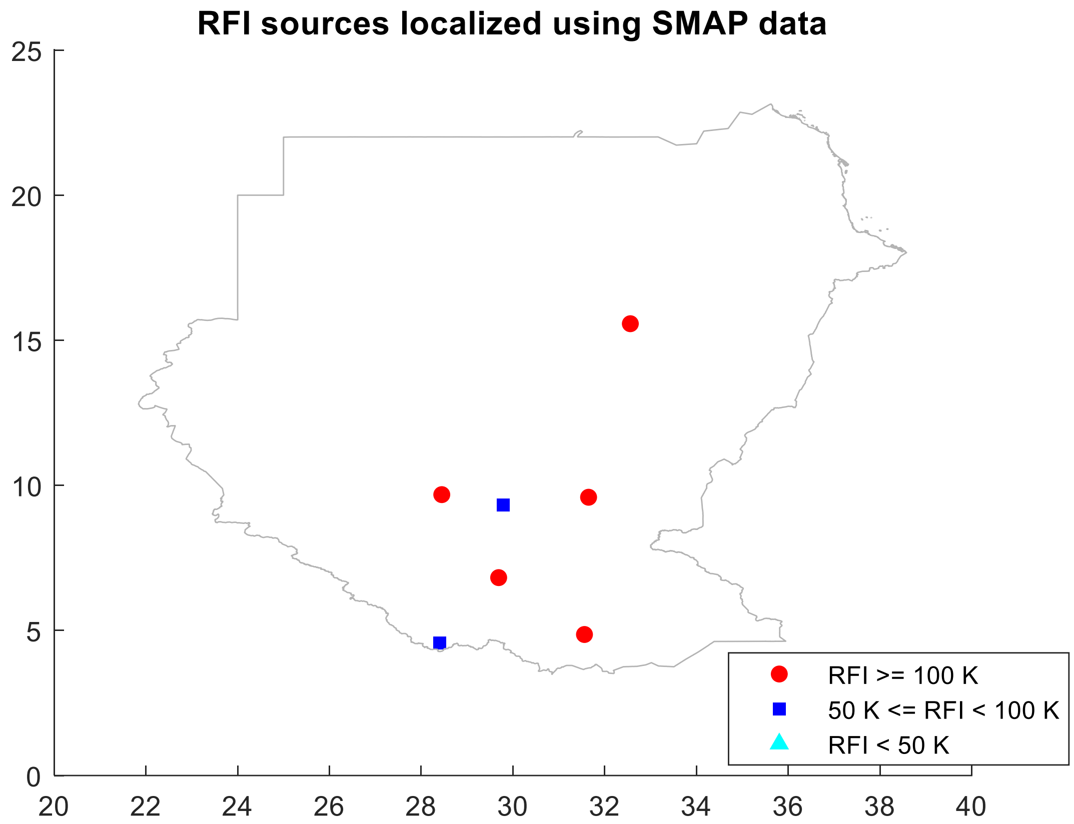

Note to Fig. 76: These locations can be easily seen in the probability and peak hold maps. The colours indicate ranges of RFI level in kelvin.

6.7.21.4 Classification of RFI sources per intensity (status as of 31/12/2019)

A general summary of the prevalence of RFI sources over the Republic of Sudan is summarized from Table 40 as follows:

Very strong RFI (RFI level >= 100 K)	5 RFI source
Strong RFI (50 K ≤ RFI level < 100 K)	2 RFI sources
Moderate RFI (RFI level < 50 K)	0 RFI sources

7 Summary

Within this Report have been presented RFI as were observed globally and over the various administrations by the SMAP L-band spaceborne active sensor in the EESS (active) band 1 215-1 300 MHz and the SMAP L-band spaceborne passive sensor in the EESS (passive) band 1 400-1 427 MHz at various periods of times.

Global maps of observed RFI levels in dBm were shown for the EESS (active) system SMAP radar in 1 215-1 300 MHz. Maps of observed BT in dB K of areas in various administrations across the globe were shown for the EESS (passive) system SMAP radiometer. Instances of high RFI were shown for the SMAP radar and radiometer.

In cases where RFI sources could not be switched off, it was very important to ensure that the RFI sources were detected and flagged accordingly. RFI filtering methods are continuously improving and evolving; however even low levels of RFI added to the signal caused difficulties in distinguishing between natural and man-made radiations and had a strong impact on the overall data quality and interpretation of the measurements.

For the case of the SMAP Scatterometer, an RFI detection and filtering algorithm was developed for ground data processing. The global survey maps of RFI at 1 225 MHz as observed at the various timepoints showed that certain land areas were contaminated with RFI. Fortunately, this land area RFI had no impact on the SMAP measurements to estimate sea salt salinity and it is not known to what degree this RFI impacted sensor measurements of soil moisture such as those obtained by SMAP.

For the case of the SMAP Radiometer, tests facilitated by the Japanese authorities (MIC) confirmed that the main interference was due to malfunctioning/poor isolation of the IF circuits of satellite direct broadcast home-TV receiver equipment.